

Aus dem Institut für Virologie und Immunbiologie der Universität Würzburg
Vorstände: Professor Dr. med. Axel Rethwilm & Professor Dr. rer. nat. Thomas Hünig
und
dem Department of Cancer Immunology and AIDS des Dana-Farber Cancer Institutes
Vorstand: Professor Harvey Cantor, M.D.

**Analysis of Cross-Clade Neutralizing Antibodies against HIV-1 Env Induced by
Immunofocusing**

Inaugural-Dissertation
zur Erlangung der Doktorwürde der
Medizinischen Fakultät
der
Julius-Maximilians-Universität Würzburg
vorgelegt von
Fabian Marc Philipp Kaiser
aus Frankfurt am Main

Würzburg, Dezember 2012

Referent: Professor Dr. med. Axel Rethwilm
Koreferent: Professor Dr. rer. nat. Thomas Hünig
Dekan: Professor Dr. med. Matthias Frosch

Tag der mündlichen Prüfung:

Der Promovend ist Arzt

Meinen Eltern in Dankbarkeit gewidmet.

TABLE OF CONTENTS

1	Introduction	1
1.1	The HIV-1 Epidemic and the Quest for a Vaccine	1
1.2	The Human Immunodeficiency Virus	2
1.2.1	The Discovery of HIV	2
1.2.2	Classification and Sequence Diversity	3
1.2.3	HIV-1 Virion Structure.....	3
1.2.4	The HIV-1 Genome and Proteome	5
1.2.5	Cellular Tropism and HIV-1 Replication	5
1.3	HIV-1 Infection and AIDS	8
1.3.1	Routes of HIV-1 Transmission.....	8
1.3.2	The Course of HIV-1 Infection	8
1.4	The HIV-1 Envelope Glycoprotein.....	10
1.4.1	Synthesis and Organization on the Viral Surface.....	10
1.4.2	Topology of Gp120	11
1.4.3	Topology of Gp41	13
1.4.4	Viral Defense Mechanisms for Antibody Evasion.....	13
1.5	HIV-1/AIDS Vaccine Development.....	14
1.5.1	Past HIV-1 Vaccine Trials.....	14
1.5.2	Protective Epitopes of HIV-1 Env.....	15
1.5.3	The V3 Loop as a Target for HIV-1 Vaccine Design	16
1.5.4	Non-Human Primate Models of HIV-1/AIDS	18
1.5.5	Epitope Identification and the Phage Display Approach.....	18
1.6	Aim of this Work	20
2	Materials and Methods	21
2.1	Materials	21
2.1.1	Antibodies.....	21
2.1.2	Bacterial Strains.....	21
2.1.3	Buffers and Solutions	21
2.1.4	Chemical Reagents	22

2.1.5	Enzymes	23
2.1.6	Equipment.....	23
2.1.7	Kits	25
2.1.8	Ladders and Loading Dyes	25
2.1.9	Media	26
2.1.10	pPEPTIDE Cloning Vector 1 (MoBiTec)	26
2.1.11	Precast Gels for PAGE	27
2.1.12	Primers.....	27
2.2	Methods	28
2.2.1	Phage Amplification	28
2.2.2	Phage Precipitation	28
2.2.3	Measurement of Phage Concentration.....	28
2.2.4	Isolation of Phage ssDNA	28
2.2.5	Amplification of Phage Mimotope DNA via PCR.....	29
2.2.6	Purification of PCR Products	29
2.2.7	Measurement of DNA Concentration.....	29
2.2.8	Amplification of pPEPTIDE Vector DNA.....	30
2.2.9	Isolation and Purification of pPEPTIDE Vector DNA (Mini-Prep).....	30
2.2.10	Digestion of Phage Mimotope and pPEPTIDE Vector DNA.....	30
2.2.11	Analysis and Purification of Digested DNA Samples.....	30
2.2.12	Ligation of Phage Mimotope DNA and pPEPTIDE Vector DNA.....	31
2.2.13	Transformation of DH5 α Cells.....	31
2.2.14	Control Digestion of Recombinant DNA	31
2.2.15	Sequencing	31
2.2.16	Site-Directed Mutagenesis.....	32
2.2.17	Transformation of BL21(DE3) Cells.....	32
2.2.18	Selection of High-Level Expression Clones.....	32
2.2.19	Expression Kinetics	32
2.2.20	Protein Expression.....	33
2.2.21	Column Preparation.....	33
2.2.22	Purification of His-tagged Fusion Proteins	33
2.2.23	Analysis of Eluted Fractions	34

2.2.24	Desalting and Buffer Exchange.....	34
2.2.25	Concentrating of Fusion Protein Samples	34
2.2.26	Bradford-Assay.....	34
2.2.27	Immunization of Mice (carried out by Robert Rasmussen)	34
2.2.28	Neutralization Assay (carried out by Helena Ong)	35
2.2.29	Western-Blots	35
2.2.30	Fusion Protein ELISA	36
2.2.31	Statistical Analysis	36
3	Results.....	37
3.1	Preliminary Results.....	37
3.1.1	Serial Passage of SHIV-1157ip Rhesus Monkeys.....	37
3.1.2	Selection of HIV-C Env-Specific Mimotopes.....	39
3.1.3	Identification of a Conformational Mimotope of HIV-1 Clade C Env	43
3.2	Results.....	44
3.2.1	Molecular Cloning and Expression of Fusion Proteins.....	44
3.2.2	Reactivity Profile of Mimotopes in the Context of Fusion Proteins	49
3.2.3	Immunization Studies in Mice.....	57
3.2.4	Analysis of Vaccination-Induced Antibodies.....	60
3.2.4	Anti-Mimotope Antibodies	61
4	Discussion	67
4.1	Identification of Protective Epitopes	67
4.2	A12.2 – A Conformational Mimotope.....	67
4.3	Time-Dependent Variation in Mimotope Recognition and Cross-Recognition of Mimotopes	68
4.4	Immunization of Mice with Selected Mimotopes.....	69
4.5	Concluding Remarks.....	70
5	Summary	72
6	References	74

ABBREVIATIONS

GENERAL ABBREVIATIONS

(+)ssRNA	positively sensed, single-stranded ribonucleic acid
AIDS	Acquired Immunodeficiency Virus
CA	capsid proteins
CD 4	Cluster of Differentiation 4
CD 8	Cluster of Differentiation 8
CD4bs	CD4 binding site
cDNA	complementary deoxyribonucleic acid
CRF	circulating recombinant form
CTL	cytotoxic T lymphocyte
DC	dendritic cell
dsDNA	double-stranded deoxyribonucleic acid
ELISA	enzyme-linked immunosorbent assay
env	envelope
gag	group-specific antigen
gp120	glycoprotein 120
gp160	glycoprotein 160
gp41	glycoprotein 41
HAART	Highly Active Anti-Retroviral Therapy
HIV	Human Immunodeficiency Virus
HIV-1	Human Immunodeficiency Virus Type 1
HIV-2	Human Immunodeficiency Virus Type 2
HLA	human leukocyte antigen
HTLV	Human T-lymphotropic virus
IgG	immunoglobulin G
IgM	immunoglobulin M
IN	integrase
kB	kilobases

kDa	kilo Dalton
LTNP	long-term non-progressor
LTRs	long terminal repeats
MA	matrix protein
mAb	monoclonal antibody
MHC	major histocompatibility complex
MPER	Membrane-proximal external region
nAb	neutralizing antibody
NC	nucleocapsid
Nef	negative effector
NHP	non-human primates
NIH	National Institute of Health
nmAb	neutralizing monoclonal antibody
ORF	open reading frame
PBS	phosphate buffered saline
pol	polymerase
PR	protease
Rev	regulator of expression of virion proteins
RT	reverse transcriptase
SHIV	Simian Human Immunodeficiency Virus
SIV	Simian Immunodeficiency Virus
SU	surface subunit
Tat	transactivator of transcription
T _H lymphocytes	T helper lymphocytes
TM	transmembrane subunit
tRNA	transfer ribonucleic acid
Vif	viral infectivity factor
Vpr	viral protein R
Vpu	viral protein u
WHO	World Health Organization

AMINO ACIDS

A	Ala	Alanine
C	Cys	Cysteine
D	Asp	Aspartic acid
E	Glu	Glutamic acid
F	Phe	Phenylalanine
G	Gly	Glycine
H	His	Histidine
I	Ile	Isoleucine
K	Lys	Lysine
L	Leu	Leucine
M	Met	Methionine
N	Asn	Asparagine
P	Pro	Proline
Q	Gln	Glutamine
R	Arg	Arginine
S	Ser	Serine
T	Thr	Threonine
V	Val	Valine
W	Trp	Tryptophan
Y	Tyr	Tyrosine

1 INTRODUCTION

1.1 THE HIV-1 EPIDEMIC AND THE QUEST FOR A VACCINE

It is an undeniable fact that infection with Human Immunodeficiency Virus 1 (HIV-1) has reached pandemic proportions. According to recent estimates by the World Health Organization (WHO), approximately 33.3 million people are currently infected with HIV-1 and more than 37 million individuals have passed away since the onset of this pandemic (1). Nearly 90% of all new HIV-1 infections are reported in resource-poor countries of Africa, Asia and Latin America, where the social, economic and political consequences hit hardest (Figure 1.1) (1). The most-affected countries are located in Sub-Saharan Africa, where approximately 60% of all people infected with HIV-1 reside (1). Although Highly Active Anti-Retroviral Therapy (HAART) has transformed HIV-1 infection into a chronic disease, the complexity and costs of treatment limit its application in those countries. Intense efforts are therefore being made to develop a vaccine that is capable of preventing infection with HIV-1. Each year, nearly 1 billion dollars is spent globally on HIV-1 research and HIV-1 vaccine development (2). However, despite these intense efforts, a safe and effective vaccine against HIV-1 has not been developed to this point.

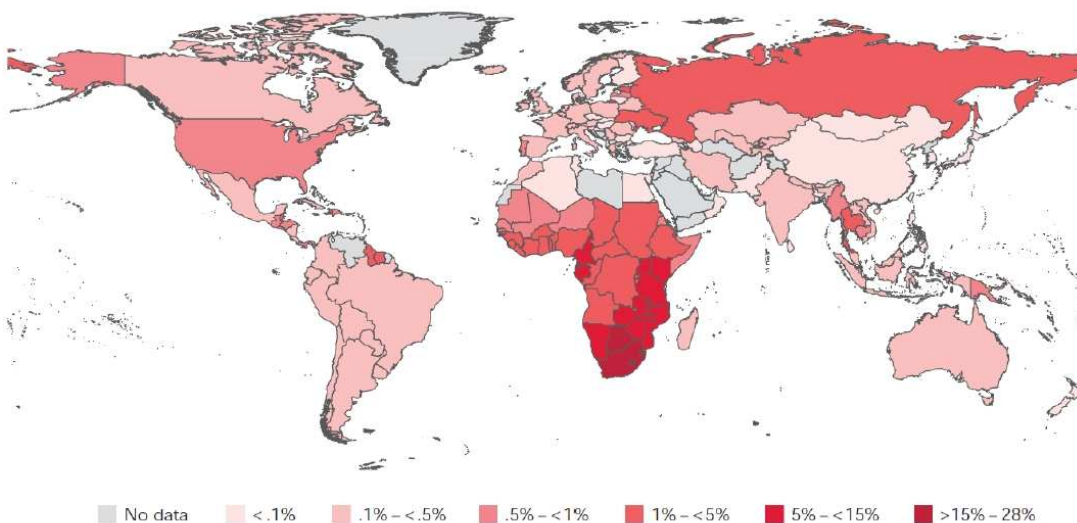


Figure 1.1 Global prevalence of HIV-1 in 2009 (1).

Most currently available antiviral vaccines induce a powerful neutralizing antibody (nAb) response that either prevents initial infection or assists in the eradication of the infectious agent before it can cause disease. Past phase III clinical trials with potential HIV-1 vaccines have been unsuccessful and rather disappointing (2, 3). These trials attempted to induce nAbs upon vaccination with the HIV-1 surface subunit (SU) glycoprotein 120 (gp120) as well as to generate cytotoxic T-lymphocyte responses (CTL) using recombinant adenoviral vectors (4). Based on the failure of the most recent STEP trial, some leaders in the field of HIV-1 vaccine research have questioned whether a vaccine can be realized based on the current knowledge (5).

1.2 THE HUMAN IMMUNODEFICIENCY VIRUS

1.2.1 THE DISCOVERY OF HIV

In 1983, the laboratory of Luc Montagnier at the Parisian Pasteur Institute in France proclaimed the isolation of a virus he believed to be the cause of a new rising pandemic, which had been named the Acquired Immunodeficiency Syndrome (AIDS) (6). This pandemic had initially been observed among homosexual men in New York and California who had suddenly begun to develop rare opportunistic infections and neoplasms. These findings had been accompanied by a rapid loss of Cluster of Differentiation 4 (CD4)-positive T lymphocytes in those patients. Shortly afterwards, the laboratory of Robert Gallo re-confirmed the previous findings (7). Both isolates bore a strong resemblance to the Human T-lymphotropic Virus (HTLV), but the high viral load and the rapid decline in CD4-positive T lymphocytes did not correlate with an HTLV infection. In 1984, the laboratory of Jay Levy reported the isolation of a virus from patients presenting with the very same symptoms (8). Comparative genomic analysis confirmed that those three isolates belonged to a novel group of retroviruses and in 1984, the International Committee on the Taxonomy of Viruses announced the official name for this new-found pathogen: Human Immunodeficiency Virus (9, 10).

In 1986, a related but less virulent and less infective retrovirus was isolated from AIDS patients in West-Africa. This isolate exhibited 40-60% sequence homology to HIV-1 and was hence named Human Immunodeficiency Virus Type 2 (HIV-2) (11). Until today, it remains confined to this area.

1.2.2 CLASSIFICATION AND SEQUENCE DIVERSITY

Both human immunodeficiency virus (HIV) species belong to the lentiviral genus of the subfamily of *Orthoretrovirinae* (12). Retroviruses such as HIV are defined as enveloped viruses containing two copies of a positively sensed, single-stranded ribonucleic acid [(+)ssRNA] genome, which is transcribed into double-stranded deoxyribonucleic acid (dsDNA) upon infection of a target cell by the viral enzyme reverse transcriptase (RT; p64) (13). Following permanent integration into the host genome by the enzyme integrase (IN; p32), the virus replicates by using the host's biosynthetic machinery to produce new virions (13). All retroviral genomes contain the genes *gag* (group-specific antigen), *pol* (polymerase) and *env* (envelope), which are flanked by long terminal repeats (LTRs) (13). In addition, HIV contains six other genes. Lentiviruses are retroviruses characterized by a long incubation period and a protracted course of disease (13).

Among the properties of HIV-1 that complicate vaccine development its enormous sequence diversity is most striking. Its remarkable capacity for mutation and adaption is due to an error-prone RT, a high chance of recombination and a very rapid turnover *in vivo* (14). Based on comparative genomic sequence analysis, HIV-1 strains are subdivided into four groups: M (main/major), O (outlier), N (non-M/non-O, new) and P, which also vary in their geographical distribution (14). Group M represents the most common group responsible for the vast majority of infections and is further subdivided into eleven distinct clades or subtypes – based on envelope sequences – which differ in geographical prevalence (A-H, J and K) (1). Clade C (56%) has established rapidly growing epidemics in the most populated countries of Sub-Saharan Africa, Asia, especially India and China, and Latin American countries, such as Brazil, whereas clade B (12%) remains confined to Europe and North America (14). In addition, many circulating recombinant forms (CRFs) have arisen due to simultaneous infections of patients with different clades (15, 16).

1.2.3 HIV-1 VIRION STRUCTURE

HIV-1 virions are round particles approximately 100 nm in diameter with viral spikes on the surface (Figure 1.2). These viral spikes represent the heterodimeric trimer complex of the heavily glycosylated surface subunit gp120 and the transmembrane

subunit (TM) glycoprotein 41 (gp41), which remain associated through weak non-covalent bonds (13). Both envelope glycoproteins are derived from the glycoprotein 160 (gp160) precursor molecule, which is cleaved by host cell proteases (17). The viral envelope spike is embedded in a phospholipid bilayer, which originates from the host cell membrane and may thus also contain several host membrane proteins, e.g. major histocompatibility complex proteins (MHC) (17). Along with the linked matrix proteins (MA; p17), this membrane composes the outer core of the virion.

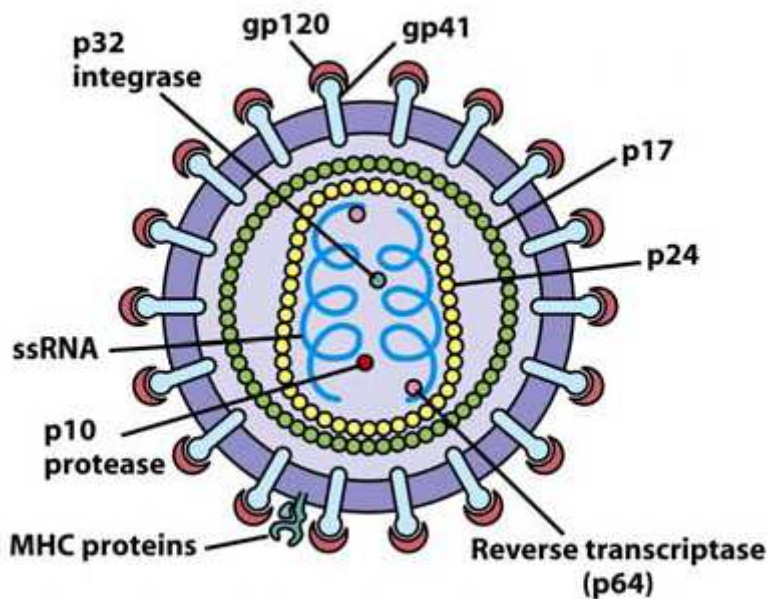


Figure 1.2 HIV-1 Virion Structure (18).

The conical inner core of the virion (viral capsid) is constituted by capsid proteins (CA; p24) and encloses the viral genome (13). The HIV-1 genome consists of two 9.7 kilobases (kB) (+)ssRNA molecules, which are stabilized by nucleocapsid proteins (NC; p7) (13). The viral enzyme RT is bound to these two (+)ssRNA molecules. In addition, the capsid contains the viral enzymes IN and protease (PR; p10), two copies of the transfer RNA lysine 3 ($tRNA^{Lys3}$) for initiation of reverse transcription, and the additional proteins Nef (negative effector) and Vif (viral infectivity factor). The three remaining additional proteins Rev (regulator of expression of virion proteins), Tat (transactivator of transcription), and Vpu (viral protein u) are not part of the viral particle and are synthesized upon infection of the host cell.

1.2.4 THE HIV-1 GENOME AND PROTEOME

The HIV-1 genome is approximately 9.7 kB in size and contains open reading frames (ORFs) for 16 different proteins, which are synthesized from at least ten transcripts (19, 20). The integrated genome is flanked by long terminal repeats (LTRs), which are composed of repetitive enhancer and promoter sequences. These regulatory elements are required for reverse transcription of the viral genome, integration of the viral dsDNA into the host genome, and regulation of viral gene expression (19). In addition to the three classic retroviral genes *gag*, *pol*, and *env*, the HIV-1 genome contains six additional genes, which are important for the replication of the virus: genes encoding for the two regulatory proteins Rev and Tat and four genes encoding for the accessory proteins Nef, Vpr, Vpu, and Vif (19).

HIV-1 *gag* encodes for all structural proteins that constitute the viral core and matrix and is first translated as Gag precursor polyprotein (pr55), which is subsequently cleaved by the viral PR (19). The genetic information for the three viral enzymes PR, RT, and IN is encoded by *pol*, which is translated as a gag-pol precursor protein (pr160) that is cleaved into the above named enzymes by PR as well (19). RT is responsible for transcribing the viral (+)ssRNA genome into dsDNA, which is subsequently integrated into the host cell DNA by the enzyme IN. The third characteristic retroviral gene *env* encodes for the Env polyprotein gp160 that undergoes cellular protease cleavage into the surface subunit gp120 and the transmembrane subunit gp41.

The regulatory HIV-1 proteins Rev and Tat are essential for HIV-1 replication (19): Rev mediates nuclear export of gag-pol, vif, vpr, and vpu-env transcripts to the cytoplasm and induces the transition between the early and late phases of viral gene expression, whereas Tat functions as the main transcriptional regulator of the LTR. In contrast to Rev and Tat, the remaining four accessory proteins Nef, Vif, Vpr, and Vpu are not necessary for viral replication *in vitro*, but play a significant role in viral replication and disease progression *in vivo* (19, 20).

1.2.5 CELLULAR TROPISM AND HIV-1 REPLICATION

HIV-1 enters the body through the exchange of bodily fluids and is capable of infecting a panel of immune cells, in particular T helper (T_H) lymphocytes, macrophages, microglial cells and dendritic cells (DCs) (13). This cellular tropism is determined by

the viral and host cell receptors: All HIV-1 strains use CD4 as the exclusive primary receptor, whereas co-receptor selectivity depends on the viral strain and the target cell (19). After CD4 binding, the trimeric surface subunit gp120 undergoes a conformational change, enabling binding to a co-receptor of the chemokine receptor family (Figure 1.3) (17). HIV-1 may either bind to the CC chemokine receptor CCR5, which is mainly found on DCs, macrophages and T lymphocytes, or the CXC chemokine receptor CXCR4, which is exclusively expressed on T lymphocytes (21). Co-receptor binding then triggers a conformational change in the trimeric transmembrane subunit gp41, which induces exposure of the fusion peptide and subsequent membrane fusion. Depending on their co-receptor selectivity, HIV-1 strains are subdivided into the group of R5 strains (“macrophage-tropic” or M-tropic) and the group of X4 strains (“T cell-tropic” or T-tropic) (21, 22). However, certain strains are capable of using both co-receptors and are thus called X4R5 strains (dualtropic).

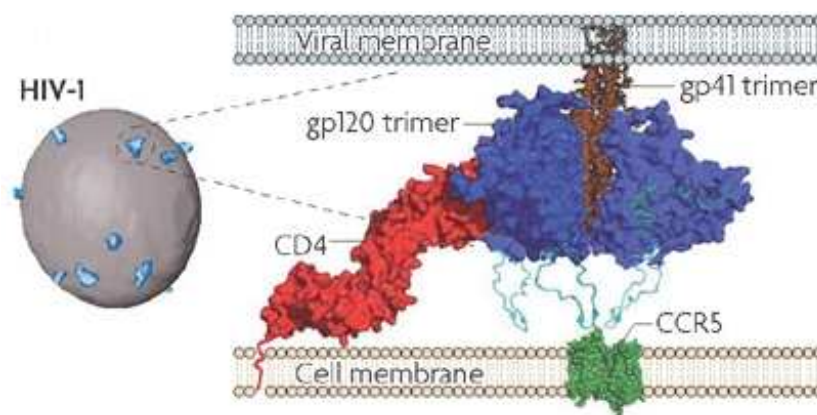


Figure 1.3 Interaction of HIV-1 Env with its primary receptor CD4 and its secondary receptor CCR5 (23). *Reproduction occurs with permission.* In order to initiate infection, the trimeric viral envelope gp120 binds its primary receptor CD4. The resulting conformational changes in the gp120-CD4 complex allow binding to the secondary receptor CCR5, which activates the trimeric viral envelope gp41 to initiate membrane fusion.

During the course of infection, co-receptor selectivity changes as the patient progresses towards AIDS: Initially, R5 strains dominate, whereas X4 strains tend to arise towards the end of infection. This switch in co-receptor selectivity reflects the pathologic processes during each stage of HIV-1 infection: Upon infection of the patient, R5 viruses predominate, seemingly to establish a latent reservoir in dendritic cells and macrophages, which can pass the virus to T_H lymphocytes. With time, X4 viruses

emerge to infect T_H lymphocytes and thus accelerate the progression towards AIDS (24). Regardless of differences among the various HIV-1 clades, 90% of primary infections occur via mucosal exposure and are almost exclusively initiated by R5 viruses [reviewed in (25)]. Clade C viruses, the predominant HIV-1 subtype, are almost entirely confined to CCR5 as co-receptor at all stages of infection, including AIDS.

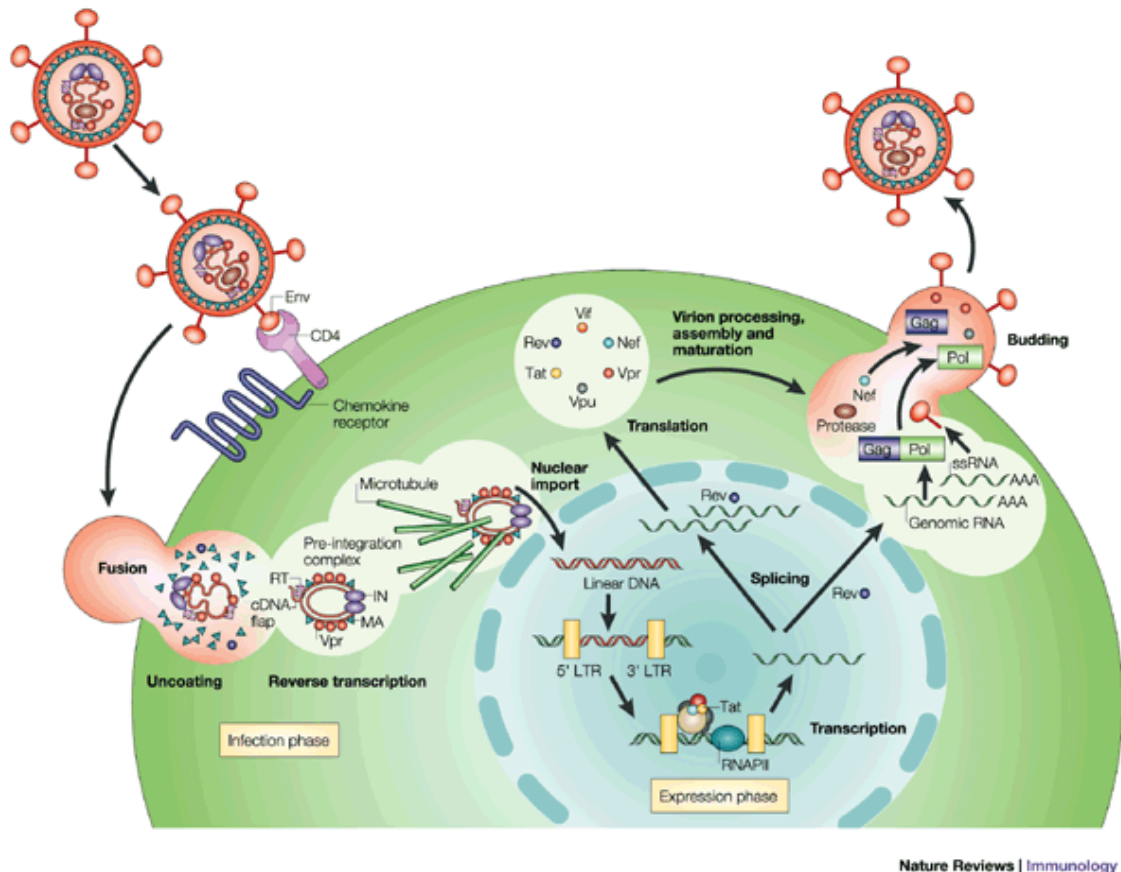


Figure 1.4 The HIV-1 Life Cycle (19). *Reproduction occurs with permission.*

Once internalized, the viral capsid is uncoated and the (+)ssRNA genome is reverse transcribed to a double-stranded complementary DNA (cDNA). Because RT lacks a proof-reading function, the process of reverse transcription is highly error-prone and results in a multitude of mutations. This contributes to the immense genetic variety of progeny viruses (26). The viral cDNA is routed to nucleopores – apparently along the microtubule network – as part of the pre-integration complex of IN, MA, RT, Vpr and host proteins that is docked at the nuclear envelope. This process does not depend on cell division and nuclear membrane disintegration. The viral cDNA then crosses the

nucleopore and is integrated into the genome of the target cell, most commonly into active euchromatin. This LTR-flanked provirus may remain latent for a long time.

The 5' LTR functions as the promoter, whereas the 3' LTR acts as the polyadenylation and termination site. The level of proviral transcription is increased by cellular activation, which is augmented by Tat. Rev mediates the nuclear export of singly spliced and unspliced genomic transcripts to the cytoplasm where HIV-1 structural and enzymatic proteins are synthesized and transported to the plasma membrane to localize in lipid rafts. Nef can support the process of viral assembly. During the last step of the HIV-1 life cycle, HIV-1 virions are assembled and the processed envelope glycoproteins gp120 and gp41 are transported to the plasma membrane into which they are anchored. Virion maturation may occur either during the budding process or afterwards. During this last step of the HIV-1 life cycle, protein cleavage by PR takes place and the structural proteins assemble to give rise to a fully matured virion, which can now infect another cell.

1.3 HIV-1 INFECTION AND AIDS

1.3.1 ROUTES OF HIV-1 TRANSMISSION

HIV-1 is transmitted via the exchange of bodily fluids and approximately 90% of all transmissions occur via sexual intercourse. Therefore, the genital or rectal mucosa is the primary site of transmission, regardless of differences among the HIV-1 clades (25). It is known that mucosal transmissions are almost exclusively initiated by R5 viruses (25), however, the mechanisms of mucosal transmission remain poorly understood (27). Other common possibilities of HIV-1 transmission are: transfusion with contaminated blood or blood products; needle sharing as part of intravenous drug abuse; and mother-to-child transmission during childbirth or via breast-feeding. The likelihood of HIV-1 infection depends on virulence of the strain, viral particle concentration and host susceptibility (28, 29).

1.3.2 THE COURSE OF HIV-1 INFECTION

HIV-1 patients undergo a three-stage transition towards AIDS with significant interindividual variability (30): the acute stage following infection, the chronic stage of

clinical latency, during which patients remain largely asymptomatic, and the final stage of clinical manifestation that results in AIDS (Figure 1.5). During the progression towards AIDS, viral diversity increases.

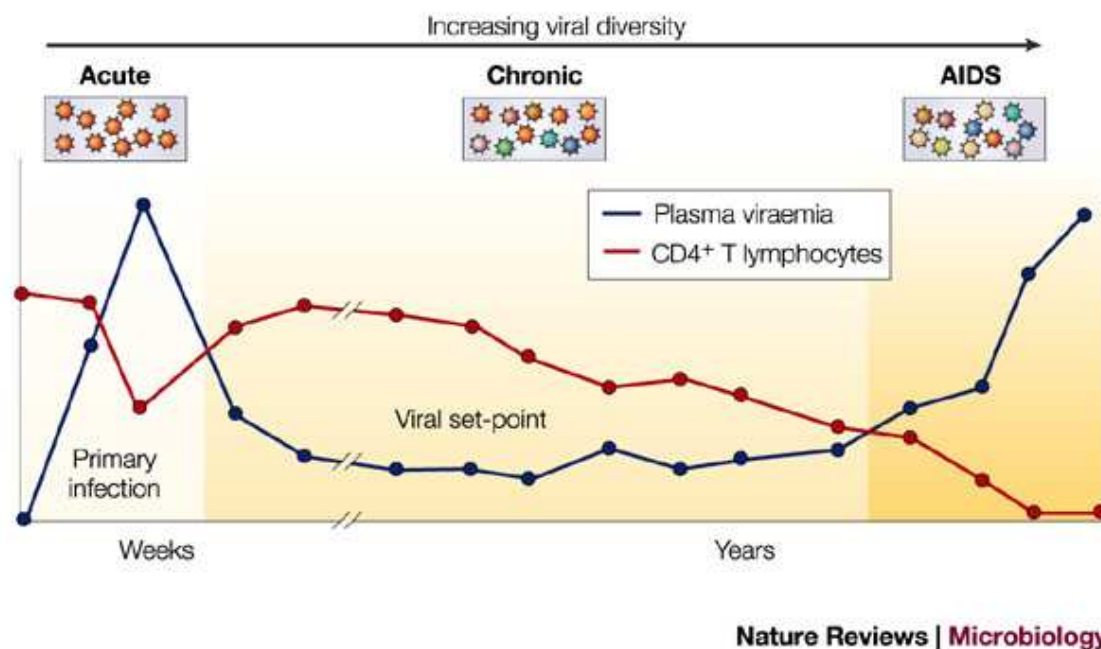


Figure 1.5 The natural course of HIV-1 infection (30). *Reproduction occurs with permission.*

The acute stage of HIV-1 infection may present as the acute retroviral syndrome, which resembles infectious mononucleosis and may last twelve to twenty weeks. During this initial stage, the plasma viral load peaks and CD4-positive T lymphocyte numbers decrease. After the first months of infection, plasma viral load stabilizes at an individual level (viral set-point) and the number of CD4-positive T lymphocytes normalizes. This subsequent chronic stage of infection is characterized by continuous viral replication at high levels. However, the patient remains asymptomatic despite a constant decrease in CD4-positive T lymphocyte numbers. During this stage, adaptive immune responses appear to control viral replication and thereby select for escape mutants, thus increasing viral diversity (27, 30). After an average time span of ten years, the clinical hallmarks of AIDS manifest and patients present with opportunistic infections and HIV-1-associated malignancies. The risk of opportunistic infections increases significantly when CD4-positive T lymphocyte numbers fall below 200 per mm^3 , which goes along with the emergence of X4-strains.

However, a small patient collective does not exhibit any signs of disease progression for more than ten years without any antiviral therapy. Several mechanisms are discussed for this long-term non-progressor (LTNP) status, such as:

- a lower viral set point (31);
- an increased diversity of the *env* region (32);
- mutations in the V3 loop of gp120 that result in an impaired co-receptor switch;
- increased secretion of natural CCR5 receptor ligands (32);
- difference in human leukocyte antigen (HLA) profiles (33);
- non-functional co-receptor proteins, such as the CCR5 Δ 32bp deletion (34).

However, it has also been postulated that these LTNPs have developed an unusually effective humoral immune response against HIV-1. Therefore, a promising approach to identify HIV-1 vaccine candidates is to dissect the humoral immune response against the virus in such patients to identify the protective epitopes and induce the appropriate antibodies (35).

1.4 THE HIV-1 ENVELOPE GLYCOPROTEIN

1.4.1 SYNTHESIS AND ORGANIZATION ON THE VIRAL SURFACE

The antibody response to HIV-1 *in vivo* is directed against several viral proteins. However, essentially all nAbs are directed against the viral envelope glycoprotein, particularly the surface subunit gp120 (17, 36). The viral envelope glycoprotein is formed as a non-covalently linked, trimeric complex between the surface subunit gp120 and the transmembrane subunit gp41 (17). During the viral life cycle, gp120 is responsible for attachment of the virion to the target cell, whereas gp41 induces virus and host cell membrane fusion.

Upon HIV-1 infection, the viral envelope glycoprotein is first synthesized as a single polypeptide precursor that subsequently undergoes oligomerization and extensive glycosylation in the Golgi apparatus (17). The glycosylation process is essential for proper folding and conformational stability of the protein (37). The resulting glycoprotein has acquired a molecular mass of approximately 160 kilo Dalton (kDa) and is subsequently cleaved in the trans-Golgi network into gp120 and gp41 (17). The glycoprotein complexes remain associated through weak noncovalent bonds and are

then expressed on the surface of infected cells. During the process of budding, the glycoprotein complexes are incorporated into the viral envelope and displayed on its surface as viral spikes (17). Although heterodimeric trimer complexes of gp120 and gp41 represent the functional envelope spike (38), it has been suggested that other nonfunctional envelope species may also be present on the surface of HIV-1, such as monomers, dimers, or tetramers (39). These envelope species may divert the humoral immune response from the intact trimer.

On the virion surface, the HIV-1 envelope glycoprotein shields its vulnerable conserved regions (40). Therefore, conserved epitopes rarely induce antibodies (low immunogenicity) and induced antibodies are rarely able of binding to conserved epitopes (low antigenicity). NAbs against conserved epitopes are a particular threat to HIV-1, as mutational escape is more difficult than for variable epitopes.

1.4.2 TOPOLOGY OF GP120

Based on comparative sequence analysis, gp120 is divided into five conserved (C1-C5) and five variable (V1-V5) segments; the latter are highly variable in sequence and structure and thus allow the virus to escape immune responses (39, 41-44). Different regions of gp120 are responsible for interaction with CD4 and co-receptors of the chemokine family. These interactions induce a series of conformational changes in gp120, which subsequently also trigger conformational changes in gp41. Gp41 then forms the coiled-coil form and exposes the fusion peptide, which triggers fusion of the host cell and viral membrane.

As determined by various crystal structures, the gp120 core is heart-shaped and is divided into three areas: the inner domain, the outer domain, and the bridging sheet (Figure 1.6). The C1 and C5 regions are the main components of the inner domain, which is largely devoid of glycans and generates the major contact interface with gp41. The inner and outer domains are linked by the bridging sheet, which is composed of four anti-parallel β -strands from the V1/V2 stem and the C4 regions. The bridging sheet engages in co-receptor binding and triggers subsequent conformational changes in gp120 and gp41 (43). Because it forms or is exposed after CD4 receptor binding, it is also referred to as the “CD4-induced epitope” (44). The outer domain constitutes the

surface of gp120 and is largely covered by glycans, which reduces the immunogenicity of the viral particle (39).

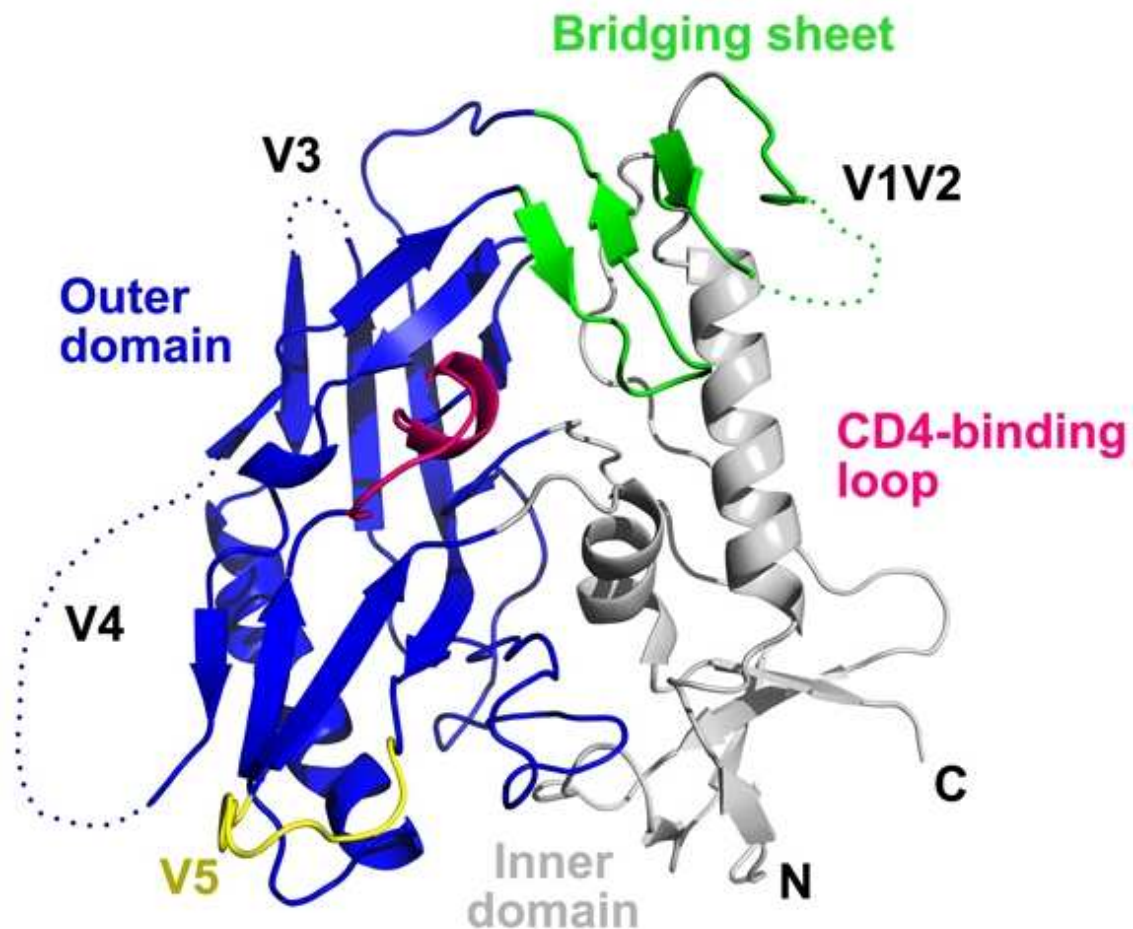


Figure 1.6 Ribbon diagram of a clade C core gp120 structure (CAP210) (45). *Reproduction occurs with permission.* This ribbon diagram shows the three main domains of gp120: the outer domain (blue), the inner domain (grey) and the bridging sheet (green). The five variable loops and the CD4-binding loop (pink) are indicated.

At the beginning of the interaction between gp120 and CD4, certain residues on the CD4 receptor, mostly phenylalanine 43 (Phe⁴³) and arginine 59 (Arg⁵⁹), make contact with a cavity formed at the interface of the outer and inner domains and the bridging sheet, which has been named the *Phe43 cavity* or the CD4-binding site (CD4bs) (43). After binding the CD4 receptor, gp120 undergoes a conformational shift (V1/V2 and V3 shifts), which unmasks the highly conserved co-receptor binding site. Amino acids important for the interaction with the co-receptor have been mapped to the bridging sheet and near the V3 stem (39). Due to the short-term transitional exposure of the co-

receptor binding site after CD4-binding, antibodies directed against this area exhibit poor neutralization ability *in vitro* without soluble CD4.

1.4.3 TOPOLOGY OF GP41

The transmembrane subunit of the viral envelope glycoprotein gp41 is located in the viral phospholipid bilayer and plays a pivotal role in the process of virus and host cell membrane fusion. The protein is more conserved than gp120 and is divided into three major domains: the extracellular region (ectodomain), the transmembrane domain, and the cytoplasmic tail (Figure 1.7). The ectodomain is mainly involved in the process of membrane fusion and contains an N-terminal hydrophobic region, which acts as a fusion peptide, a polar region, two α -helix repeat regions (N-terminal heptad repeat and C-terminal heptad repeat), a disulfide-bridged hydrophilic loop connecting the two heptad repeats and containing the immunodominant KLIC motif, and a tryptophan (Trp)-rich region (membrane-proximal external region, MPER) (44, 46).

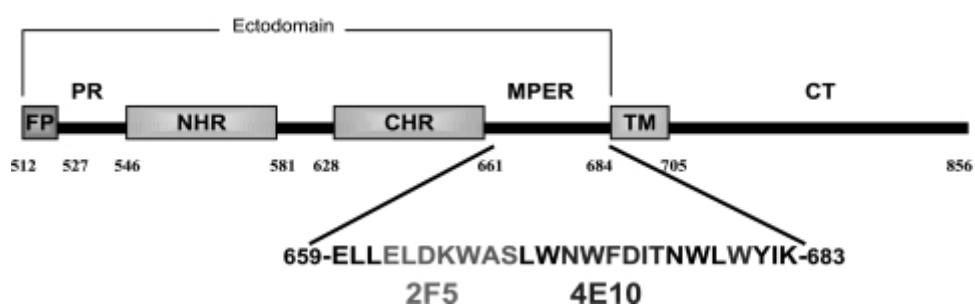


Figure 1.7 Schematic illustration of gp41 domains and the epitopes of the human mAbs 2F5 and 4E10 (46). *Reproduction occurs with permission. See text for details.*

1.4.4 VIRAL DEFENSE MECHANISMS FOR ANTIBODY EVASION

Several structures of HIV-1 and Simian Immunodeficiency Virus (SIV) envelope glycoproteins have illustrated how conserved regions are shielded from antibody recognition. The variable regions of gp120 play a fundamental role by diverting the immune system and shielding conserved neutralization-sensitive elements (17, 47), such as the co-receptor binding site (48). The envelope glycoprotein also frequently changes its primary structure in response to selective pressure and thus exhibits high variability. Furthermore, the trimeric structure shields important domains of the protein core and thereby protects them from antibody-mediated neutralization (49). In addition, the highly neutralization-sensitive co-receptor binding site is only transiently uncovered by

conformational Env re-orientation after CD4 receptor binding and immediately masked during virus and host cell membrane fusion. Moreover, heavy glycosylation on the outside of gp120 protects the protein core from antibody recognition [reviewed in (39, 50)].

1.5 HIV-1/AIDS VACCINE DEVELOPMENT

1.5.1 PAST HIV-1 VACCINE TRIALS

To date, vaccination protects from many human viral infections that may otherwise cause severe disease, such as hepatitis caused by the hepatitis B virus. All of these clinically approved vaccines are based upon the induction of a humoral immune response. This includes the subunit vaccine against hepatitis B (51), which inspired the first attempt to develop a vaccine against HIV-1. This first vaccine was based upon the surface subunit gp120 and successfully passed Phase I and II clinical trials. The vaccine was approved as safe and induced antibodies that neutralized laboratory-adapted strains of HIV-1 but failed to neutralize primary isolates (52-54). Consequently, two subsequent Phase III clinical trials in the US and in Thailand did not show efficacy (54, 55).

Because of the observed difficulties in inducing nAbs against primary HIV-1 isolates by vaccination, the pendulum of opinion swung to the other extreme: the induction of CTL responses only (44). During the following years, the interest in pursuing nAb-response-based vaccine strategies waned but was rekindled after several groups proved that infection could be prevented by means of passive immunization in primate models. These studies were based upon the challenge of rhesus monkeys with Simian Human Immunodeficiency Viruses (SHIVs) after administration of anti-HIV-1 nAbs [reviewed in (56, 57)]. These experiments showed that nAbs alone are protective and even provide complete protection when administered as post-exposure immunoprophylaxis after mucosal challenge.

The most recently tested vaccine, a collaboration between Merck and the National Institutes of Health (NIH), had only been the second HIV vaccine candidate to complete efficacy testing in humans. Unfortunately, the outcome was disastrous: The vaccine did not only fail to prevent infection, but it also could not contain viral replication in those

who became infected and even increased susceptibility to infection in patients with preexisting antibodies to the adenovirus vector used to deliver the HIV vaccine antigens (5).

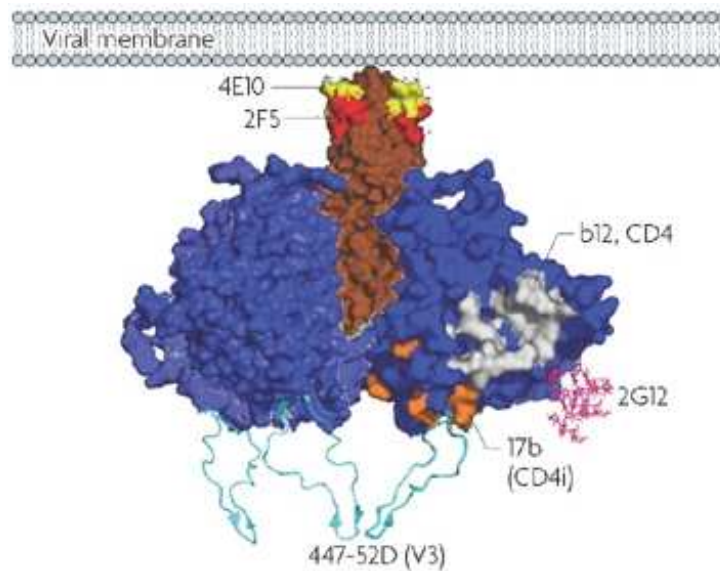
1.5.2 PROTECTIVE EPITOPES OF HIV-1 ENV

Antibodies may prevent or modulate viral infection (58, 59) by reducing the size of the infecting inoculum and by neutralizing or eliminating virions during the initial rounds of replication, so that CTLs can expand and eliminate infected cells later in the course. Passive immunization studies in primates that had been challenged with SHIVs have shown that several neutralizing monoclonal antibodies (nmAbs) are able to completely prevent infection [(60-68), reviewed in (69)]. The epitopes recognized by these antibodies can therefore be considered as protective epitopes. The nmAbs used in these passive immunization experiments also neutralized a number of primary strains of HIV-1 of different clades *in vitro*, particularly when used in combination (70-73), which illustrates their broad reactivity. The following nmAbs had been involved in passive immunization studies and provided complete protection from infection (Figure 1.8): 2G12, which binds to mannose residues on gp120 (74); b12, an antibody against the CD4bs (75, 76); as well as 4E10 and 2F5, which bind to neighboring epitopes in the MPER of gp41 (77). Unfortunately, three out of four human nmAbs seem to have arisen as part of an autoimmune response (78). Both 4E10 and 2F5 cross-react with the self-antigen cardiolipin, an important component of the inner mitochondrial membrane. This observation might explain the inability to induce 4E10/2F5-like nAbs (79, 80), since repetitive boosting may eliminate autoreactive B lymphocytes.

The protective epitopes of these antibodies may also be poorly immunogenic because of their location in recessed regions of gp120 (CD4bs) or their transient accessibility (the nmAbs targeting the extracellular domain of gp41). Furthermore, b12 contains an unusually long, finger-like structure, which might be difficult to induce with current immunization strategies (81).

Other important but less potent neutralizing monoclonal antibodies (nmAbs) are 17b and 447-52D (44). 17b is directed against the co-receptor binding site, but only antigen-binding fragments of this monoclonal antibody (mAb) are neutralizing because of the close proximity to the viral membrane and the resulting steric interference. Intact

immunoglobulin G (IgG) molecules specific for the co-receptor binding site do not neutralize primary isolates (23). The V3 loop of gp120 targeted by 447-52D is also highly immunogenic, but antibody specificity broadens only after extended antigen stimulation.



Nature Reviews | Microbiology

Figure 1.8 Modeling of the HIV-1 envelope spike showing epitopes of broadly nmAbs (23). *Reproduction occurs with permission.* The HIV-1 trimeric envelope glycoprotein is illustrated with gp120 and gp41 shown in blue and brown, respectively. The epitopes of the nmAbs are modeled on the structure: 4E10 (yellow), 2F5 (red), 2G12 (pink), b12 (grey), 17b (orange) and 447-52D (light blue).

1.5.3 THE V3 LOOP AS A TARGET FOR HIV-1 VACCINE DESIGN

Similar to the V2 loop, the V3 loop is highly variable in its primary structure. However, it differs from the V2 loop in its structural characteristics and function (44). Due to its highly variable primary structure, many V3-specific antibodies are isolate-specific and only induced early after infection or after brief immunization protocols (82-85). Although some V3-specific mAbs from HIV-1 infected individuals show crossreactivity, most exhibit poor neutralization activity for primary isolates (86-88). Of note, these antibodies had been selected with linear V3 peptides.

However, broadly nAbs against the V3 loop have also been isolated. These polyclonal and monoclonal V3-specific antibodies are conformation sensitive rather than specific

for linear epitopes in the V3 loop (89). The most broadly reactive of these nmAbs neutralize many clade B HIV-1 primary isolates (90-93) and also clade A and F viruses, which, by definition, must have shared or crossreactive epitopes (89). Such antibodies (similar to 447/52-D, 19b and 2182) seem to arise later in the course of infection as a result of somatic hypermutation (94). Because of the need for prolonged antigenic stimulation, such antibodies may be difficult to induce with a vaccine (44). To this point, clinical vaccine trials have not addressed whether prolonged immunization regimens induce more broadly reactive nAbs, in general, and more highly crossreactive V3-specific antibodies, in particular (44).

Structural and functional characteristics of the V3 loop offer an explanation for the crossreactivity of such V3-specific antibodies against conformational epitopes. Despite its name, the V3 loop is considered a semi-conserved region with many constant features, such as a fixed size of approximately 30-35 amino acids, a conserved type II turn at its tip, a disulphide bond at its base, and a net positive charge (48). These conserved structural features reflect its fundamental role in co-receptor binding and selectivity (95, 96). The conserved nature of the V3 loop is further explained by its structural homology to natural ligands of the HIV-1 co-receptors [reviewed in (44)]. These findings illustrate the essential function of the V3 loop in virus infectivity and in determining co-receptor selectivity and thus explain its conserved nature and the high crossreactivity of antibodies directed against conserved V3 motifs (44).

The past assumption that V3-specific antibodies are isolate specific and unable to neutralize primary isolates has also been questioned by the observation that such antibodies are produced early after infection or immunization (82-84) and that broadly reactive V3-specific nAbs are characteristic of a more mature immune response (89, 91). Furthermore, the assumption that V3-specific antibodies are incapable of neutralizing primary isolates is challenged by the fact that HIV-1-positive sera had only been depleted with linear V3 peptides and thus failed to remove antibodies directed against conformational epitopes of the V3 loop (97, 98). Moreover, it has been shown that epitopes in the V3 loop are not hidden but are at least partially exposed on the surface of R5 virions and R5-virus-infected cells (92, 93, 99-102), and that V3-specific mAbs can neutralize both R5 and X4 viruses (89, 90, 92, 93, 103). In summary, the V3 loop may thus be a promising target for HIV-1 vaccine development.

1.5.4 NON-HUMAN PRIMATE MODELS OF HIV-1/AIDS

There is strong evidence that HIV has evolved from SIV, a related retrovirus that appears to have been transmitted from monkeys to humans at several independent occasions. HIV-1 and SIVcpz are believed to have evolved from a common ancestor in chimpanzees (104, 105), whereas HIV-2 is related to SIVsm, a strain of SIV found in sooty mangabeys (106). After the discovery that SIV causes AIDS-like disease in Asian macaques, non-human primates (NHP) have become very popular in HIV-1/AIDS vaccine research [reviewed in (107)]. In order to mimic human HIV-1/AIDS pathogenesis, hybrid SIV strains containing HIV-1 genes (*vpu*, *tat*, *rev*, *env*) have been developed. These SHIV strains combine several advantages in comparison to natural SIV strains [reviewed in (69)], such as the evaluation of vaccines based on HIV-1 envelope glycoproteins and the isolation of corresponding anti-HIV-1 antibodies.

In order to simulate human HIV-1 infection and AIDS in NHP as closely as possible, SHIV challenge strains must mimic human HIV-1 transmission as closely as possible and thus fulfill several criteria [reviewed in (69)]. SHIV strains have to exhibit mucosal transmission, since 90% of all newly acquired HIV-1 infections result from mucosal exposure through sexual contact or via mother-to-child transmission. Furthermore, SHIV strains need to be R5 tropic, since almost all mucosally transmissible HIV-1 strains exhibit R5 tropism (108, 109). In addition, SHIV strains need to cause gradual rather than acute pathogenicity and need to be susceptible to antibody-mediated neutralization.

Such a SHIV strain has been developed by the Ruprecht laboratory: SHIV-1157ip is a highly replication competent, mucosally transmissible R5 clade C SHIV strain, equipped with the viral envelope glycoprotein of a recently transmitted HIV isolate from a 6-month-old Zambian infant (HIV1157i) that has been passaged through several rhesus monkeys for host adaptation (110).

1.5.5 EPITOPE IDENTIFICATION AND THE PHAGE DISPLAY APPROACH

In order to identify promising HIV-1 vaccine candidates, immunogenic regions of HIV-1 Env must be identified and analyzed to show whether they are able to induce protective antibodies in the host (44). X-ray crystallography studies have revealed important structural features of the HIV-1 envelope protein and its sites of interaction

with cellular receptors. Unfortunately, conserved parts are masked and thus inaccessible to the immune system (39, 111). However, these findings have not been translated into a potent vaccine so far.

Valuable sources to study natural immune responses against HIV-1 Env are sera with high-titer, cross-clade nAbs, such as those obtained from LTNPs (35). The analysis of such effective humoral immune responses might help unmask structures on the HIV-1 envelope glycoprotein that are conserved across many clades. The Ruprecht laboratory has identified a cohort of rhesus macaques infected with SHIV-1157ip, a chimera that encodes *env* of a recently transmitted HIV-1 clade C strain, or the related SHIV-1157ipd3N4 (110) that developed high-titer nAb responses against homologous SHIV clade C as well as heterologous primary strains of HIV-1 of different clades. The Ruprecht laboratory has used the phage display technology to identify the HIV-1 clade C Env structures recognized by such broadly reactive sera.

Phage display (112) is a commonly applied technique to analyze humoral immune responses (35, 113-118), to map antibody epitopes (100, 119-121) or to identify protein interaction sites in general (122). However, so far, the identification of conformational epitopes was limited because of the difficulties in projecting the linear mimotope sequence onto a protein structure. Fortunately, computer programs have been developed (123-128) that allow three-dimensional (3D) analysis. These programs project the linear peptide sequence onto the 3D surface structure of target proteins by using published protein structure files. The computer program 3DEX (128), which is used by the Ruprecht laboratory, maps conformational mimotopes in 3D surface structures of target proteins by using an algorithm that takes into account the physicochemical neighborhood of individual amino acids. Thereby, a discontinuous epitope is localized within the 3D protein structure by searching for a 3D fit with partial amino acid strings of a given mimotope in a pre-set distance on the surface of the protein. This algorithm is repeated for each string of amino acids until the full peptide sequence is analyzed.

1.6 AIM OF THIS WORK

The Ruprecht laboratory has dissected the humoral immune response of rhesus monkeys with broadly reactive nAb responses by applying the phage display technology in conjunction with 3DEX computational analysis (128). Several groups of linear and conformational mimotopes of various regions of the HIV-1 clade C envelope glycoprotein have been identified. As part of this work, these mimotopes will be (1) evaluated for cross-reactivity with other sera from rhesus monkeys of the Top-Ten Cohort and also (2) analyzed for immunogenicity in a new DNA prime/phage boost immunization strategy. This immunization strategy has been designed to focus the humoral immune response on the regions represented by these mimotopes. This “immunofocusing” approach may yield new epitopes, which are capable of inducing the very same broadly reactive nAbs. These epitopes might then be incorporated into potential HIV-1 vaccine candidates.

2 MATERIALS AND METHODS

2.1 MATERIALS

2.1.1 ANTIBODIES

- Donkey anti-rabbit HRP conjugate (The Jackson Laboratory)
- Goat anti-human HRP conjugate (The Jackson Laboratory)
- Goat anti-human HRP conjugate (The Jackson Laboratory)
- Mouse anti-M13 HRP conjugate (Amersham GE)
- Rabbit anti-his-Tag mAb (kindly provided by MoBiTec)
- Rabbit anti-monkey HRP conjugate (Sigma-Aldrich)

2.1.2 BACTERIAL STRAINS

- BL21(DE3) (Novagen)
- *E. coli* K12 ER2738 (New England BioLabs Inc.)
- One Shot MAX Efficiency DH5 α -T1 Competent Cells (Invitrogen)
- XL1-Blue Competent Cells (Stratagene)

2.1.3 BUFFERS AND SOLUTIONS

- 10x FastDigest Buffer (Fermentas)
- 10x Phosphate buffered saline (PBS) (GIBCO)
- 10x Tris/glycine buffer (Bio-Rad Laboratories, Inc.): Added 20% methanol.
- 10x Tris/glycine/SDS buffer (Bio-Rad Laboratories, Inc.)
- 1x Phosphate buffered saline (PBS)
- 1x Phosphate buffered saline (PBS) (GIBCO)
- Binding/washing buffer:
 - 50 mM sodium phosphate
 - 300 mM sodium chloride
 - 5 mM imidazole

Adjusted to pH 8.0 and autoclaved.

- Carbonate-Bicarbonate Buffer (Sigma-Aldrich)
- Coomassie staining solution:
 - 50% methanol
 - 10% acetic acid
 - 0.05% Brilliant Blue R-250

Dissolved dye in methanol before adding acetic acid and water.

- Elution buffer:
 - 50 mM sodium phosphate
 - 300 mM sodium chloride
 - 100 mM imidazole

Adjusted to pH 8.0 and autoclaved.

- Laemmli Sample Buffer (Bio-Rad Laboratories, Inc.):
Added 1/20 β -mercaptoethanol.

- PBS-CT:
 - 0.5%: PBS
 - 3% casein
 - 0.5% Tween 20

- PBS-T:
 - 0.5%: PBS
 - 0.5% Tween 20

- Phage precipitation buffer
 - 20% PEG-8000
 - 2.5 M sodium chloride

Autoclaved and stirred while cooling.

- Phosphate-Citrate Buffer, pH 5.0 at 25 °C (Sigma-Aldrich)

2.1.4 CHEMICAL REAGENTS

- Ampicillin (Sigma-Aldrich)
- Bond-Breaker TCEP Solution, Neutral pH (Pierce Biotechnology)
- Bright-Glo luciferase substrate (Promega)
- BugBuster Protein Extraction Reagent (Novagen)
- DEAE-Dextran solution (Sigma-Aldrich)

- Ethidium bromide (Sigma-Aldrich)
- Guanidine hydrochloride (Sigma-Aldrich)
- Hydrochloric acid (Sigma-Aldrich)
- Hydrogen peroxide (Sigma-Aldrich)
- Imidazole (Sigma-Aldrich)
- Incomplete Freund's Adjuvant (Sigma-Aldrich)
- Isopropyl- β -D-thiogalactopyranosid (Invitrogen)
- Methanol (Fisher Scientific)
- Molecular Biology Grad Water (Sigma-Aldrich)
- Monophosphoryl-Lipid A (Sigma-Aldrich)
- N-Z-Case Plus (Sigma-Aldrich)
- PEG-8000 (Fisher Scientific)
- Sodium azide (Sigma-Aldrich)
- Sodium chloride (Fisher Scientific)
- Sodium dodecyl sulfate (Sigma-Aldrich)
- Sodium hydrochloride (Sigma-Aldrich)
- Sodium hydroxide, solid (Fisher Scientific)
- Sodium phosphate (Sigma-Aldrich)
- Tween 20 (Sigma-Aldrich)
- β -mercaptoethanol (Bio-Rad Laboratories, Inc.)
- σ -Phenylenediamine (Sigma-Aldrich)

2.1.5 ENZYMES

- FastDigest Acc65I (Fermentas)
- FastDigest AseI (Fermentas)
- FastDigest BamHI (Fermentas)
- FastDigest SphI (Fermentas)

2.1.6 EQUIPMENT

- 14 ml/50 ml Falcon Tubes (Becton Dickinson)
- -20 °C Freezer (Marvel Scientific)
- 96-well round-bottom plates (Becton Dickenson)

- Adventurer SL AS1502 (scale) (OHAUS Corporation)
- All-Purpose-Laboratory Wrap PVC (FISHERbrand)
- AT261 Delta Range (scale) (Mettler-Toledo)
- Avanti Centrifuge J-25 (Beckman Coulter)
- Bar Seal (Nunc)
- BD 5 ml/20 ml/30 ml Syringe (BD Bard-Parker)
- Biological Safety Cabinet Class II Type A/B3 (Nuair)
- Buffer Dam (Bio-Rad Laboratories, Inc.)
- Centrifugal Tubes Polycarbonate Thick Wall (Beckman Coulter)
- ELISA-Platte, Microlon (ELISA plates) (Greiner Bio-One)
- ELx 405 (ELISA plate washer) (BioTek)
- Eppendorf 0.2 ml PCR tubes (Eppendorf)
- Falcon Ten-twenty-nine Petri Dish (Becton Dickinson)
- Foodservice Foil (Durable Packaging International)
- Fridge (Whirlpool)
- HI-Flow 2000cc Suction Canister (Bemis)
- MAXYMum Recovery 1000 μ l max (Axygen Scientific)
- Microfuge 18 Centrifuge (Beckman Coulter)
- Microfuge 22R Centrifuge (Beckman Coulter)
- Microvol. Tips 10 μ l Filter Tip (Corning)
- Mini PROTEAN 3 Cell (SDS-PAGE) (Bio-Rad Laboratories, Inc.)
- Mini Trans-Blot Filter Paper (Bio-Rad Laboratories, Inc.)
- Parafilm "M" Laboratory Film (Pechiney Plastic Packaging)
- pH meter 440 (Corning)
- pH Test Strips, 4.5-10.0 (Sigma-Aldrich)
- Pipet Basin 50 ml, PVC, Non-Sterile, Bulk (Fisherbrand)
- Pipetman 2 μ l/10 μ l/20 μ l/200 μ l/1000 μ l (Gilson)
- Precision-Gilde Needle (BD Bard-Parker)
- Protected Disposable Scalpel (BD Bard-Parker)
- Repeater Plus (Eppendorf)
- RT7 Benchtop Centrifuge (Sorvall)
- Safe-Lock Tubes 1.5 ml/2 ml (Eppendorf)

- Syringe Filters (Nalgene)
- TipOne 1-200 µl Yellow Pipet Tips (USA Scientific)
- TipOne Graduates Filter Tips (all sizes) (USA Scientific)
- Trans-Blot Transfer Medium Supported Nitrocellulose Membrane (0.45 µm), 7x8.4 cm (Bio-Rad Laboratories, Inc.)
- Transfer Pipets Disposable (Polyethylene) (Fisherbrand)
- Turntable microwave oven (GE)
- Vortex Genie 2 (Fisherbrand)
- Whatman Schleicher & Schuell R-F Reaction Folders (Whatman)

2.1.7 KITS

- Amicon Ultra-15 Centrifugal Filter Devices – Ultracel 10 k (Millipore)
- Amicon Ultra-4 Centrifugal Filter Devices – Ultracel 10 k (Millipore)
- AminoLink Plus Immobilization Kit (Pierce Biotechnology)
- Econo-Pac 10DG Columns (Bio-Rad Laboratories, Inc.)
- GeneTailor Site-Directed Mutagenesis System (Invitrogen)
- NucleoSpin Extract II (Macherey-Nagel)
- NucleoSpin Plasmid (Macherey-Nagel)
- Opti-4CN Substrate Kit (Bio-Rad Laboratories, Inc.)
- Profinity IMAC Resin (Bio-Rad Laboratories, Inc.)
- Qiagen HotMasterMix (2.5x) (Qiagen)
- Quantum Prep Freeze 'N Squeeze DNA Gel Extraction Spin Columns (Bio-Rad Laboratories, Inc.)
- Quickstart Bradford Dye Reagent, 1x (Bio-Rad Laboratories, Inc.)
- Rapid DNA Ligation Kit (Fermentas)

2.1.8 LADDERS AND LOADING DYES

- 6x Loading Dye Solution (Fermentas)
- 6x Orange Loading Dye Solution (Fermentas)
- PageRuler Prestained Protein Ladder (Fermentas)
- PCR Marker (New England Biolabs)
- ZipRuler Express DNA Ladder Set, ready-to-use (Fermentas)

2.1.9 MEDIA

- 2x YT (Capsules) (MP Biomedicals)
- DMEM/10% FCS (Gibco)
- LB Broth (Tablets) (MP Biomedicals)
- LB Medium (Capsules) (MP Biomedicals)
- LB Medium (Powder) (MP Biomedicals)
- LB-Agar Medium (Plates) (Sigma-Aldrich)
- SOC Medium (Invitrogen)

2.1.10 PPEPTIDE CLONING VECTOR 1 (MOBITEC)

The pPEPTIDE Cloning Vector 1 is a fusion construct based on the pET-3a expression system and contains a novel sequence that induces the expression of recombinant target proteins and, in particular, peptides as small as five residues in *E. coli* as desired in this experiment. The peptides are purified using a poly(his) affinity tag. The original target peptide sequence is flanked by restriction sites for BamHI and AseI. Restriction with these single-cutters results in excision of the target peptide sequence, which can subsequently be replaced by the sequence of the protein of interest. The expression of the fusion protein is controlled by the T7 promoter. The pPEPTIDE Cloning Vector 1 contains an ampicillin resistance gene.

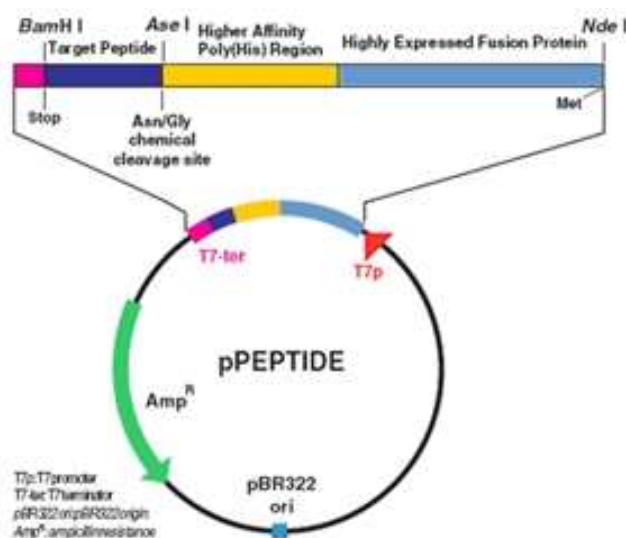


Figure 2.1 Map of the pPEPTIDE Cloning Vector 1.

2.1.11 PRECAST GELS FOR PAGE

All precast gels were ordered from Bio-Rad Laboratories, Inc.

- Precast Gel for 2D PAGE, 12% Tris-HCl
- Precast Gel for PAGE, 12% Tris-HCl, 10 well, 50 μ l comb
- Precast Gel for PAGE, 12% Tris-HCl, 15 well, 15 μ l comb

2.1.12 PRIMERS

All primers were ordered from Invitrogen (5' to 3').

- Sequencing of M13 phage ssDNA: CCCTCATAGTTAGCGTAACG
- Amplification of phage mimotope DNA:
pPEPTIDE fwd. primer:
CGCCCGCGGATTAATGGCCCTTTAGTGGTACCTTTCTATTCTCACTCT
pPEPTIDE rev. primer:
GGCCCGGGGATCCTAACTTTCAACAGTTTCGGCCGAACCTCCACC
- Sequencing of recombinant plasmids:
 - T7 fwd. primer: TAATACGACTCACTATAGGG
 - T7 rev. primer: AAACCCCTCAAGACCCG
- Site-directed mutagenesis:
 - SDM fwd. primer: CTGCGGACCAAGATGAATCATCTTAGAGTG
 - SDM rev. primer: ATTCATCTTGGTCCGCAGCAGACTTTTCCG

2.2 METHODS

2.2.1 PHAGE AMPLIFICATION

2 ml of LB media were inoculated with 20 μ l of ER2738 overnight culture (1:100) and 10 μ l of the designated phage stock. The culture was incubated at 37°C and 250 rpm for 4.5 h.

2.2.2 PHAGE PRECIPITATION

The culture was centrifuged at 12,000 rpm and 4°C for 20 min. 1.5 ml of supernatant were added to 500 μ l 20% PEG-8000/2.5 M NaCl and thoroughly vortexed. The phages were incubated at 4°C overnight and centrifuged at 12,000 rpm and 4°C for 20 min on the next day. The supernatant was subsequently aspirated and the phage pellet was re-suspended in 200 μ l PBS.

2.2.3 MEASUREMENT OF PHAGE CONCENTRATION

10 μ l of the phage solution were diluted in 490 μ l of PBS (1:50), thoroughly vortexed, and spin centrifuged. A wavelength scan was performed between 240 nm and 320 nm and the phage concentration was calculated using the following formula:

$$C_{Phages} = \frac{(A_{269} - A_{320}) \times 6 \times 10^{16}}{7223} \times 50(\text{dilution factor})[\text{phages/ml}]$$

2.2.4 ISOLATION OF PHAGE SSDNA

500 μ l of supernatant of the overnight culture were added to 200 μ l of 20% PEG-8000/2.5 M NaCl after centrifugation (see phage precipitation) and thoroughly vortexed. The suspension was incubated at 4°C overnight and centrifuged at 12,000 rpm and 4°C for 20 min on the following day. The supernatant was subsequently aspirated and the phage pellet was re-suspended in 100 μ l iodide buffer and vortexed. Afterwards, 300 μ l of 100% ice-cold ethanol were added and the mixture was centrifuged at 12,000 rpm and 4°C for 20 min. The supernatant was disposed and the pellet was washed with 300 μ l of 70% room-tempered ethanol. After 20 min of centrifugation at 12,000 rpm and 4°C, the supernatant was removed and the phage ssDNA pellet was air-dried and subsequently re-suspended in 15 μ l of dH₂O.

2.2.5 AMPLIFICATION OF PHAGE MIMOTOPE DNA VIA PCR

The phage ssDNA was diluted 1:10 in dH₂O. 2 µl of the diluted phage ssDNA were added to the following reagents:

Qiagen HotMasterMix (2.5x):	20 µl
pPEPTIDE forward-primer (10 µmol/µl, final 200 nM):	1 µl
pPEPTIDE reverse-primer (10 µmol/µl, final 200 nM):	1 µl
dH ₂ O:	26 µl
<hr/>	
total volume incl. phage ssDNA:	50 µl

Afterwards, the PCR mixture was thoroughly vortexed, spin centrifuged, and the following PCR program was run:

94 °C	10 s	
<hr/>		
94 °C	10 s	
53°C	10 s	30 cycles
65°C	10 s	
<hr/>		
65°C	10 min	
4°C	∞	

2.2.6 PURIFICATION OF PCR PRODUCTS

The PCR reaction was purified using the NucleoSpin Extract II Kit (Macherey Nagel), according to the manufacturer's instructions. The DNA was eluted twice with 25 µl dH₂O each.

2.2.7 MEASUREMENT OF DNA CONCENTRATION

The 2 µl of each DNA sample were diluted in 98 µl of dH₂O (1:50) and measured at OD_{260/280}. The DNA concentration was determined by applying the following formula:

$$C_{DNA} = OD_{260} \times 50 \times 50(\text{dilution factor})[\text{ng}/\mu\text{l}].$$

2.2.8 AMPLIFICATION OF PPEPTIDE VECTOR DNA

XL1-Blue cells were transformed with 5 ng of pPEPTIDE Vector DNA according to the manufacturer's instructions. Cells were plated on LB_{amp} plates and incubated at 37°C overnight. Five colonies were picked using sterile pipette tips and used to inoculate 3 ml of LB_{amp} media. The clones were incubated at 37°C and 250 rpm overnight.

2.2.9 ISOLATION AND PURIFICATION OF PPEPTIDE VECTOR DNA (MINI-PREP)

pPEPTIDE Vector DNA was isolated and purified using the NucleoSpin[®] Plasmid Kit (Macherey-Nagel), according to the manufacturer's instructions. The DNA was eluted twice with 25 µl dH₂O each.

2.2.10 DIGESTION OF PHAGE MIMOTOPE AND PPEPTIDE VECTOR DNA

1 µg of DNA was double-digested using the restriction enzymes BamHI and AseI at 37°C for 1h in a water thermostat:

Phage Mimotope DNA/pPEPTIDE Vector DNA (1 µg):	X µl
10x FastDigest Buffer:	2 µl
BamHI (1 U):	1 µl
AseI (1 U):	1 µl
dH ₂ O:	X µl
total volume:	20 µl

2.2.11 ANALYSIS AND PURIFICATION OF DIGESTED DNA SAMPLES

Digested insert and vector DNA samples were run at 100 V on 1.6% and 0.8% agarose gels, respectively. The desired bands were excised using a clean scalpel and the DNA was eluted using the Freeze 'N Squeeze Kit, according to the manufacturer's instructions. The volume of the eluted sample was measured and 1/10 volume of NaOAc was added. The sample was vortexed and 2.5x volume of 100% ice-cold ethanol were added. The sample was vortexed and incubated at -20°C for 2 h. Afterwards, the sample was centrifuged at 15,000 rpm and 4°C for 1 h. The supernatant was aspirated and the pellet was washed with 500 µl of 70% room-tempered ethanol.

The sample was centrifuged at 15,000 rpm and 4°C for 20 min. The supernatant was removed and the pellet was air-dried and subsequently re-suspended in dH₂O.

2.2.12 LIGATION OF PHAGE MIMOTOPE DNA AND pPEPTIDE VECTOR DNA

1.8 ng of digested mimotope insert DNA were ligated with 100 ng of digested pPEPTIDE Vector DNA (ratio 3:1), using the Rapid DNA Ligation Kit, according to the manufacturer's instructions:

Purified phage mimotope DNA (1.8 ng):	X μ l
Purified pPEPTIDE Vector DNA (100 ng):	X μ l
5x Rapid DNA Ligation Buffer:	4 μ l
T4 DNA Ligase (5 u):	1 μ l
dH ₂ O:	X μ l
total volume:	20 μ l

2.2.13 TRANSFORMATION OF DH5A CELLS

DH5 α Cells were transformed with 5 μ l of the ligation mixture, according to the manufacturer's instructions. After transformation, the cells were plated on LB_{amp} agar plates and incubated at 37 °C overnight.

2.2.14 CONTROL DIGESTION OF RECOMBINANT DNA

16 colonies were picked on the day following transformation and used to inoculate 4 ml of LB_{amp} media. Cultures were incubated at 37°C and 250 rpm overnight. In order to determine successful recombination, isolated plasmid DNA was digested with the restriction enzyme EagI, according to the manufacturer's instructions. The digestion reaction was mixed with 4 μ l 6x Loading Dye and run on a 1% agarose gel.

2.2.15 SEQUENCING

600 ng of isolated plasmid DNA were supplemented with the T7 forward primer, thoroughly vortexed, and spin centrifuged. Sequencing was conducted by the Dana-Farber Sequencing Core Facility. Sequences were checked for correctness, using the freeware Finch TV.

2.2.16 SITE-DIRECTED MUTAGENESIS

Site-directed mutagenesis was performed according to the manufacturer's instructions.

2.2.17 TRANSFORMATION OF BL21(DE3) CELLS

BL21(DE3) cells were transformed with 5 ng of plasmid DNA, according to the manufacturer's instructions.

2.2.18 SELECTION OF HIGH-LEVEL EXPRESSION CLONES

Seven distinct colonies were chosen and used to inoculate 3 ml of 2x YT media supplemented with 100 µg/ml ampicillin. The cultures were grown until OD = 1.2, at which a 100 µl sample was taken for subsequent SDS-PAGE analysis. Afterwards, the cultures were induced with 0.4 mM IPTG (final concentration) and further incubated for 5 h. Another 100 µl sample was taken and the samples were centrifuged for 5 min at 14,000 rpm. The supernatant was decanted and the pellet re-suspended in 50 µl Laemmli buffer and 25 µl dH₂O. The mixture was boiled for 15 minutes and afterwards centrifuged for 5 min at 14,000 rpm. 15 µl of supernatant were run on a 12% polyacrylamide gel at 200 V. Afterwards, the gel was stained with Coomassie dye for 1 h and later boiled in dH₂O for 10 min to destain. The high level expression clone was chosen based upon the largest amount of protein produced after 5 h. This clone was used to make a 50% glycerol stock.

2.2.19 EXPRESSION KINETICS

The high level expression clone was used to inoculate 4 ml of 2x YT media supplemented with 100 µg/ml ampicillin. The culture was grown until OD = 1.2. Afterwards, a 100 µl sample was taken for subsequent SDS-PAGE analysis and the culture was induced with 0.4 mM IPTG (final concentration) and grown for 8 h. 100 µl samples were taken every hour and centrifuged for 5 min at 14,000 rpm. The supernatant was decanted and the pellet re-suspended in 50 µl Laemmli buffer and 25 µl dH₂O. The mixture was boiled for 15 minutes and centrifuged for 5 min at 14,000 rpm. 50 µl supernatant were run on a 12% polyacrylamide gel at 200 V. Afterwards, the gel was stained with Coomassie-dye for 1 h and later boiled in dH₂O for 10 min to destain.

2.2.20 PROTEIN EXPRESSION

Recombinant BL21(DE3) cells from the glycerol stock were used to inoculate 30 ml of 2x YT media supplemented with 100 µg/ml ampicillin. The culture was grown overnight and centrifuged on the next morning at 8,000 rpm and 4°C for 20 min. The cells were re-suspended in 300 ml of fresh media supplemented with 100 µg/ml ampicillin and grown until OD = 1.2. Afterwards, a 100 µl sample was taken for subsequent SDS-PAGE and the culture was induced with 0.4 mM IPTG (final concentration) and grown for 5 h. Another 100 µl sample was taken and the culture was centrifuged at 10,000 rpm and 4°C for 10 min. The supernatant was decanted and the pellet was frozen at – 20°C for ensuing protein extraction and purification.

2.2.21 COLUMN PREPARATION

20 ml of Profinity™ IMAC Resin slurry (pre-charged with Ni²⁺) were transferred to a 147 ml glass column (Bio-Rad). After the storage solution had been removed, the column was washed with three column volumes of dH₂O. 20 ml of dH₂O were added to make a 50% slurry.

2.2.22 PURIFICATION OF HIS-TAGGED FUSION PROTEINS

The bacterial pellet was re-suspended in room temperature BugBuster reagent, using 5 ml of reagent per gram of wet cell paste, and the cell suspension was incubated on a rotating mixer at a slow setting for 20 min at room temperature. The lysate was centrifuged at 16,000x g and 4°C for 20 min and the supernatant was subsequently mixed with an equal volume of 2x binding/washing buffer supplemented with 8 M GuHCl to reach a final concentration of 4 M GuHCl. The lysate was filtered applying Millipore Steriflip® Sterile 50 ml Disposable Vacuum Filtration System according to the manufacturer's instructions and the clarified lysate was added to the column. The resin-lysate mixture was gently swirled in the column and incubated at 4°C for 30 min on a rocking platform. Afterwards, the resin was allowed to settle. Flow-through samples were collected for subsequent SDS-PAGE analysis. The column was washed with five column volumes of binding/washing buffer and wash fractions were collected. The protein was eluted with five column volumes of elution buffer. The eluates were saved for further analysis.

Afterwards, the column was sanitized with five column volumes of 0.5 M NaOH. The solution was rinsed from the column with five column volumes of dH₂O/0.02% NaN₃ for storage.

2.2.23 ANALYSIS OF ELUTED FRACTIONS

15 µl samples of all fractions were mixed with 2x Laemmli buffer, boiled for 5 min, and run on a 12% polyacrylamide gel. Afterwards, the gel was stained with Coomassie dye for 1 h and later boiled in dH₂O for 10 min to destain.

2.2.24 DESALTING AND BUFFER EXCHANGE

Following purification, the elution steps containing the highest amount of protein were used for desalting and buffer exchange using Econo-Pac[®] 10DG columns, according to the manufacturer's instructions. Proteins were eluted in PBS.

2.2.25 CONCENTRATING OF FUSION PROTEIN SAMPLES

Protein solutions were concentrated using Amicon[®] Ultra Centrifugal Devices (30 kDa MWCO), according to the manufacturer's instructions.

2.2.26 BRADFORD-ASSAY

20 µl of concentrated protein solution were diluted in 980 µl of Bradford Quick Dye Solution (1:50) and incubated at room temperature for 10 min. The amount of total protein was calculated using the following formula according to the standard curve with BSA:

$$X = \frac{OD_{595} - 0.051}{0.0007}$$

2.2.27 IMMUNIZATION OF MICE (carried out by Robert Rasmussen)

Recombinant phages were allocated according to motifs into groups of 5-6 phages with similar but not identical peptide sequences. Phages of each group were combined and used as five different mixtures for immunization. Mice were primed once with SHIV-1157ip *env* DNA intramuscularly (100 µg in 100 µl PBS) and boosted subcutaneously (s.c.) with 10¹² phage particles in 100 µl PBS/MPL every 4-5 weeks. Serum samples

were collected 2-5 weeks after each boost. After four phage boosts, serum samples were tested for their neutralizing capacity against HIV-1_{SF162.LS} and SHIV-1157ip. In a pilot study, 11 mice were given an additional boost with trimeric SHIV-1157ip gp160 s.c. [20 µg in 100 µl PBS with incomplete Freund's adjuvant (IFA)] and their sera were tested for the presence of neutralizing antibodies.

2.2.28 NEUTRALIZATION ASSAY (carried out by Helena Ong)

SHIV-1175ip was prepared in rhesus monkey PBMC, HIV pIndieC was prepared in human PBMC and HIV_{SF162.LS} pseudovirus (kindly provided by David Montefiori) was prepared using cotransfection of 293T cells with an *env* expression plasmid and Δ*env* backbone vector. TZM-bl cells encode the luciferase gene under the control of the HIV-1 promoter; both CD4 and CCR5 are also expressed on the cell surface (AIDS Research and Reference Program, Division of AIDS, NIAID, NIH). A total of 5,000 cells/well were seeded overnight in 100 µl DMEM/10% FCS. Serial 2-fold dilutions of immune sera were prepared in triplicates in 96-well round-bottom plates. In parallel, the pre-immune sera were serially diluted and used as controls. "Virus only" wells received 50 µl medium. The virus was diluted (1:500 for SHIV-1157ip: 36 ng/ml p27; 1:500 for HIV pIndieC: 35 ng/ml p24; 1:300 for HIV_{SF162.LS}: 300 ng/ml p24) and 50 µl of virus was added to all wells. The plate was incubated for 1 h at 37°C in 5% CO₂, after which time 10 µl of a 400 µg/ml DEAE-Dextran solution was added to all wells and the entire mixture was transferred into the 96-well flat-bottom plate with the seeded TZM-bl cells. The next day, medium was replaced with fresh medium and incubated another 24 h. Bright-Glo luciferase substrate (Promega, Madison WI, USA) was added to the plate the following day and luciferase activity was measured. The percent neutralization was calculated using the following equation:

$$\%Neutralization = \left[1 - \left(\frac{Luciferase\ immune\ serum}{Luciferase\ pre-immune\ serum} \right) \right] \times 100.$$

2.2.29 WESTERN-BLOTS

40 µg of protein were run on a 12% polyacrylamide gel (BioRad) at 200 V. Afterwards, the gel, the nitrocellulose membrane, the fiber pads and the filter pads were incubated in

transfer buffer for 15 min and the protein transfer was conducted for 60 min at 100 V using a wet blot apparatus. The membrane was cut into strips, blocked with 3% PBS-CT for one hour and individual strips were incubated with the appropriate sera/primary antibodies in 3% PBS-CT at 4°C overnight (rhesus monkey sera: 1:200; primary antibodies: 1:1,000). On the following day, the blot was washed three times with PBS-T and incubated with the adequate HRP-conjugated antibody for one hour at room temperature (1:2,000 in 3% PBS-CT). Afterwards, the blot was washed five times with PBS-T and developed with Opti-4CN substrate, according to the manufacturer's instructions.

2.2.30 FUSION PROTEIN ELISA

The ELISA plates were coated overnight at 4°C with 100 ng/well native or reduced (10 mM TCEP/1% SDS; boiled for 2 min) proteins in 100 µl 0.05 M carbonate coating buffer. The ELISA plates were washed three times with 300 µl dH₂O on the following day, and blocked with 200 µl PBS-CT for one hour at room temperature. Afterwards, the plate was washed three times with 300 µl dH₂O and incubated with the appropriate sera, diluted in 100 µl/well 3% PBS-CT (monkey: 1:800; mouse: 1:175); and incubated overnight at 4°C. The ELISA plates were subsequently washed three times with 300 µl dH₂O and incubated with the appropriate HRP-conjugated secondary antibody diluted 1:2,000 in 100 µl/well 3% PBS-CT for 1 h at room temperature. Afterwards, the plate was washed five times with 300 µl dH₂O and incubated with 100 µl of ODP in phosphate-citrate buffer for six minutes. The reaction was stopped using 100 µl/well 1 N H₂SO₄ and read at 490 nm and 620 nm (corrected OD values = 490 – 620 nm). All reactions were run in duplicates.

2.2.31 STATISTICAL ANALYSIS

Statistics were calculated using a two-tailed paired t test and only applied to matching pairs of mice comparing the significance between the post-phage boosts and post-gp160 boost.

3 RESULTS

3.1 PRELIMINARY RESULTS

These experiments have been performed by Michael Humbert, Helena Ong, and Robert Rasmussen.

3.1.1 SERIAL PASSAGE OF SHIV-1157IP RHESUS MONKEYS

The Ruprecht laboratory has generated several clade C R5-tropic SHIV's based upon *env* of a Zambian pediatric isolate of HIV-1 clade C. At the beginning of these studies, the parental infectious proviral clone, SHIV-1157i, was passaged through five rhesus monkeys to generate the adapted SHIV-1157 ip (Figure 3.1) (129). Several rhesus monkeys infected with SHIV-1157ip or the related late isolate SHIV-1157ipd3N4 produced high-titer, broadly reactive nAbs against homologous SHIV-C as well as heterologous primary strains of HIV-1 of other clades (Table 3.1) (110). High nAb titers against the early isolate SHIV-1157ip, the late isolate SHIV-1157ipd3N4 (110), as well as against a heterologous R5 SHIV-C (SHIV-2873Nip) were detected. All of these sera were also tested against a spectrum of heterologous HIV clade C and B strains (Table 3.1) and cross-clade nAbs against various strains were detected, including HIV_{pIndieC}, HIV_{SF162.LS}, and HIV_{NL4-3}. The serum of rhesus monkey RKI-8 was particularly effective at neutralizing a broad spectrum of viruses of both clade C and B. This cohort of rhesus monkeys, which has been called the "Top-Ten Cohort", is a precious source to study natural humoral immune responses against the HIV-1 envelope glycoprotein, and might help to identify novel conserved structures, which may then serve as immunogens to be incorporated into potential vaccine candidates.

Because of the breadth and strength of its humoral immune response to HIV-1 Env, animal RKI-8 was chosen to select HIV-C Env-specific mimotopes.

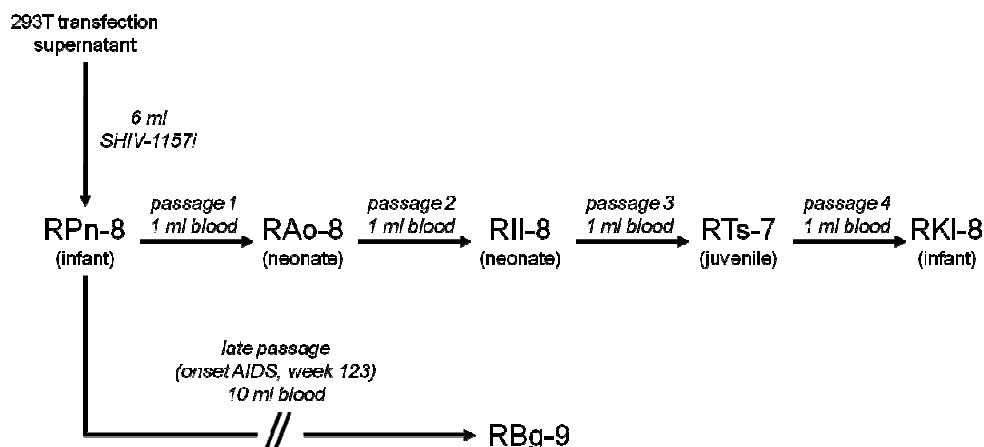


Figure 3.1 Serial passage of SHIV-1157i in rhesus monkeys for viral adaptation. The first animal (RPn-8) was inoculated i.v. with cell-free supernatant from 293T cells transfected with the infectious molecular clone SHIV-1157i; all following animals were inoculated i.v. through serial transfer of blood. The neonatal period covers the time from birth to one month; infancy comprises the period up to one year, and juvenile monkeys are between one and five years of age.

Animal #	Clade C							Clade B		
	Homologous		Heterologous					Heterologous		
	SHIV-1157ip (early) ¹	SHIV-1157ipd3N4 (late) ²	HIV _{paideC} ¹	ZM135M ¹	ZM233M.PB6 ¹	ZM109F ¹	SHIV-2873Nip ²	SHIV _{SF162P3} ¹	HIV _{SF162LS} ¹	HIV _{NL4-3} ¹
RKl-8 ³	2,048	>640	2,048	24	160	26	>640	96	3,741	512
RAo-8 ³	2,048	>640	128	<20	42	<20	>640	<40	220	32
RJa-9 ³	1,800	>10,240	128	<20	59	22	2,048	68	35,770	128
RMf-9 ³	2,048	>640	128	<20	<20	35	>640	78	18,303	128
RTs-7	2,048	>640	128	n.d.	n.d.	n.d.	>640	n.d.	n.d.	32
RHy-8	600	>10,240	90	<20	<20	<20	>640	n.d.	173	n.d.

*IC₅₀, 50% inhibitory concentration given as reciprocal serum dilution for 50% neutralization.
¹determined in TZM-bl assays.
²determined in human PBMC-based assays.
³phage display selection performed; n.d. not determined.
 ZM135M, ZM233M.PB6, and ZM109F are primary HIV clade C isolates from Zambia. No neutralization was seen against five HIV clade C isolates from South Africa and four others from Zambia (not shown). SHIV-2873Nip is a Tier 1 (i.e. neutralization-sensitive) R5 virus that encodes *env* of a recently transmitted, R5 HIV clade C isolated from a Zambian infant (130). SHIV_{SF162P3} is a Tier 2 virus (i.e. more difficult to neutralize and representative of most primary HIV isolates), HIV_{SF162LS} is a Tier 1 virus.

Table 3.1 IC₅₀ for selected rhesus monkeys with high-titer nAb activity.

3.1.2 SELECTION OF HIV-C ENV-SPECIFIC MIMOTOPES

To select HIV-C Env-specific mimotopes, polyclonal IgG from RKI-8 was used. RKI-8 serum IgG was immobilized on paramagnetic beads and used to screen three different phage-displayed random peptide libraries (7mer, cyclic 7mer, 12mer) (summarized in Figure 3.2). For each screening, 94 single clones were tested in a phage ELISA for their specificity by using SHIV-positive and SHIV-negative serum in parallel. The positive clones were then amplified and sequenced. The corresponding peptide insert sequences were allocated to different groups according to the peptide motifs and analyzed for linear homology to gp160_{SHIV-1157ip}. By using monkey RKI-8 serum (110), 78 different clones were isolated. Thirty-eight of these mimotopes resembled three regions on gp120: the V2 loop (9 clones), the V3 loop (21 clones) and the C-terminal domain (8 clones). Thirty-four of the 78 clones resembled regions on gp41: The majority represented a subdomain of the immunodominant region (IDR), which is referred to as the immunodominant loop (44) and contains the KLIC motif (20 clones); seven clones exhibited homology to IDR outside the immunodominant loop as well as several amino acid residues of the N-terminal heptad repeat. Seven additional clones showed homology to the MPER. The remaining six phage inserts failed to show linear homology to gp160_{SHIV-1157ip}.

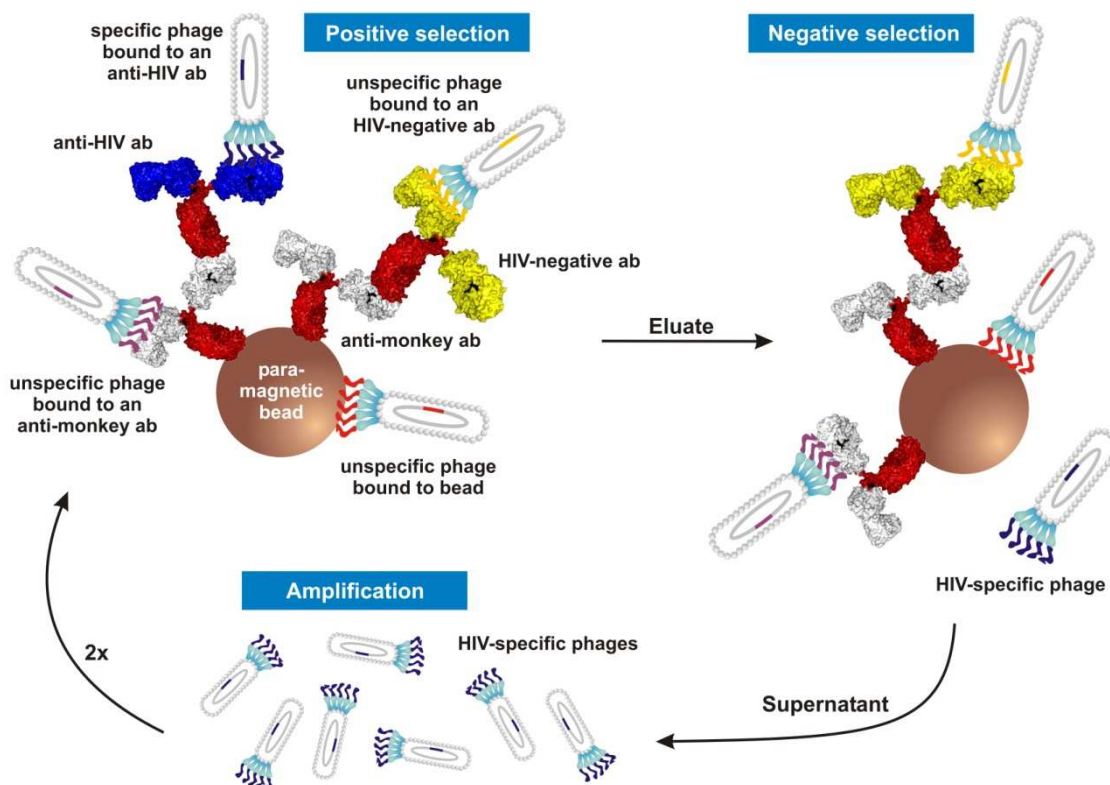


Figure 3.2 Selection of HIV-1 clade C Env-specific mimotopes. Paramagnetic beads were coated with a rabbit anti-monkey IgG. Coated beads were pre-incubated with rhesus monkey serum and subsequently incubated with the original phage-displayed peptide library. Biopannings of all three libraries (7mer, cyclic 7mer and 12mer) were performed in parallel using separate tubes. Beads were washed to remove unbound phages and bound phages were eluted by pH shift. Following neutralization, eluted phages were subjected to negative selection as described above using pooled sera from non-infected control monkeys. Phages remaining from the negative selection were amplified in *E. coli* and used for a second and third round of selection. After the third positive selection, the phages were titered, and single clones were picked and tested by phage ELISA for specific binding. Positive clones were amplified and sequenced to deduce their peptide insert.

Several mimotopes exhibited only minimal linear homology to gp160_{SHIV-1157ip}. Since these mimotopes might represent conformational eptiopes on the HIV-1 envelope glycoprotein, computational analysis with 3DEX was performed. Using the software 3DEX (128) and a published structure of gp120 (131), an interesting V3 mimotope with combined linear and structural homology was identified (Table 3.2, clone A12.2; Figure 3.3). Comparison of the primary envelope sequence of the structure file (PDB-ID: 2B4C; HIV-1 subtype B strain JR-FL) and SHIV-1157ip showed that the amino acids in

this segment of the V3 loop are almost identical in sequence (inset Figure 3.3). By performing 3DEX analysis, two motifs were identified – each spanning four amino acids – at the crown of the V3 loop (Figure 3.3, yellow/orange) and nearby (Figure 3.3, green). Although these eight amino acids are discontinuous, they could be located on neighboring spots on the surface of gp120.

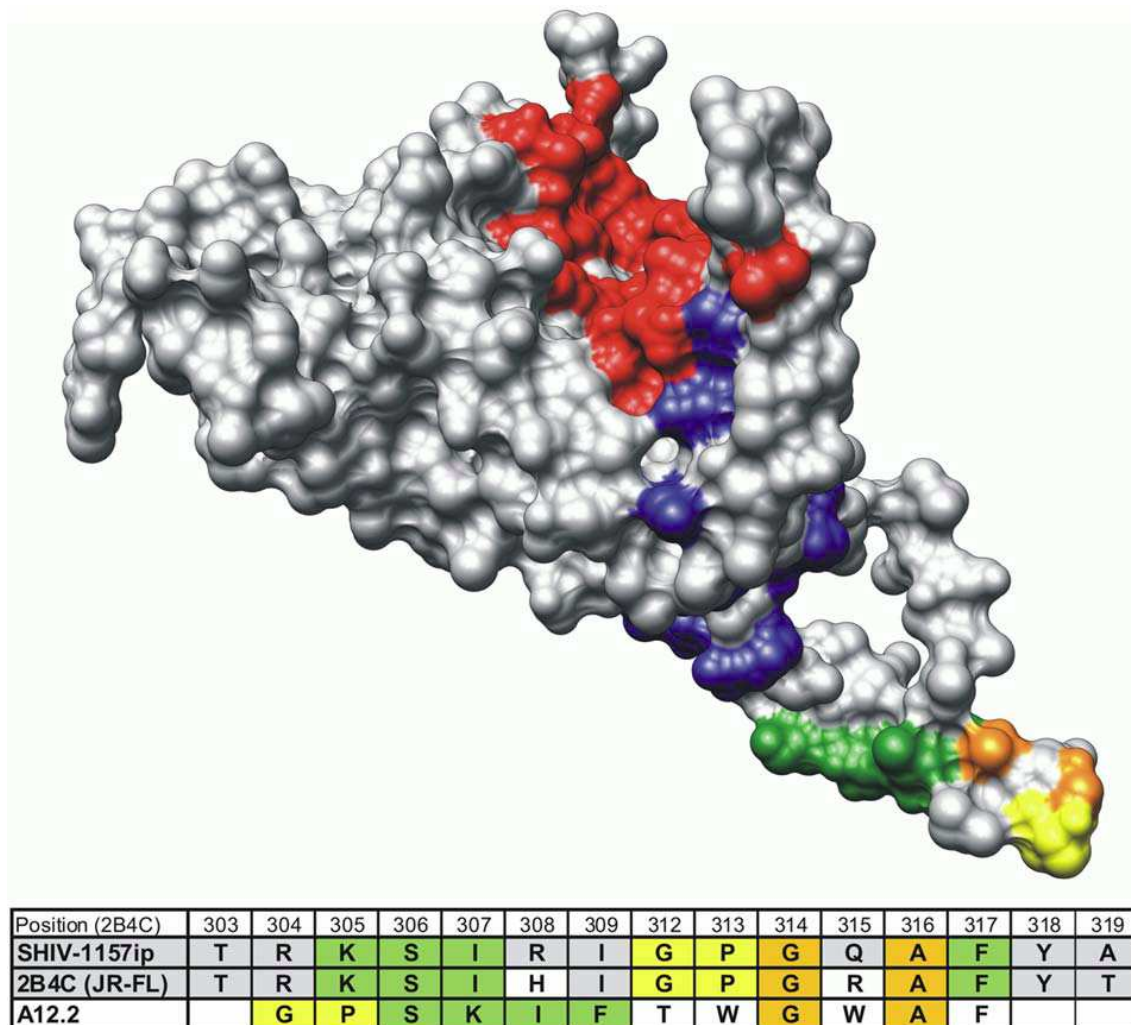


Figure 3.3 Location of mimotope A12.2 on gp120 (132). 3DEX analysis (6) was used to find structural homology between A12.2 (yellow, orange and green) and the surface of gp120 (PDB ID: 2B4C) with the CD4 binding site shown in red and CCR5 coreceptor contact sites in blue. The inset table shows partial V3 sequences for SHIV-1157ip, the protein structure used for 3DEX analysis (2B4C), and A12.2. Amino acid residues resembling the parental sequence but too few to form a linear epitope are shown in yellow and orange. Residues identified by 3DEX as showing 3D homology are shown in green. All amino acids are in close proximity on the molecule's surface and form a potential conformational mimotope of gp120.

Group	Clone	Number	Sequence																			
	SHIV-1157ip		R	K	S	I	R	I	G	P	G	Q	A	F	Y	A	T	G	D	I		
Group 1 V3 loop gp120	AIV3p12.7					I	R	P	H	P	G	H	M	Y	Y	S	W					
	AIV3p12.5				Q	V	R	M	G	P	G	Q	P	D	Y	L						
	AIII12.11					V	R	L	P	P	G	A	S	G	Y	T	P					
	AIV12.1	3				I	R	P	G	P	A	A	G	G	Y	P	A					
	AIV12.4	2			K	M	I	H	L	G	P	Q	Q	T	F	P						
A12.2	12	G	P	S	K	I	F	T	W	G	W	A	F									
	SHIV-1157ip		Y	K	V	V	E	I	K	P	L	G	I	A	P	T	K	A	K	R		
Group 2 C-terminus gp120	AIII7.7									K	T	L	R	I	A	P						
	AIV7.1	4								K	L	L	R	I	A	P						
	AIV7.5	4							A	T	W	R	I	G	P							
	AIII7.5				K	D	V	-	-	-	-	-	R	I	A	P						
	AIII7.9				K	V	V	-	-	-	-	-	R	I	E	P						
	SHIV-1157ip		L	A	I	E	R	Y	L	Q	D	Q	Q	L	L	G	I	W	G	C		
Group 3 IDR gp41	AIII12.10	2					S	L	L	Y	S	S	E	Y	S	G	I	W				
	AIII12.14	2						K	L	L	S	S	N	T	Y	G	I	W	M			
	AIII12.13							K	L	L	G	Y	T	T	S	A	G	I	W			
	AIV3p12.10						L	C	Y	H	R	D	G	S	Y	P	T	S				
	AIV12.8						S	L	L	K	H	S	L	S	A	G	I	W				
	SHIV-1157ip		L	G	I	W	G	C	S	G	K	L	I	C	T	T	A	V	P	W		
Group 4 KLIC gp41	AIIIc.1	12						S	H	G	K	L	L	A								
	AIVc.6	3							T	G	K	L	Q	C	I							
	AIV3p12.6		Q	H	S	W	S	C	S	G	K	L	L	C								
	AIII12.1	3		S	L	W	T	L	H	G	S	L	I	S	A							
	AIII12.6			S	I	W	Q	T	S	G	V	L	I	S	Y							
	SHIV-1157ip		N	L	W	N	W	F	S	I	T	K	W	L	W	Y	I	K	I	F		
Group 5 MPER gp41	AIII7.6					N	I	L	S	-	T	-	L	L								
	A7.1					N	V	F	N	-	-	-	W	K	W							
	A7.2						E	F	R	-	-	-	W	A	W	A						
	A7.5					D	W	T	-	-	-	-	W	S	W	N						
	A7.4												W	S	W	G	W	M	A			

Table 3.2 Alignment of mimotopes selected with serum from monkey RKL-8 with the sequence of homologous gp160_{SHIV-1157ip}. Phage peptide sequences (clones) were grouped according to their motifs (V3, gp120 C-terminus, gp41 immunodominant region (IDR), KLIC, and membrane proximal external region (MPER)) and aligned to gp160_{SHIV-1157ip} (grey rows). Linear homologies are shaded grey. Numbers in parentheses indicate how many times a given mimotope was selected independently. Mimotopes were considered linear if they exhibited more than 50% linear amino acid identity.

3.1.3 IDENTIFICATION OF A CONFORMATIONAL MIMOTOPE OF HIV-1 CLADE C ENV

In order to confirm that mimotope A12.2 represents a conformational epitope and antibody binding thus depends on the structural integrity of the target HIV-1 clade C envelope glycoprotein, antibody binding was compared using both native and reduced protein. By using immobilized recombinant phages, the corresponding antibodies were isolated from the polyclonal rhesus monkey serum through affinity purification. The obtained phage-affinity-purified antibodies were then subjected to a dot spot analysis with homologous, trimeric gp160_{SHIV-1157ip}, which was spotted under native and denaturing conditions (Figure 3.4). When the protein was denatured, binding of antibodies specific for clone A12.2 was not detected (Figure 3.4, field A1 and B1), although specific binding was shown to the native protein. As control, antibodies specific for a phage clone with greater linear homology to the V3 loop were purified (AIV12.4). Antibody binding to the protein was observed both under native and denaturing conditions (Figure 3.4, field A2 and B2). The negative control without spotted protein (Figure 3.4, row C) did not show nonspecific antibody interaction with the membrane. As an additional positive control, anti-monkey IgG was used (Figure 3.4, row D) to confirmed that equal amounts of antibodies had been applied to all strips.

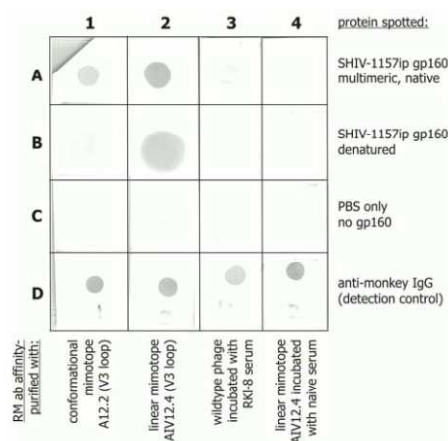


Figure 3.4 The conformational dependence of mimotope A12.2 by dot spot analysis with phage affinity-purified serum antibodies (132). The following were spotted onto the membrane: row A, native gp160_{SHIV-1157ip}; row B, denatured gp160_{SHIV-1157ip}; row C, no protein spotted; row D, anti-rhesus monkey IgG. In columns 1-4, rhesus monkey antibodies affinity-purified with the following reagents were applied: (1) recombinant phage A12.2 encoding mimotope identified as conformational by 3DEX analysis; (2) phage AIV12.4 encoding linear mimotope; (3) WT phage; and (4) AIV12.4 incubated with naïve rhesus monkey serum.

3.2 RESULTS

3.2.1 MOLECULAR CLONING AND EXPRESSION OF FUSION PROTEINS

In order to analyze if the HIV-1 Env mimotope motif groups represent common antibody epitopes found in Top-Ten Cohort rhesus monkey sera with broadly reactive nAbs (Table 3.1) and to assess the success of the immunization studies in mice, selected mimotopes of all groups (except MPER) were cloned into fusion proteins and analyzed with Western blots and enzyme-linked immunosorbent assays (ELISAs).

In order to produce the desired mimotopes as part of fusion proteins, the phage mimotope DNA, encoding for the mimotope expressed on the M13KE phage, was cloned into the pPEPTIDE Cloning Vector 1. The flanking sequences framing the mimotope were also included to ensure that the mimotope would reach the identical conformation as expressed on the M13KE phage. Following ssDNA extraction, the phage mimotope DNA was amplified via PCR (Figure 3.5). As controls for the Western blot and ELISA experiments, a random phage insert obtained during negative selection (Nc.19; cyclic 7mer) was used.

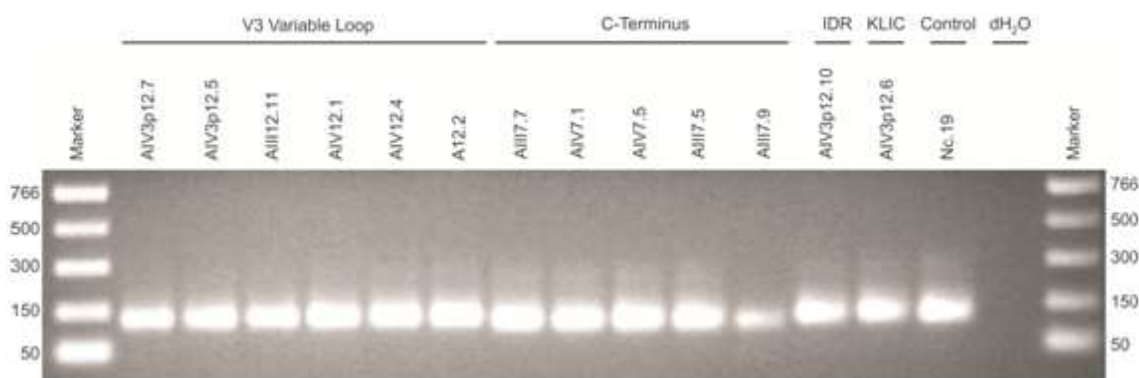


Figure 3.5 Amplification of phage mimotope DNA via PCR. All phage mimotope DNA samples were successfully amplified via PCR. No contaminants are seen in the dH₂O control.

Phage mimotope DNA and pPEPTIDE Cloning Vector 1 DNA were both double-digested using the restriction enzymes BamHI and AseI to create complementary sticky ends for ligation. The digested phage mimotope DNA samples were run on a 1.6% agarose gel (Figure 3.6, exemplary for group 1 mimotope samples and Nc.19). The digested samples run at a smaller size than the undigested sample, proving that the digestion was successful. The digested phage mimotope samples were extracted from the agarose gel and purified.

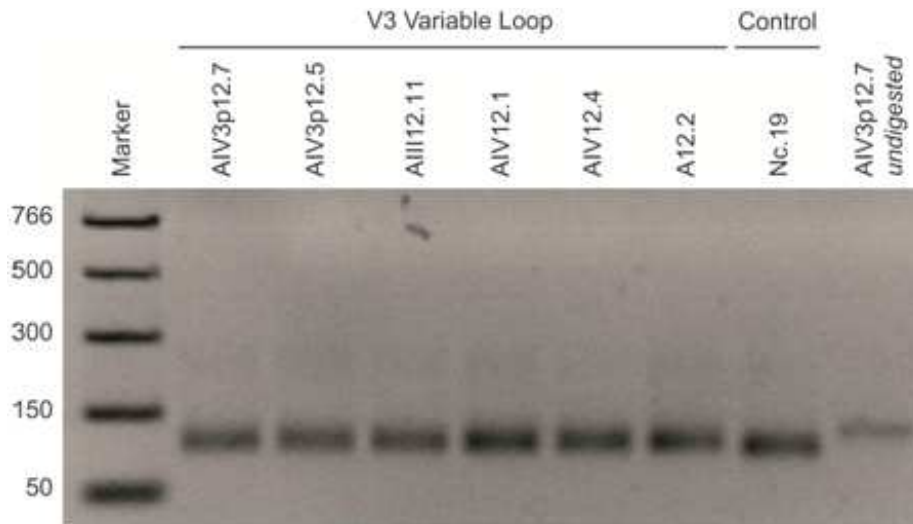


Figure 3.6 Digestion of phage mimotope DNA samples. All samples were double-digested with BamHI and AseI. As expected, all digested samples run slightly lower than the undigested samples.

The digested pPEPTIDE Cloning Vector 1 DNA was run on a 0.8% agarose gel to analyze the digestion. As shown in Figure 3.7, the plasmid DNA was successfully digested, resulting in two bands at 5022 bp and 124 bp, representing the pPEPTIDE Cloning Vector 1 backbone and the excised target protein insert. The backbone was extracted from the agarose gel and purified.



Figure 3.7 Digestion of pPEPTIDE Cloning Vector DNA. The samples was double-digested with BamHI and AseI. The excised insert DNA runs at the expected size of 124 bp.

Phage mimotope samples and pPEPTIDE Cloning Vector 1 were ligated in a 3:1 ratio and 5 μ l of the ligation mixture were subsequently transformed into DH5 α TM-T1^R competent cells.

Phages of the random peptide library require the *E. coli* strain ER2738 as their host. This bacterial strain has a reduced genetic code – it encodes all 20 amino acids with only 32 codons – thereby increasing the relative frequency of residues with a single codon, as well as removing two of the three stop codons. The DNA of phage AIV12.4 contains such a removed stop codon (TAG), which encodes for the amino acid glutamine in ER2738. However, the BL21(DE3) strain used for protein expression does not employ a reduced genetic code. In this strain, TAG encodes for a stop codon, resulting in a truncated fusion protein. This stop codon was removed by site-directed mutagenesis: The first base thymine was exchanged with cytosine to produce the codon CAG, encoding for glutamine. The mutated plasmids were sequenced and successful mutagenesis was analyzed using the freeware BioEdit (Figure 3.8A and Figure 3.8B).

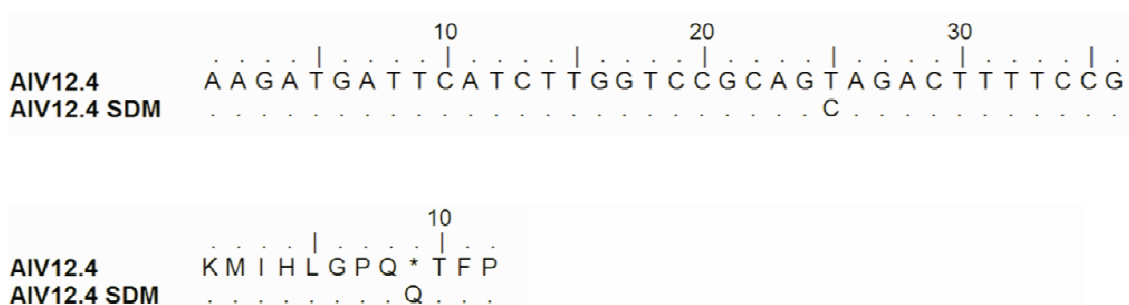


Figure 3.8 Site-directed mutagenesis. In order to remove the stop-codon, site-directed mutagenesis was conducted. Thymine at base 25 was replaced by cytosine, thus exchanging the stop-codon for the original amino acid glutamine.

Sixteen colonies of each transformation were picked and recombinant plasmid DNA was isolated from an overnight culture. 1 μ g of recombinant plasmid DNA was digested with the restriction enzyme EagI in order to check for successful recombination. Successful recombination yielded two bands at 3956 bp and 1157 bp. Figure 3.9 shows the restriction analysis of the obtained AIV3p12.7 plasmid DNA samples isolated from DH5 α TM-T1^R competent cells. Restriction digestion of plasmids of several clones yielded two bands at 3956 bp and 1157 bp (see #1, #2, #4, #5, #6, #7, #8, #9, #10, #11, #13, #14). Several negative clones showed bands running at different sizes (#3, #12, #15, #16). Clone AIV3p12.7 #1 was chosen for subsequent

transformation of BL21(DE3) cells. Clones defined as positive by restriction analysis were also sequenced to screen for potential mutations.

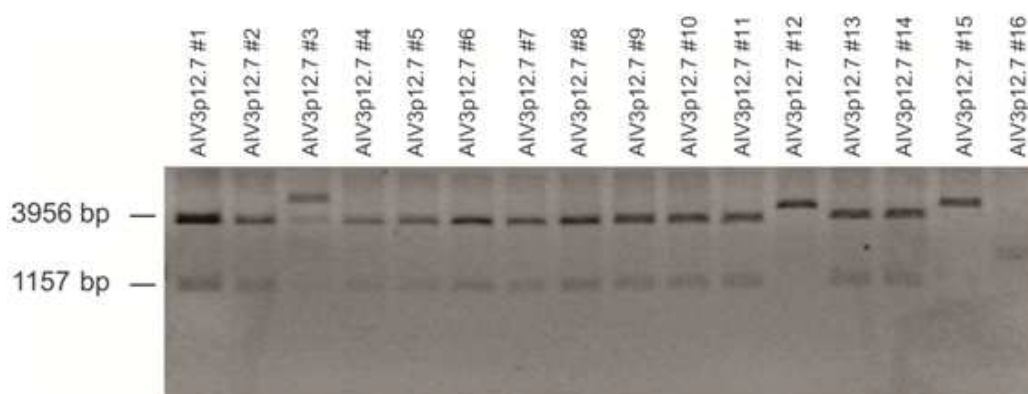


Figure 3.9 Restriction analysis of AIV3p12.7 plasmid DNA samples. Purified plasmid DNA samples were digested with *Eag*I to screen for positive clones. As shown for AIV3p12.7, most clones could be defined as positive by two bands running at 3956 bp and 1157 bp.

Transformed bacteria do not produce protein in equal quantities upon induction. Thus, in order to select a clone with high protein expression for purification, an expression screen was performed. Using AIV3p12.7 as an example (see Figure 3.10), some clones show poor expression of the fusion protein (#2, #4) compared to others (#3, #5, #7). For each mimotope fusion protein, a high level expression clone was selected (here #5) and conserved for protein expression and purification by preparing a 50% glycerol stock for further usage.

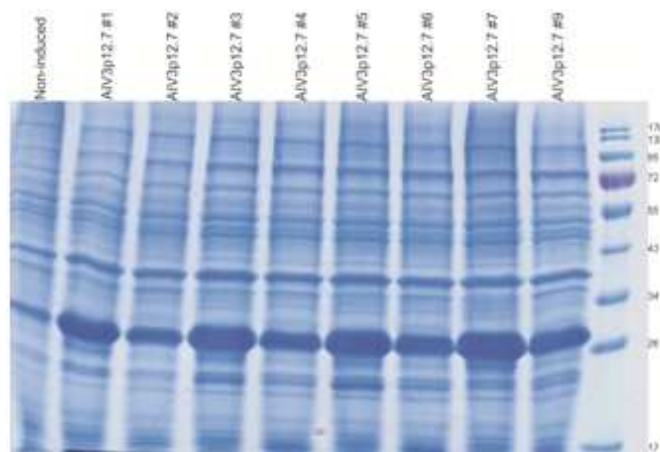


Figure 3.10 Expression screen. In order to determine the clone with the highest protein expression, nine clones were induced with IPTG and protein expression was compared after 5 h. As shown for mimotope AIV3p12.7, protein expression varied markedly. In this case, clone AIV3p12.7 #5 was selected for protein purification.

Protein purification is shown for fusion protein AIV3p12.7 (Figure 3.11). Little protein is lost during the filtering process and in the flow through and washing steps. Most protein is eluted during the elution steps E1 and E2. The elution fractions containing the highest amount of protein were pooled for subsequent buffer exchange and ensuing protein concentration. The amount of total protein purified from a 300 ml culture varied between 5 to 10 mg. As shown for the proteins of the V3 loop, most samples lacked other contaminating proteins (Figure 3.12).

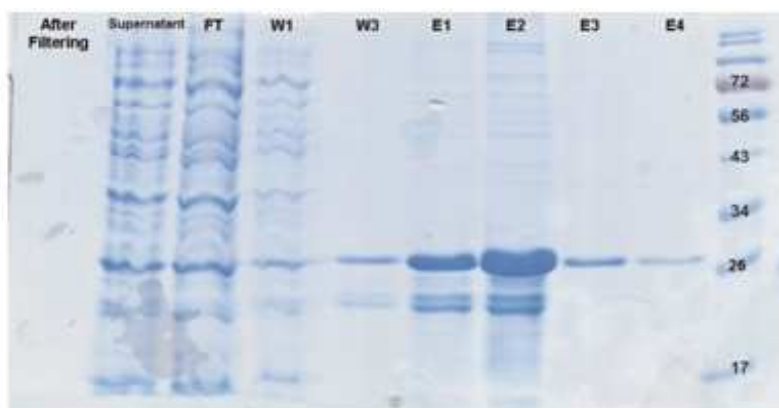


Figure 3.11 Protein purification. As shown for mimotope fusion protein AIV3p12.7, little protein is lost during in the flow through (FT) and washing steps 1 (W1) and 3 (W3). Most protein is eluted during elution step 1 (E1) and 2 (E2), which were combined for subsequent protein gel elution.

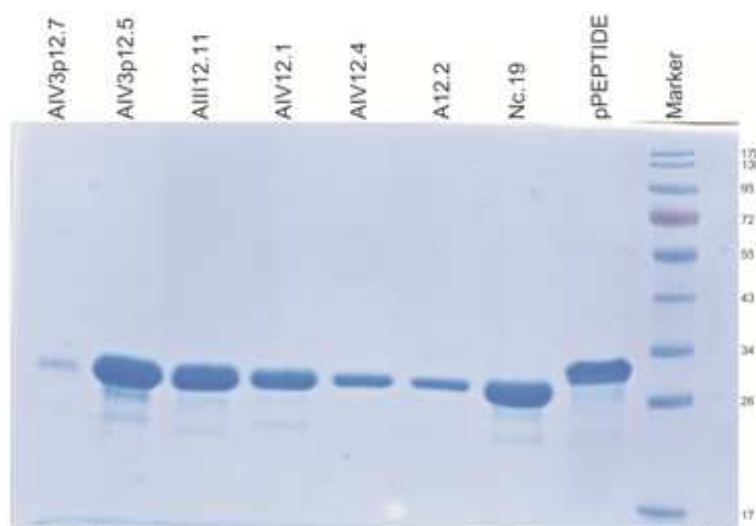


Figure 3.12 Purified proteins of V3 loop group and both controls. As shown for all fusion proteins of the V3 loop group and both controls (Nc.19 and pPEPTIDE) most samples were free of major contaminants.

3.2.2 REACTIVITY PROFILE OF MIMOTOPES IN THE CONTEXT OF FUSION PROTEINS

In order to assess whether the mimotopes are recognized as part of a fusion protein, Western blots were performed. RKI-8 sera of different time points between 2004 and 2007 were used, as well as a panel of rhesus monkey sera with broadly neutralizing activity against different HIV-1 clades (Top-Ten Cohort) (Figures 3.13 – 3.15). Specific binding to the mimotopes in the context of three fusion proteins was observed, especially AIV12.4, which was recognized by RKI-8 sera of various time points as well as several other rhesus monkey sera. Both naïve control sera (RJI2, CF12) did not bind to the mimotope fusion protein, whereas the positive anti-His antibody control detected the fusion protein migrating at a MW of 26 kDa. In the case of AIV12.4, parental serum from the HIV1157i-infected human (1157MVP41m) taken at 41 months of age and a serum pool of HIV-C-infected individuals recognized the mimotope as well (Figure 3.14).

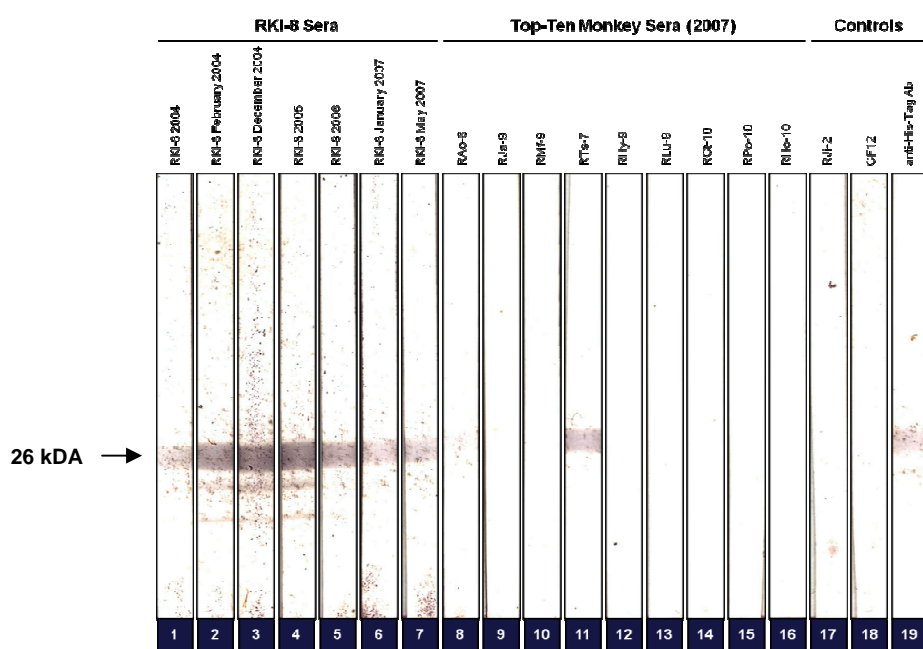


Figure 3.13 Detection of AIV3p12.5 with RKI-8 sera and sera of the Top-Ten Cohort by Western blot. Mimotope fusion protein AIV3p12.5 was detected by all RKI-8 rhesus monkey sera samples and serum of the rhesus monkey RTs-7.

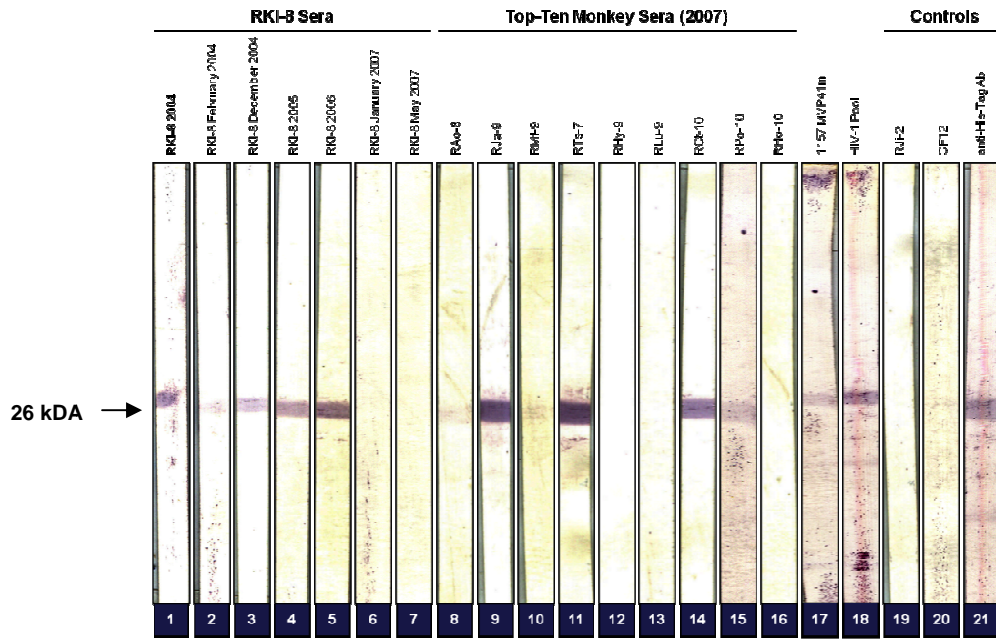


Figure 3.14 Detection of AIV12.4 with RKI-8 sera and sera of the Top-Ten Cohort by Western blot. Mimotope fusion protein AIV12.4 was detected by most RKI-8 rhesus monkey sera samples. Particularly serum of the rhesus monkeys RAO-8, RHy-9, and RTs-7 detected the mimotope fusion protein as well as two human sera samples.

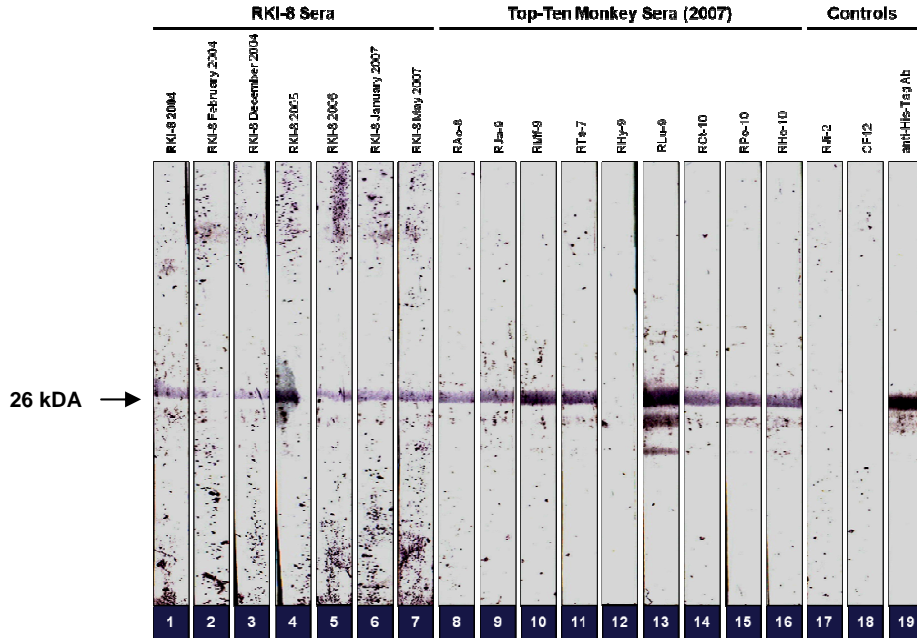


Figure 3.15 Detection of AIV3p12.6 with RKI-8 sera and sera of the Top-Ten Cohort by Western blot. Mimotope fusion protein AIV3p12.6 was detected by all RKI-8 rhesus monkey sera samples as well as all sera of the Top-Ten Cohort except for rhesus monkey RHy-9.

To assess whether the mimotopes in the context of a fusion protein have conserved their structure, ELISAs with sera from RKI-8 were performed. All mimotope fusion proteins were recognized by serum antibodies of RKI-8, including the conformational mimotope A12.2 (Figure 3.16). In order to re-confirm that recognition of the mimotope A12.2 depends on its structural integrity, a conformational ELISA was performed. All mimotopes except A12.2 showed similar signals both under native and reduced conditions. However, for A12.2 the signal was reduced when the protein was denatured (Figure 3.17).

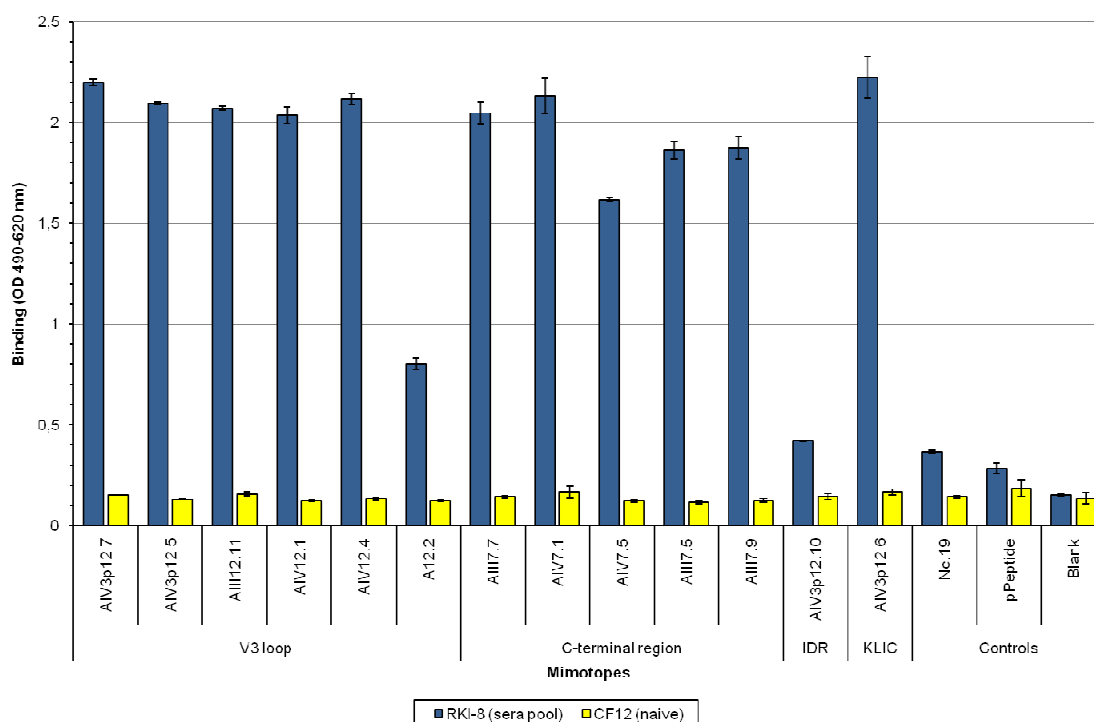


Figure 3.16 Reactivity profile of mimotope fusion proteins by ELISA. All mimotope fusion proteins were tested by ELISA with sera from rhesus monkeys RKI-8 and CF12 (naive). RKI-8 sera recognized all fusion proteins except for AIV3p12.6. A fusion protein with a random phage-displayed peptide (Nc.19) and the original vector backbone were used as negative controls.

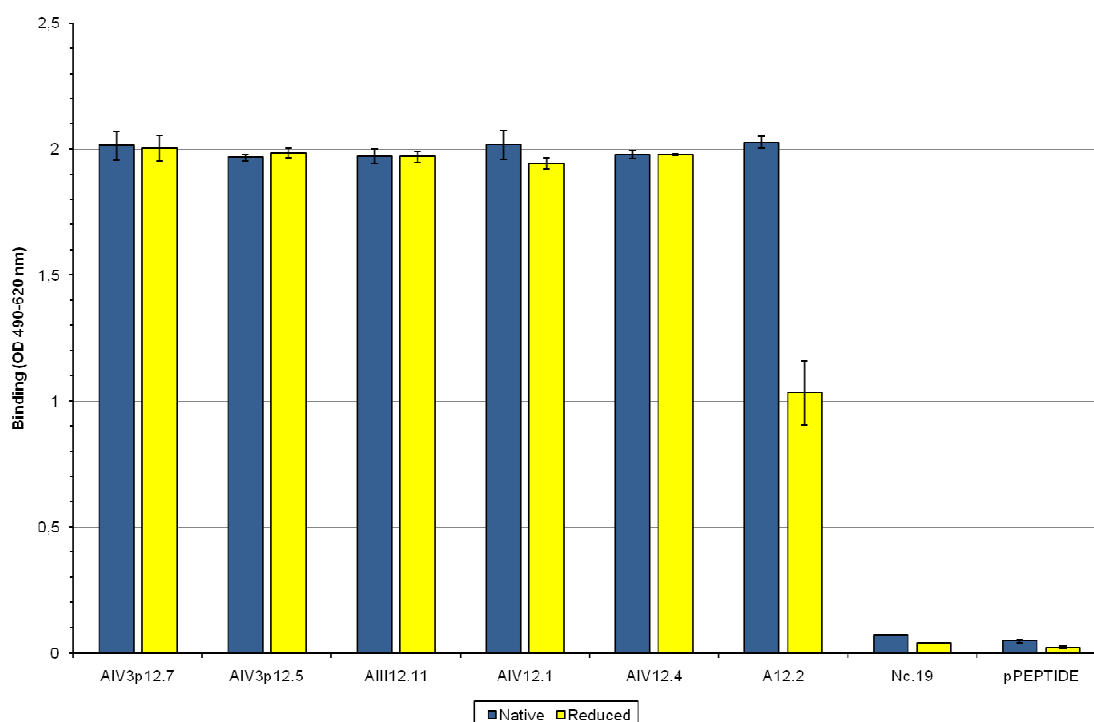


Figure 3.17 **Reactivity profile of V3 loop mimotope fusion proteins under native and reduced conditions by ELISA.** Detection of mimotope fusion proteins of the V3 loop group under native and reduced conditions did not vary markedly except for the conformational mimotope A12.2 whose detection was decreased under reduced conditions. A fusion protein with a random phage-displayed peptide (Nc.19) and the original vector backbone were used as negative controls.

The binding pattern for RKI-8 was confirmed with sera taken at different time points between 2003 and 2007 (Figure 3.18 – 3.21). Interestingly, the reactivity of RKI-8 serum samples taken from different years with AIV12.4 varied as this animal progressed to AIDS (110, 129). Both Western blot and ELISA analysis showed a high affinity for the early time point in 2004. However, reactivity with this linear mimotope varied with serum samples taken at later time points (2005 to 2007). Similar results were observed with mimotope fusion proteins AIII12.11 and AIV12.1.

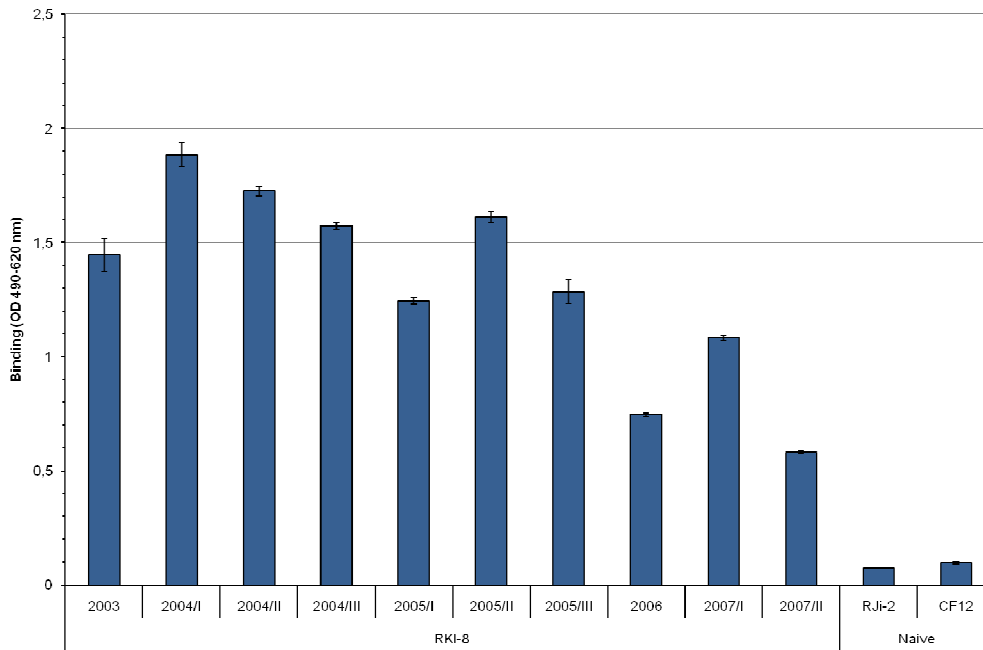


Figure 3.18 Cross-reactivity of mimotope fusion protein AIII12.1 with RKI-8 sera of different time points. Sera of naïve rhesus monkeys RJI-2 and CF12 were used as negative controls.

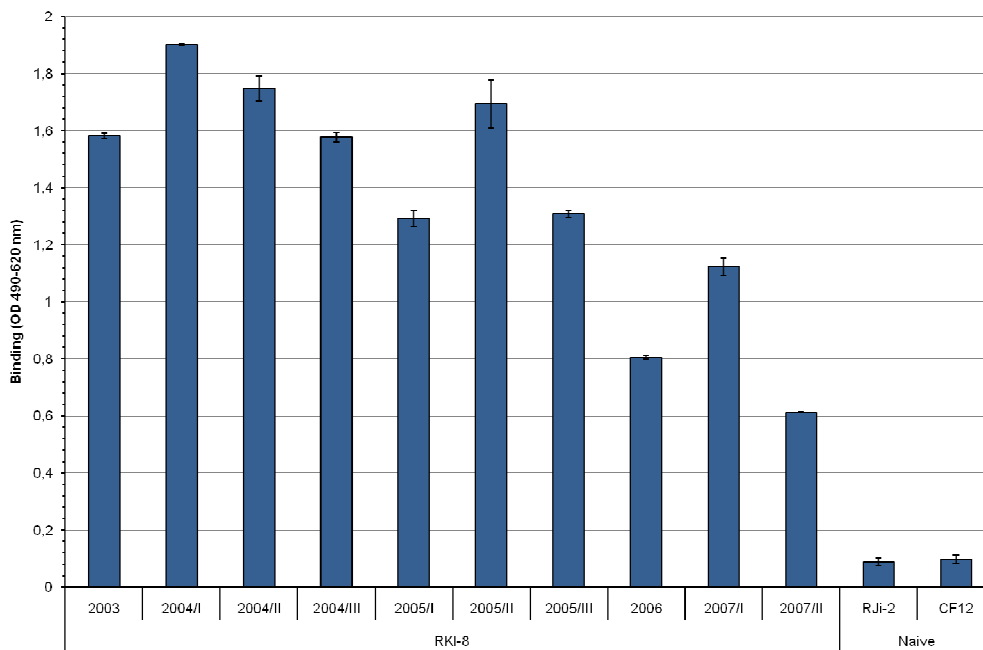


Figure 3.19 Cross-reactivity of mimotope fusion protein AIV12.1 with RKI-8 sera of different time points. Sera of naïve rhesus monkeys RJI-2 and CF12 were used as negative controls.

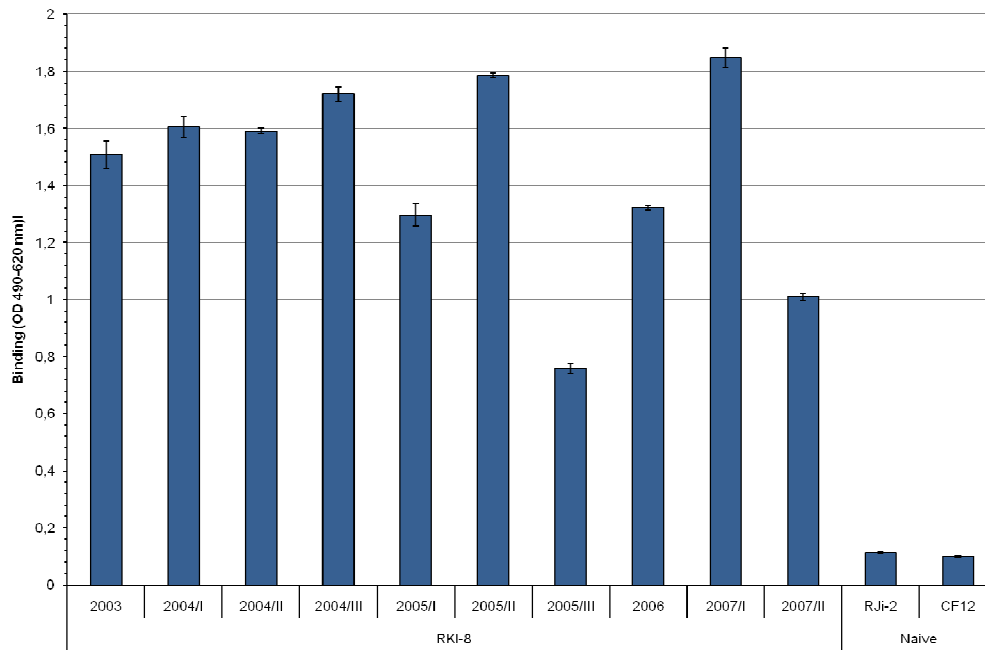


Figure 3.20 Cross-reactivity of mimotope fusion protein AIV12.4 with RKI-8 sera of different time points. Sera of naïve rhesus monkeys Rji-2 and CF12 were used as negative controls.

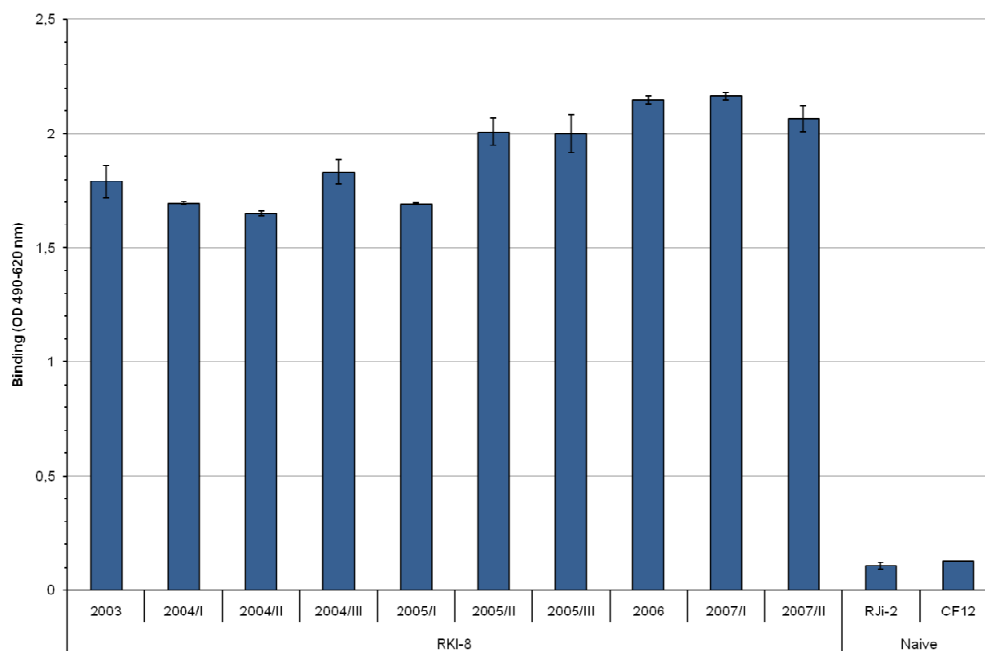


Figure 3.21 Cross-reactivity of mimotope fusion protein AIV3p12.6 with RKI-8 sera of different time points. Sera of naïve rhesus monkeys Rji-2 and CF12 were used as negative controls.

In order to analyze whether the HIV-1 Env mimotope motif groups represent common antibody epitopes found in sera with broadly reactive nAbs, all fusion proteins were tested by ELISA analysis using Top-Ten Cohort rhesus monkey sera with broadly neutralizing activity against different HIV-1 clades (Table 3.1, Figures 3.22 – 3.24). Individual serum samples from three rhesus monkeys were used. Notably, rhesus monkey sera recognized selected V3 loop mimics and the mimotope representing the KLIC motif. Mimotope AIV12.4 was shown to be most cross-reactive.

In summary, the Western blot and ELISA results show that the mimotopes expressed in the context of fusion proteins have conserved their structural integrity and were detected by the rhesus monkey serum from which they had been selected as well as by other sera from the cohort.

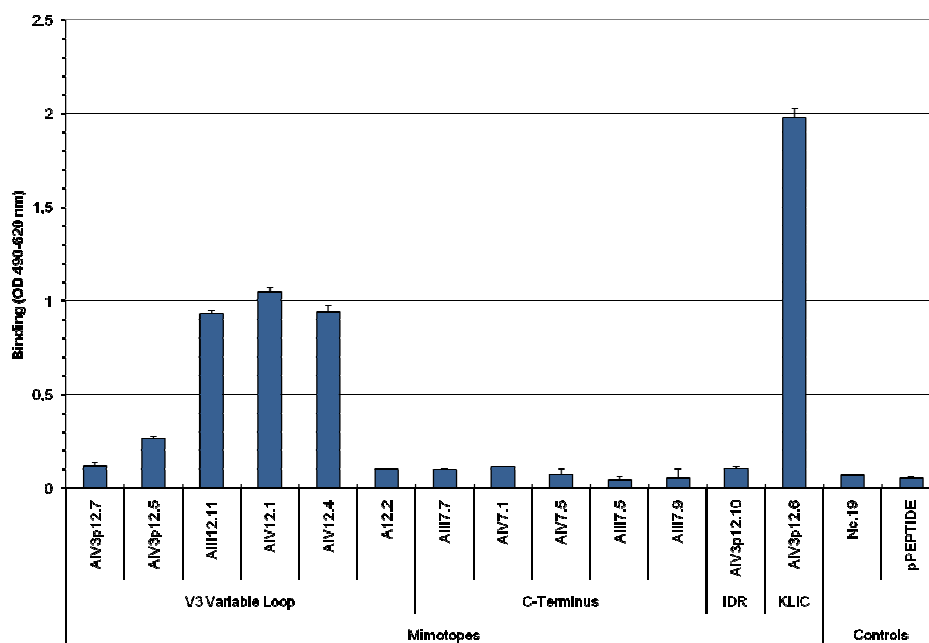


Figure 3.22 Cross-reactivity of RAO-8 serum with mimotope fusion proteins. Serum of rhesus monkey RAO-8 cross-reacted with mimotope fusion proteins AIII12.11, AIV12.1, and AIV12.4 of the V3 loop group, and AIV3p12.6 resembling the KLIC motif.

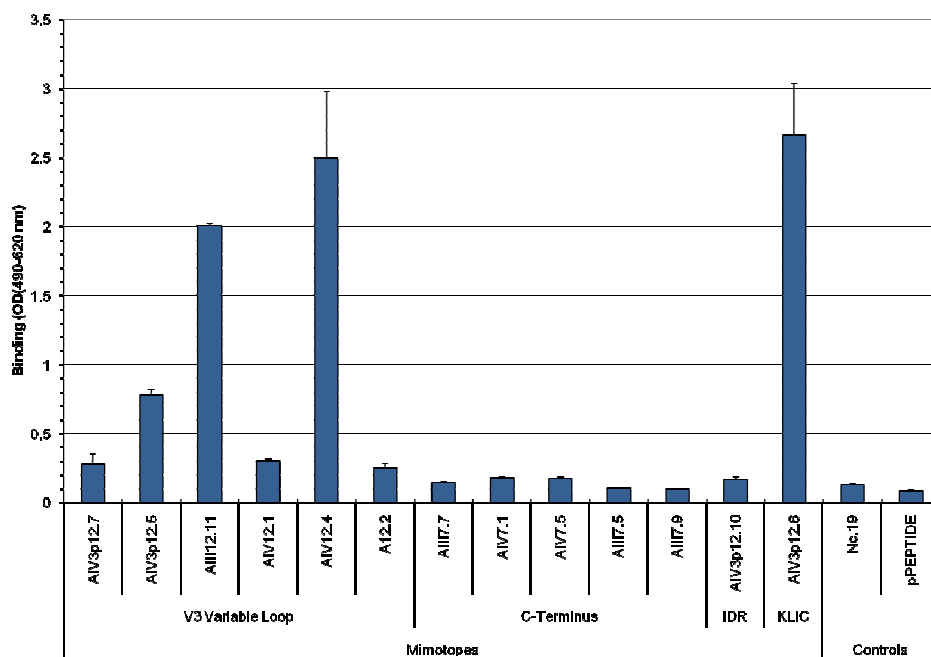


Figure 3.23 Cross-reactivity of RTs-7 serum with mimotope fusion proteins. Serum of rhesus monkey RAO-8 cross-reacted with mimotope fusion proteins AIV3p12.5, AIII12.1, and AIV12.4 of the V3 loop group, and AIV3p12.6 resembling the KLIC motif.

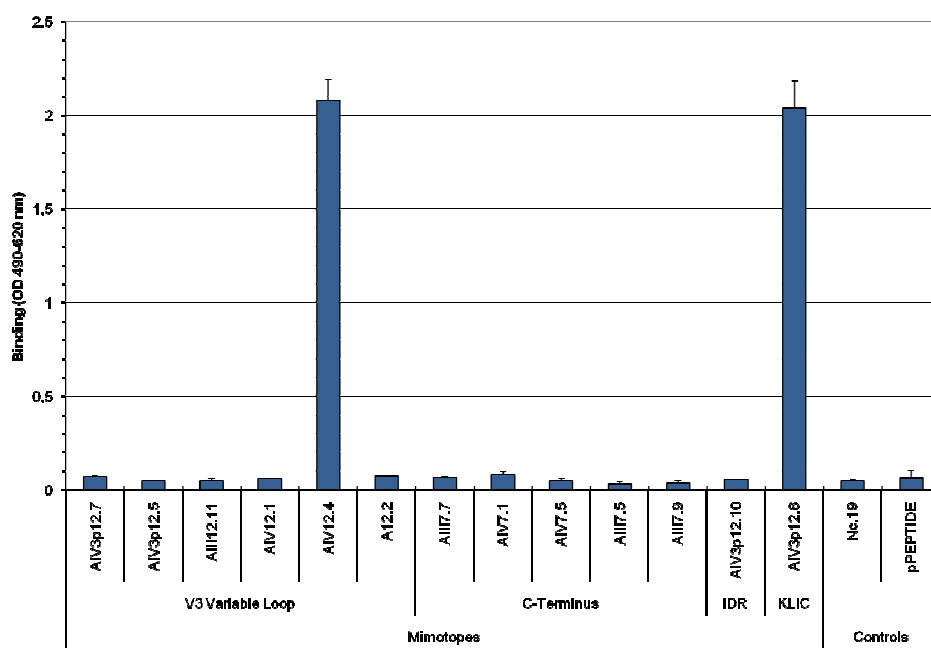


Figure 3.24 Cross-reactivity of RJa-9 serum with mimotope fusion proteins. Serum of rhesus monkey RAO-8 cross-reacted with mimotope fusion proteins AIV12.4 of the V3 loop group, and AIV3p12.6 resembling the KLIC motif.

3.2.3 IMMUNIZATION STUDIES IN MICE

In order to analyze whether the identified mimotopes are immunogenic, a vaccine study in mice was performed. One DNA inoculation was used to prime the immune system with the entire HIV-1 envelope glycoprotein, followed by phage boosting to focus the antibody response to a certain area of the molecule (Figure 3.25).

Recombinant phages were grouped according to their peptide motifs and selected phages were combined into five mixtures to immunize mice (Table 3.2). All mice received one initial priming immunization with a DNA vector encoding gp160_{SHIV-1157ip}; this single DNA inoculation was previously shown to be insufficient to induce binding antibodies or nAbs (133). After one DNA prime, all mice were boosted four times with recombinant phage particles (intervals of 4-5 weeks) (Figure 3.25). The obtained immune sera were checked for binding antibodies and the presence of nAbs.

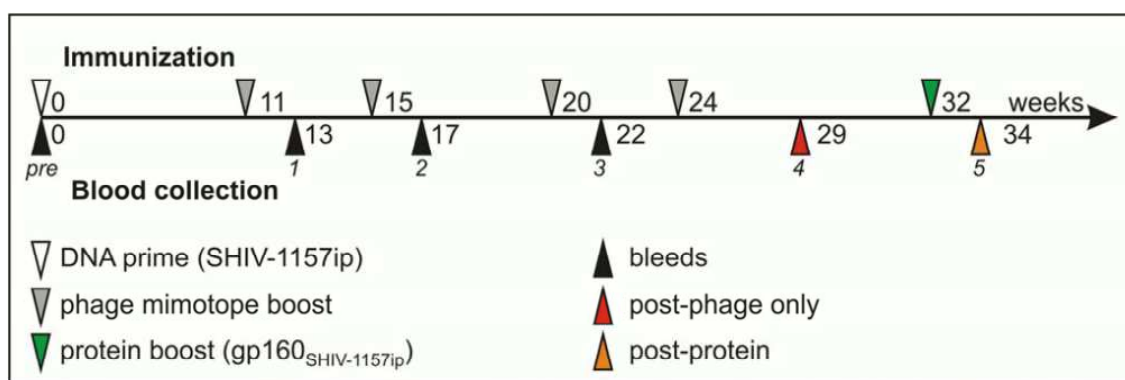


Figure 3.25 Schedule for immunizations and blood collections in mouse study (132). After collecting the initial pre-bleed samples, all mice were primed with SHIV-1157ip *env* DNA (white triangle; Methods) and subsequently immunized with four phage boosts (grey triangles) every 4-5 weeks. Blood samples were drawn 2-5 weeks after each boost (black/red/orange triangles). Furthermore, 11 mice received a final boost with trimeric gp160_{SHIV-1157ip} (green triangle).

Antibody binding titers for each group against homologous gp160_{SHIV-1157 ip} were measured after the four phage boosts using ELISA analysis (Figure 3.26A). The mean titers ranged from 1:125 to 1:1362, and almost all mice developed antibodies against the viral envelope glycoprotein. The lowest titer was observed in the MPER group, whereas the highest was observed for the C-terminal domain. However, antibody binding to HIV-1 gp160 does not necessarily correlate with neutralization of HIV-1. Therefore, post-phage boost sera (4th bleed) were analyzed for neutralization of a

heterologous HIV-1 clade B strain, HIV_{SF162.LS}; indeed, 59% of the animals had developed cross-clade anti-HIV-1 nAbs (Figure 3.26B). The mean IC₅₀ in all groups ranged from 1:19 to 1:70. Of note, four out of the six mice immunized with mimotopes representing the C-terminal domain had nAbs, including two animals with IC₅₀ values > 1:100.

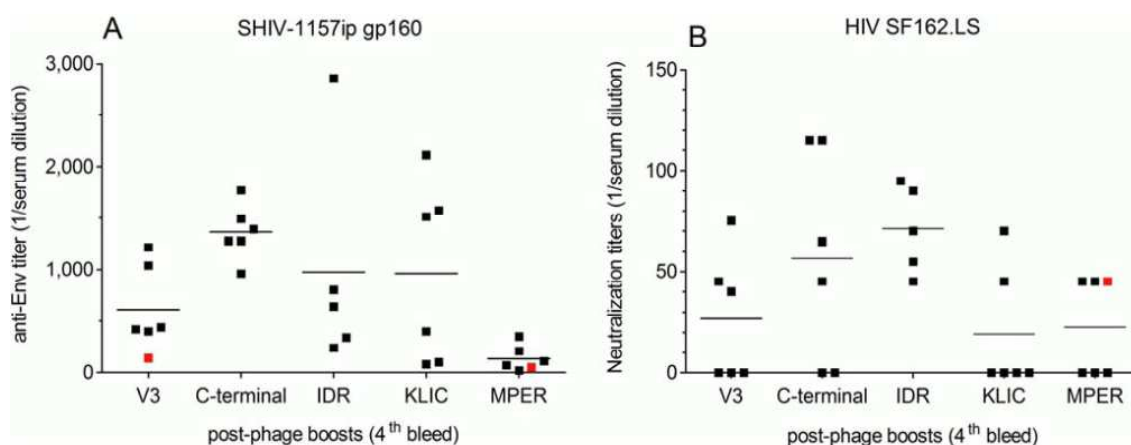


Figure 3.26 Analysis of post-phage boost (4th bleed) mouse immune sera (132). (A) Anti-Env titers. Reciprocal serum dilution of each mouse for trimeric SHIV-1157ip gp160 is shown. (B) Neutralization. Bleeds were tested for 50% neutralization (IC₅₀) against heterologous HIV-1_{SF162.LS}. IC₅₀ of each group are shown. Groups represent mimotopes from the V3 loop (V3) and C-terminal domain of gp120 (C-terminal); immunodominant (IDR), KLIC, and membrane proximal external region (MPER) of gp41. Red symbols indicate the use of the 3rd bleed due to limited serum availability.

In order to assess whether additional boosting with native, multimeric gp160 could enhance nAb responses, the mice with the highest titers (6 from the V3, 1 from the C-terminal, 2 from each, the IDR and KLIC group) were boosted with gp160_{SHIV-1157ip}. The sera obtained after completion of the DNA prime/recombinant phage boosts were compared with the sera obtained after the additional protein boost. Mean Env-ELISA titers were 1:1,220 after four phage-boosts compared to 1:2,748 after the additional protein boost. This increase did not reach statistical significance ($p = 0.1574$, Figure 3.27A). NAb titers against both homologous SHIV-1157ip and heterologous HIV-1_{SF162.LS} were not significantly raised either ($p = 0.8544$ and $p = 0.3935$, respectively; Figure 3.27B), which suggests that maximal immune responses had already been induced by DNA prime/phage boosting. Therefore, the higher ELISA antibody titer after the additional protein boost did not correlate with higher neutralizing ability.

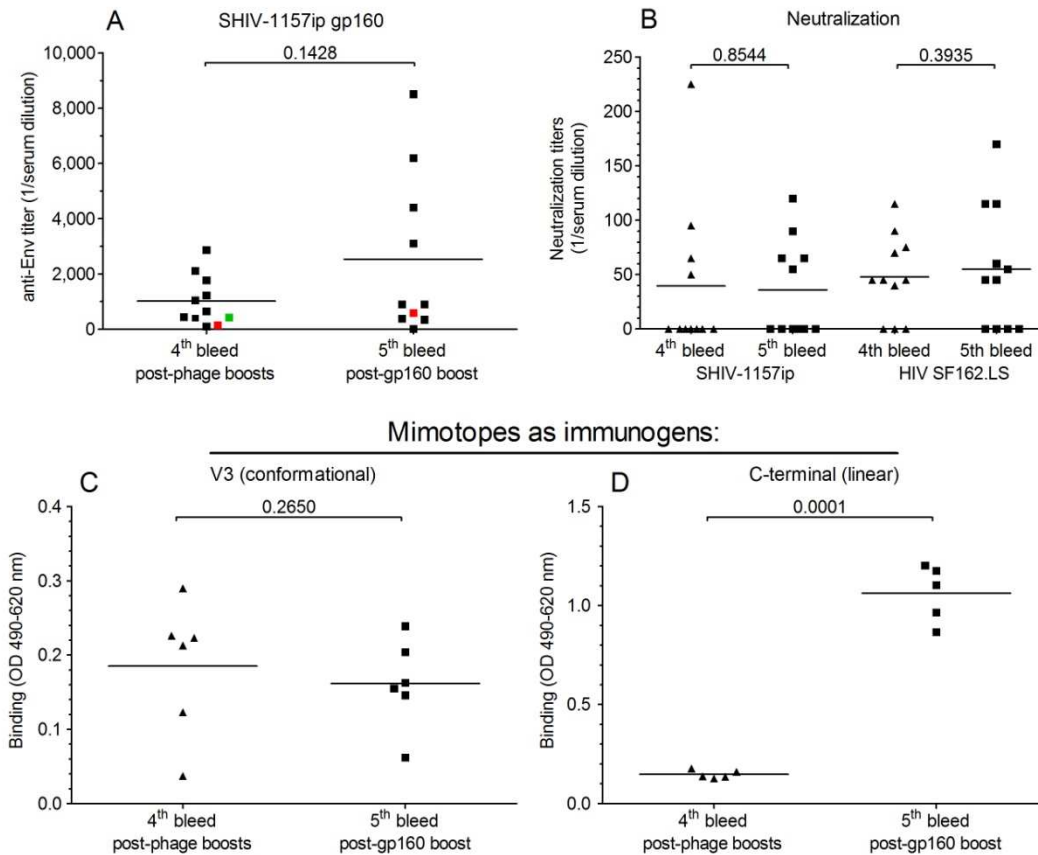


Figure 3.27 Analysis of immune mouse sera after DNA prime/phage boosting or DNA prime/phage + gp160 boosting (132). (A) Anti-Env titers. Reciprocal serum dilution of each mouse for the post-phage boosts and post-gp160 boost is shown. Red symbols indicate 3rd vs. 5th bleed, green symbol indicates no matching 5th bleed, both due to serum restrictions. (B) Neutralization with mouse immune sera. Bleeds were tested for 50% neutralization (IC₅₀) against homologous SHIV-1157ip and heterologous HIV-1SF162.LS. Post-phage boosts (triangles) are compared to post-gp160 boost (squares). (C, D) Vaccination-induced antibody responses against conformational and linear mimotopes. Mimotopes were cloned and expressed as fusion proteins. The latter were used to test whether DNA priming/phage boosting (triangles) or DNA priming/phage+gp160 boosting (squares) of mice had induced antibodies against the original phage-encoded peptide mimotopes. Sera from two selected mice were tested for reactivity to each of the mimotopes used in the immunization mixture. (C) Mouse #1.4, immunized with potential conformational V3-loop mimotopes. (D) Mouse #2.5, immunized with linear C-terminal mimotopes.

3.2.4 ANALYSIS OF VACCINATION-INDUCED ANTIBODIES

In further experiments, it was tested whether antibodies induced by the different immunogens reacted differently with native versus denatured HIV-1 gp160. It is possible that the mixture of similar but not identical mimotopes may broaden the immune response and induce antibodies against conformational rather than linear epitopes. The V3 mimotopes show incomplete linear homology to gp160 and may contain conformational homologies, whereas the gp120 C-terminal mimotopes are linear.

The post-protein boost sera (5th bleed) were analyzed for reactivity against native and reduced HIV-1 gp160 by ELISA analysis (Figure 3.28). Two sera from mice immunized with V3-loop mimotopes showed decreased binding to denatured Env (7-14-fold). In contrast, the signal obtained with serum from the mouse boosted with mimotopes representing the HIV-1 gp120 C-terminus decreased only 1.7-fold. These findings suggest that the V3-loop mimotopes induced antibody responses to conformational regions, whereas the gp120 C-terminal mimotopes mainly induced linear antibody responses.

Mimotope-induced antibodies against the gp41 IDR (Figure 3.28; mouse #3.2) showed slightly higher binding upon denaturation of gp160_{SHIV-1157ip}; whereas serum antibodies from mouse #4.2 immunized with the potentially conformational KLIC motifs exhibited decreased binding to denatured protein (Figure 3.28), suggesting that they recognize conformational epitopes on the viral envelope glycoprotein.

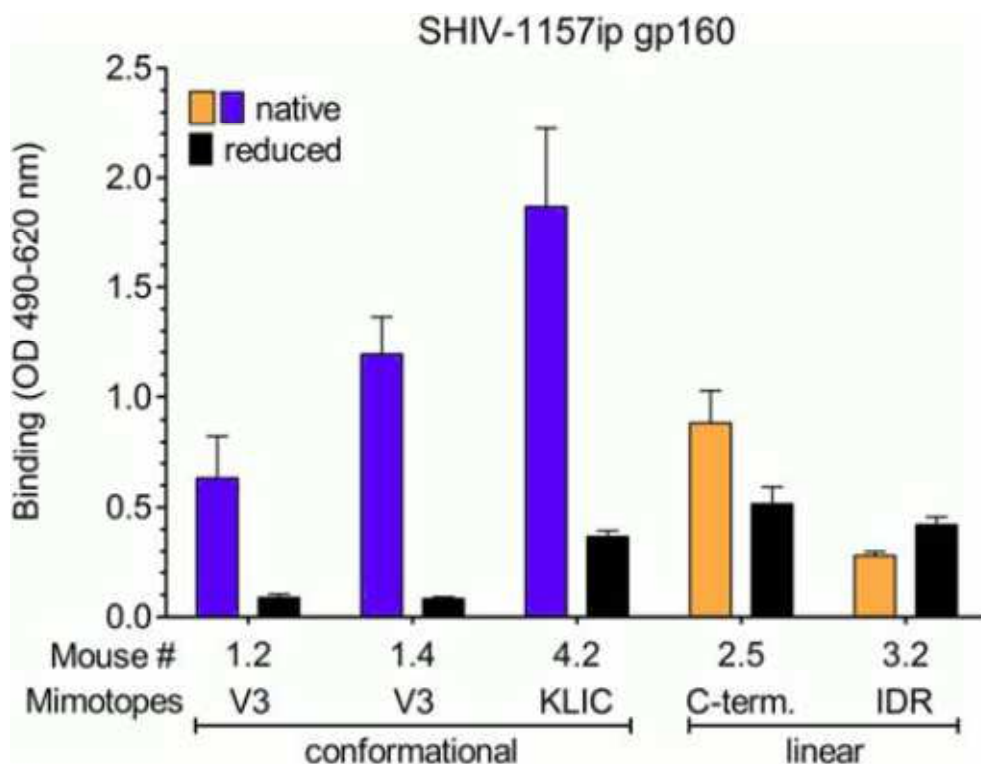


Figure 3.28 Reducing Env ELISA (132). Mouse immune sera were tested for binding to native (blue/orange bars) and reduced Env (black bars). Three mice were immunized with potential conformational mimotopes (#1.2, 1.4 and 4.2; blue), two mice with linear mimotopes (#2.5 and 3.2; orange).

3.2.4 ANTI-MIMOTOPE ANTIBODIES

In order to analyze whether the last boost with trimeric gp160_{SHIV-1157ip} enhanced the immune response against the actual mimotopes, all sera were tested against the mimotope fusion proteins by ELISA analysis. Due to limited availability of mouse sera, one mouse from each group was selected and the 4th and 5th bleeds were used for analysis (#1.4 and #2.5) (Figure 3.27 C and D). It was shown that the protein boost did not increase binding antibody titers against the six mimotopes representing the V3 loop (Figure 3.27 C). In contrast, the HIV gp160 boost significantly increased the immune response against the linear mimotopes of the C-terminal gp120 domain by 6 to 9-fold (Figure 3.27 D). These findings suggest that the conformational V3-loop mimotopes induced structure-specific antibody responses that were stimulated maximally by the one-time DNA priming followed by recombinant phage boosting. As mentioned above, the additional Env protein boost did not increase nAb titers.

These findings support the data shown in Figure 3.28 that mainly antibodies to linear epitopes were boosted by the additional gp160 protein boost, which resulted in higher binding antibody titers. However, gp160 boost-induced antibodies did not significantly improve the neutralization capacity as shown in Figure 3.27 B. Potentially conformational anti-mimotope responses (as represented by the V3 and KLIC groups) were not boosted by the last protein boost (Figure 3.27 C; data for KLIC not shown). It seems that the DNA prime/phage boost strategy already achieved maximum responses in nAb titers, although the binding titers showed moderate but still insignificant increases after the additional boost with the entire protein.

The antibody induction against the individual mimotopes of each group was also analyzed with ELISA studies (Figures 3.29 – 3.36) and re-confirmed the previous result. It was shown that an additional protein boost with trimeric gp160_{SHIV-1157ip} further augmented the antibody response to linear mimotopes of the C-terminal domain of gp120, the IDR, or the KLIC motif. However, there was no additional increase in nAbs (Figure 3.27 B). In contrast, the antibody response to mimotopes of the V3 loop on gp120 was not enhanced by the additional protein boost, which re-confirmed the previous observation that only linear epitopes were boosted by trimeric gp160_{SHIV-1157ip}.

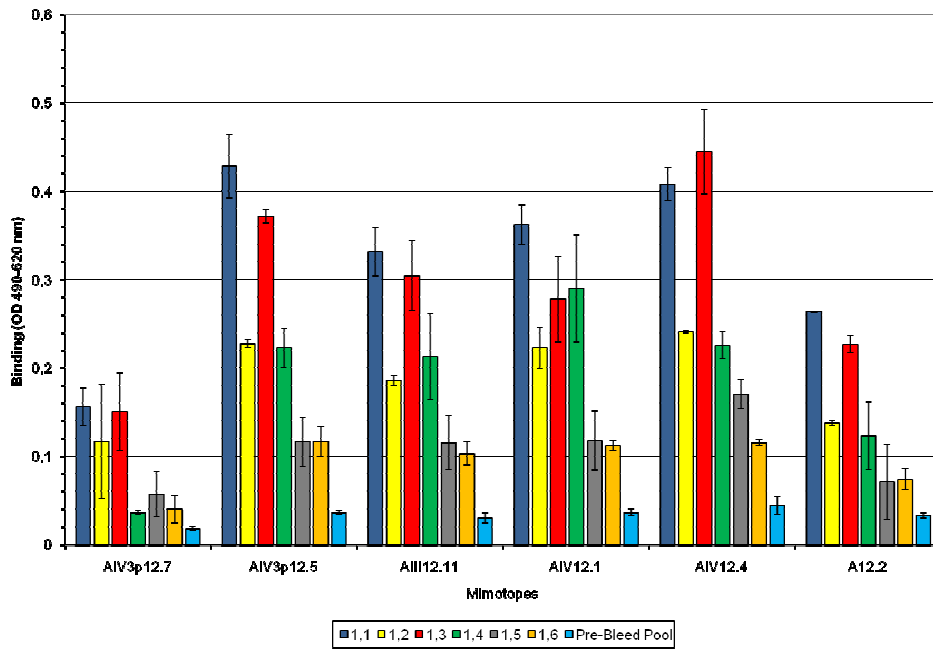


Figure 3.29 Binding to individual mimotopes of the V3 loop group after 4th boost. Mouse immune sera samples taken after the 4th boost were tested for binding to individual mimotopes.

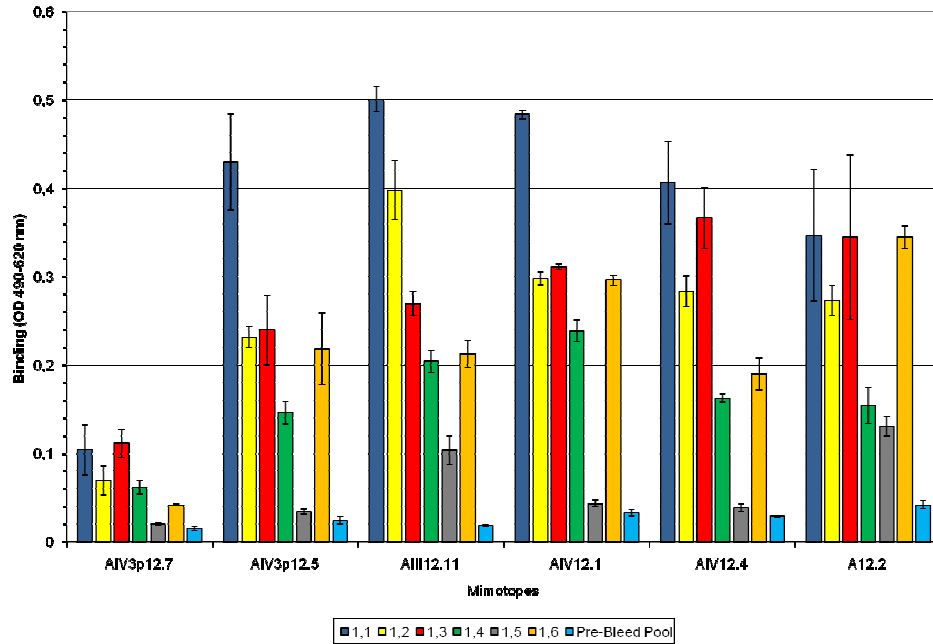


Figure 3.30 Binding to individual mimotopes of the V3 loop group after 5th boost. Mouse immune sera samples taken after the 5th boost were tested for binding to individual mimotopes.

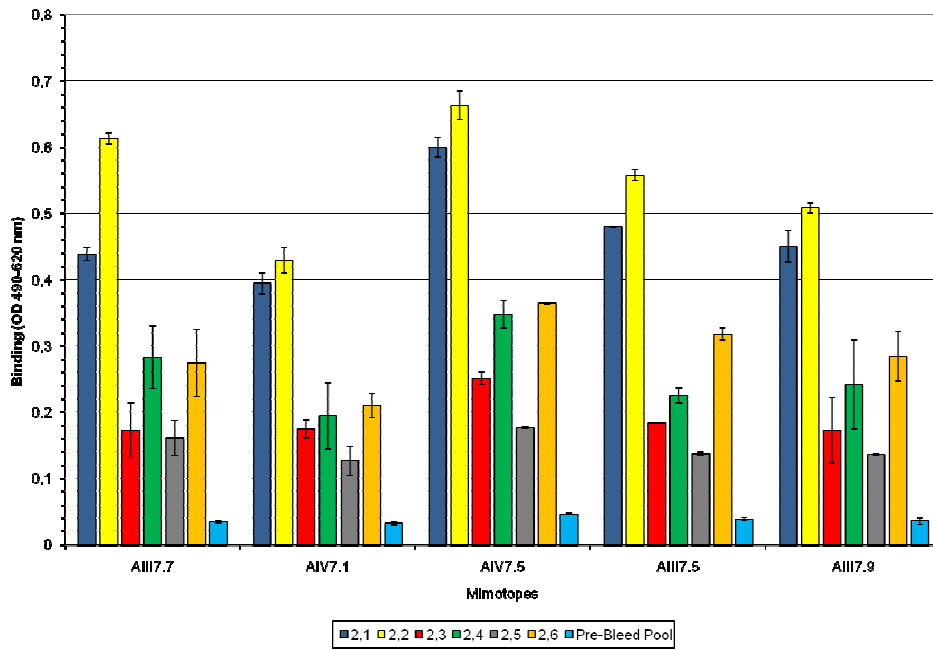


Figure 3.31 Binding to individual mimotopes of the C-terminus group after 4th boost. Mouse immune sera samples taken after the 4th boost were tested for binding to individual mimotopes.

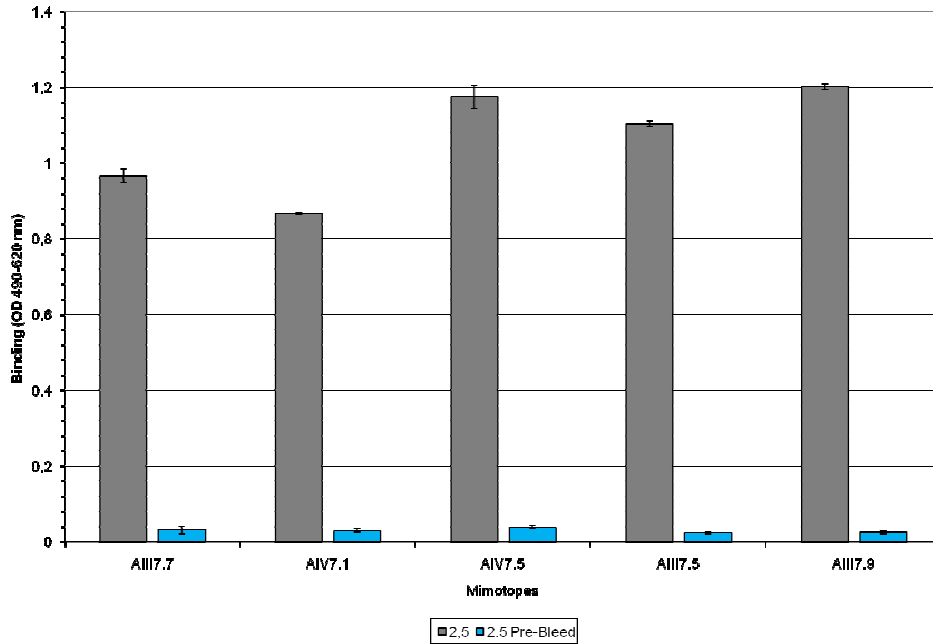


Figure 3.32 Binding to individual mimotopes of the C-terminus group after 5th boost. Mouse immune sera samples taken after the 5th boost were tested for binding to individual mimotopes.

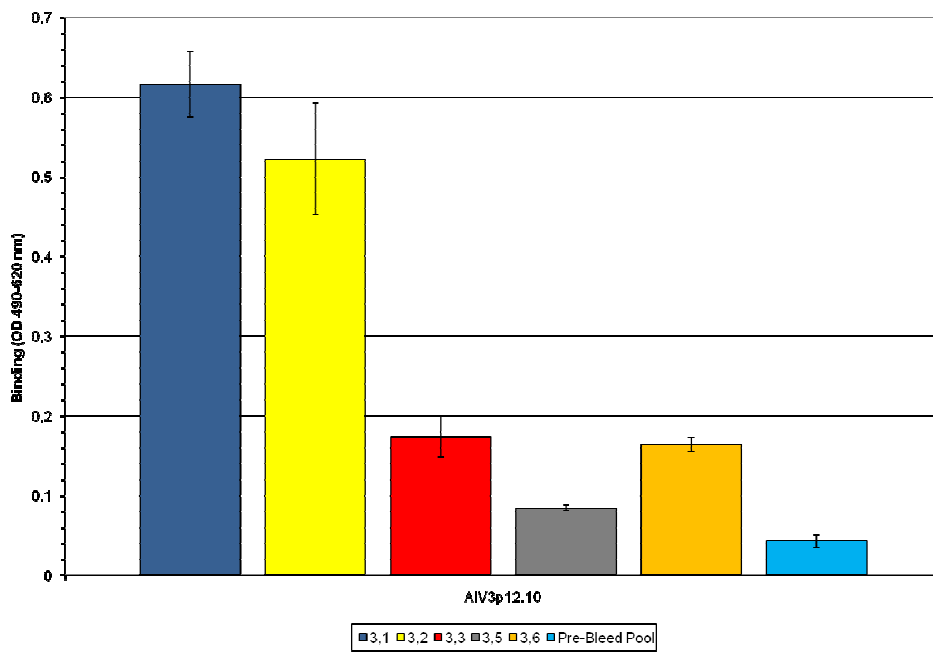


Figure 3.33 Binding to individual mimotopes of the IDR group after 4th boost. Mouse immune sera samples taken after the 4th boost were tested for binding to individual mimotopes.

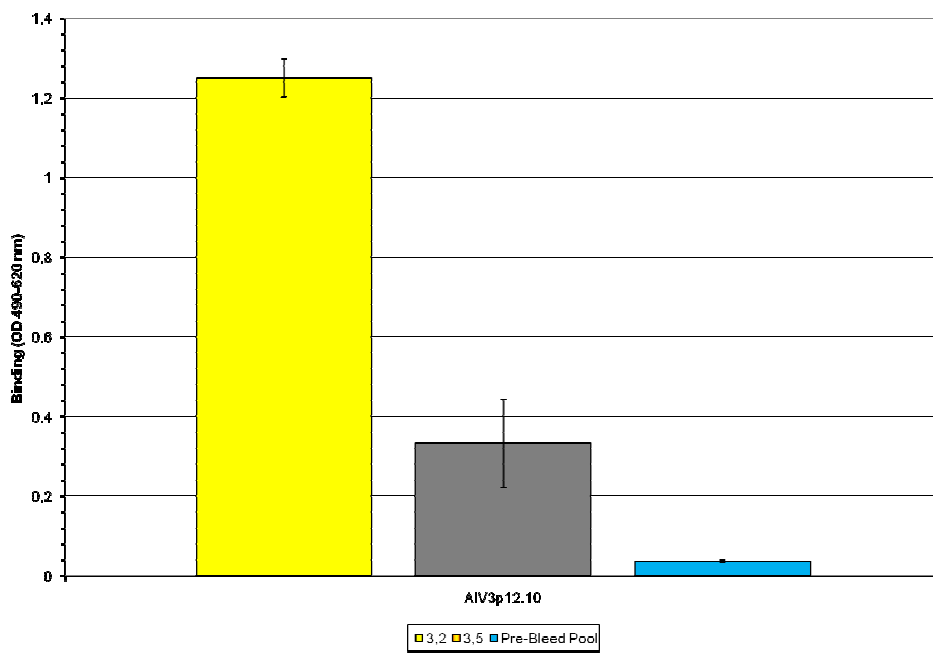


Figure 3.34 Binding to individual mimotopes of the IDR group after 5th boost. Mouse immune sera samples taken after the 5th boost were tested for binding to individual mimotopes.

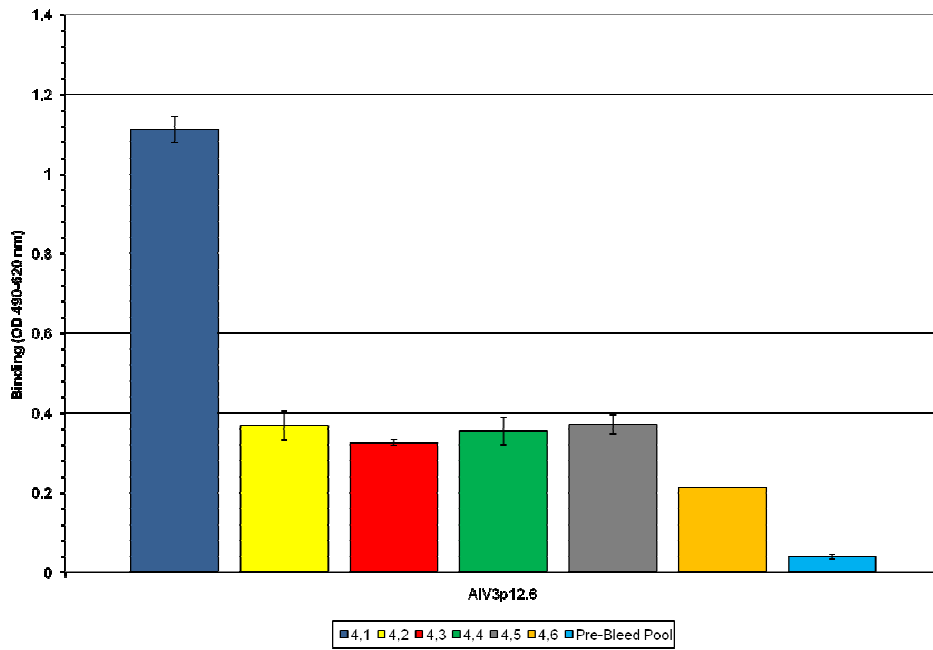


Figure 3.35 Binding to individual mimotopes of the KLIC group after 4th boost. Mouse immune sera samples taken after the 4th boost were tested for binding to individual mimotopes.

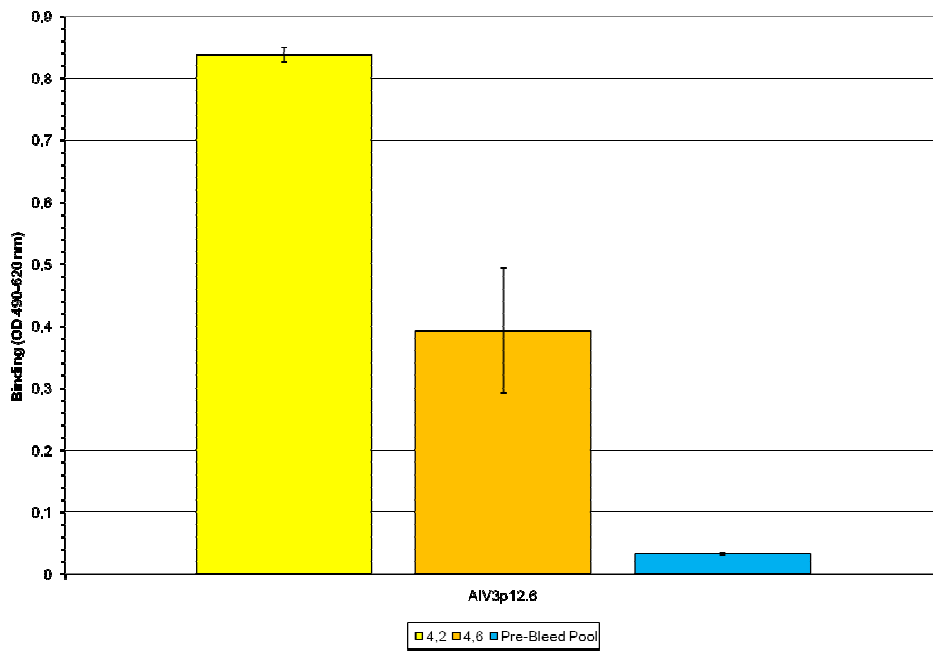


Figure 3.36 Binding to individual mimotopes of the KLIC group after 5th boost. Mouse immune sera samples taken after the 5th boost were tested for binding to individual mimotopes.

4 DISCUSSION

4.1 IDENTIFICATION OF PROTECTIVE EPITOPES

Passive immunization studies in primates challenged with recombinant SHIVs have provided strong evidence that antibodies provide complete protection from infection. These animal studies were based on the challenge of primates with SHIVs before or after passive administration of several human nmAbs (60-68) [reviewed in (69)]. The corresponding epitopes that have induced these nmAbs can therefore be considered as protective. Additional *in vitro* neutralization studies also proved the broad reactivity of these nmAbs. These nmAbs neutralized many primary strains of HIV-1 of various clades alone and particularly well when used in combination (70-73). One way to identify such antibodies and their cognate epitopes, is to analyze sera with high-titer, cross-clade nAbs. Conformational epitopes are of particularly high interest, as they might represent conserved regions on the HIV-1 envelope glycoprotein.

One such epitope is A12.2, which had been identified by computational analysis. Its dependence on structural integrity had been confirmed by dot spot analysis, which demonstrated recognition of native HIV-1 clade C gp160 by phage affinity-purified rhesus monkey antibodies, but none when the protein was denatured. By screening sera with high-titer, cross-clade nAbs with random peptide phage display libraries in conjunction with computational analysis for conformational epitopes, it is possible to select disease-specific mimotopes that may lead to the identification of novel immunogens.

4.2 A12.2 – A CONFORMATIONAL MIMOTOPE

Despite its sequence variability, the V3 loop appears to have a highly specific and conserved structure because of its role in co-receptor interaction and selectivity (134, 135). Its specificity in co-receptor interaction may pose a target for antibody-mediated neutralization (92, 136). The V3 loop mimotopes identified as part of these studies may represent conformational mimics of this loop and successfully induced nAbs in mice.

Binding of these nAbs to HIV-1 Env was significantly reduced after protein denaturation, which suggests that they are specific for conformational epitopes on HIV-1 Env. This finding was further confirmed by ELISA studies with recombinant fusion proteins. In contrast, sera from mice boosted with mimotopes that represent the linear HIV-1 gp120 C-terminus failed to show significant differences in binding upon denaturation of Env. This finding implies that the V3-loop mimotopes induced conformational antibody responses, whereas the gp120 C-terminus mimotopes induced predominantly linear antibody responses. Because of the importance of the V3 loop in co-receptor selectivity and its conserved structure, these results provide new impulses for HIV-1 vaccine research.

4.3 TIME-DEPENDENT VARIATION IN MIMOTOPE RECOGNITION AND CROSS-RECOGNITION OF MIMOTOPES

Mimotope fusion proteins AIII12.11, AIV12.1, AIV12.4 of the V3 loop group, and mimotope AIV3p12.6 representing the KLIC motif exhibited the highest recognition by other sera samples from different time points. For the KLIC motif, this is not surprising, given the overall immunogenicity of this structural element. More detailed analyzes of mimotope recognition across the course of the disease and their correlation with the viral load might provide additional insight as to how strongly these antibodies correlate with protection of disease progression.

Since all rhesus monkeys of the Top Ten-Cohort had developed high-titer, broadly reactive nAbs, cross-recognition of the RKI-8 mimotopes in the context of fusion proteins was tested by ELISA for rhesus monkeys RAo-8, RTs-7, and RJa-9. Cross-recognition was observed for mimotopes of the V3 loop except for mimotopes AIV3p12.7 and A12.2. Particularly mimotope AIV12.4 exhibited high cross-reactivity with all three sera. Interestingly, all mimotopes representing the conserved C-terminus of gp120 did not show binding to other rhesus monkey sera. Similar results for mimotope AIV12.4 were obtained with Western blot analysis. Comparative analysis of the humoral immune response of sera from rhesus monkeys or patients with high-titer, broadly reactive nAbs may lead to the identification of common epitopes that have induced the very same antibodies that conveyed protection. Of course, this approach

would yield the greatest success if conducted on a large scale basis, which might not be feasible in an academic setting.

Epitopes or mimotopes cross-recognized by various sera from HIV-infected individuals with high nAb-titers are frequently considered to be vulnerable elements of HIV-1 Env that may induce effective abs. Dissection of the humoral immune response of such patients, e.g. by phage display analysis, usually results in the identification of immunodominant regions, such as the KLIC motif, which predominantly induce antibodies (118). The immunodominance of such regions is frequently correlated with vulnerability to neutralization. However, the frequency of epitope-detection is not linked to neutralization and mimotopes with little or no cross-reactivity may be of greater use for the generation of nAbs. The rhesus monkey of the Top Ten-Cohort may have developed an unusually effective immune response against the HIV-1 envelope glycoprotein in the context of natural infection, perhaps due to the fact that the SHIV strain, SHIV-1157ip, encodes the *env* gene of a recently transmitted virus. Newly infected partners from a cohort of HIV discordant couples were shown to be infected with HIV-1 clade C strains that were more easily neutralized than contemporaneous virus from the person that transmitted the virus to them, but the recently transmitted HIV-1 clade C isolated also had shorter V-loops (137, 138). Env molecules of recently transmitted HIV-1 clade C viruses may exhibit a more open configuration with a higher likelihood of inducing broadly reactive nAbs. The rhesus monkey sera with broadly nAbs from the Top Ten-Cohort may help identify non-immunodominant but structurally conserved domains of HIV-1 Env. Although this might be a rare response in the context of a natural infection, it may be induced with mimotopes that direct the immune response only to the part linked to nAbs.

4.4 IMMUNIZATION OF MICE WITH SELECTED MIMOTOPES

Past immunization studies with whole phage particles generated peptide-specific antibodies and protective immune responses in animals (35, 139, 140). However, these studies were of limited efficacy. Thus, a novel DNA prime/recombinant phage boost strategy was developed as part of this work instead of using serial immunization regimens with recombinant phages expressing mimotopes. An initial, single priming

with a DNA vector encoding for the entire gp160 molecule was introduced, which has not been shown to induce binding or nAb responses (133). This initial, single DNA priming was intended to imprint the immune system with the correct image of native gp160 structures, without diverting antibody responses to immunodominant but ultimately insignificant regions of the viral envelope glycoprotein. It was hypothesized that the subsequent multiple phage immunizations with mimotopes of a defined, singular Env region would focus the humoral immune response on significant structural domains. This immunofocusing strategy was shown to be successful and resulted in anti-Env antibodies. The repetitive immunization with distinct mimotopes to focus the immune response on one or a few neutralizing epitopes might yield a larger proportion and higher titer of nAbs. Although the use of selected epitopes or mimotopes as vaccines to focus the humoral immune response on neutralizing domains is still in its beginning, several studies have shown the successful induction of nAbs against V2 and/or V3 (141-143). The phage boosts in this study were performed with five different mimotope groups, each corresponding to designated regions of the envelope glycoprotein, and helped identify novel HIV Env regions that are capable of inducing nAbs in the absence of the overpowering and distorting influence of immunodominant regions, which would have otherwise diverted the immune response: For the first time, the C-terminal domain of gp120, which had previously been identified as immunogenic but never linked to nAb responses, was shown to induce nAbs. It is important to note that the DNA prime/phage mimotope boosts strategy seems to have induced the maximal nAb response to a given domain, since additional boosting with native, multimeric gp160 failed to produce higher nAb titers.

4.5 CONCLUDING REMARKS

To conclude, these results confirmed the success of this novel approach to induce cross-clade neutralizing antibodies against HIV-1 Env via immunofocusing. By combining phage display and 3DEX analysis, the humoral immune response of a rhesus monkey with broadly reactive nAbs was dissected and novel antigenic mimics that represent functionally conserved Env domains, such as the V3 loop or the C-terminus of gp120, were identified. The employed DNA prime/phage boost strategy yielded cross-clade

nAbs against HIV clades B and C and was able to link the C-terminus of gp120 to antibody-mediated neutralization in mice for the first time.

Given the time-dependent differences in epitope recognition, it might be interesting to isolate mimotopes from various time points after infection. This might lead to the identification of epitopes that are recognized throughout the course of infection, which either may protect from disease progression or represent immunodominant regions that induce antibodies that do not convey protection.

These findings suggest that it might be useful to direct the humoral immune response to well-defined neutralizing epitopes rather than to immunize with native molecules or constructs based on entire molecules. Large molecules contain both neutralizing and non-neutralizing epitopes and the latter might divert the humoral immune response. In addition, most neutralizing epitopes are conformation-dependent, which has not been incorporated into HIV-1 vaccine design so far. Peptide immunogens representing linear epitopes might therefore fail to induce antibodies to conserved regions and rather promote the induction of antibodies to regions that may easily escape the selective pressure exerted by the immune system.

The results further strengthen the hypothesis that the V3 loop represents a “semi-conserved region” on HIV-1 Env. Although its primary structure is not well-conserved, its conserved tertiary structure and conformation qualify the V3 loop as a promising target for the development of a HIV-1 vaccine. Since several rhesus monkeys of the Top-Ten Cohort recognized mimotopes representing the V3 loop, it may be proposed that such antibodies play a fundamental role in controlling infection in these animals.

Since the induction of antibodies against HIV-1 in mice does not necessarily correlate with the induction of similar and equally potent antibodies in human beings, potential vaccine candidates need to be tested in non-human primate models for the induction of nAbs prior to testing in patients. This requirement is emphasized by the fact that the adenovirus-based vaccine of the STEP trial showed promising results in mice, but failed in clinical trials. Therefore, non-human primate models will have to be further optimized to mimic HIV-1 infection in human beings as closely as possible.

5 SUMMARY

ENGLISH

Despite intense research efforts, a safe and effective HIV-1/AIDS vaccine still remains far away. HIV-1 escapes the humoral immune response through various mechanisms and until now, only a few nAbs have been identified. A promising strategy to identify new epitopes that may elicit such nAbs is to dissect and analyze the humoral immune response of sera with broadly reactive nAbs. The identified epitopes recognized by these antibodies might then be incorporated into a vaccine to elicit similar nAbs and thus provide protection from HIV-1 infection.

Using random peptide phage display libraries, the Ruprecht laboratory has identified the epitopes recognized by polyclonal antibodies of a rhesus monkey with high-titer, broadly reactive nAbs that had been induced after infection with a SHIV encoding *env* of a recently transmitted HIV-1 clade C. The laboratory analyzed phage peptide inserts for conformational and linear homology with computational assistance. Several of the identified peptides mimicked domains of the original HIV-1 clade Env, such as conformational V3 loop epitopes and the conserved linear region of the gp120 C-terminus.

As part of this work, these mimotopes were analyzed for cross-reactivity with other sera obtained from rhesus monkeys with nAbs and antibody recognition was shown for several mimotopes, particularly those representing the V3 loop. In addition, these mimotopes were incorporated into a novel DNA prime/phage boost strategy to analyze the immunogenicity of such phage-displayed peptides. Mice were primed only once with HIV-1 clade C gp160 DNA and subsequently boosted with mixtures of recombinant phages. This strategy was designed to focus the humoral immune response on a few, selected Env epitopes (immunofocusing) and induced HIV-1 clade C gp160 binding antibodies and cross-clade nAbs. Furthermore, the C-terminus of gp120, a conserved HIV Env region, was linked to the induction of nAbs for the first time. The identification of such conserved antigens may lead to the development of a vaccine that is capable of inducing broadly reactive nAbs that might confer protection from HIV-1 infection.

DEUTSCH

Trotz enormer Forschungsleistungen liegt ein sicherer und effektiver Impfstoff gegen HIV-1/AIDS immer noch in weiter Ferne. HIV-1 entkommt der humoralen Immunantwort aufgrund mehrerer Mechanismen und daher wurden bis zu diesem Zeitpunkt nur wenige neutralisierende Antikörper identifiziert. Eine vielversprechende Strategie zur Identifizierung neuer Epitope, die neutralisierende Antikörper induzieren könnten, ist die Analyse von Seren mit solchen Antikörper. Die dabei identifizierten Epitope könnten dann zur Herstellung eines Impfstoffes verwendet werden, der ähnliche neutralisierende Antikörper induziert und damit vor einer Infektion mit HIV-1 schützt.

Mittels Phage-Display hat das Labor von Ruth Ruprecht mehrere solcher Epitope von polyklonalen Antikörpern aus Rhesus Affen mit hochtitrigen, breit-neutralisierenden Antikörpern identifiziert. Diese Antikörper wurden nach einer Infektion mit einem SHIV induziert, das das virale Hüllprotein eines kürzlich übertragenen HIV-1 clade C Virus enthält. Die Phagenpeptide wurden auf konformelle und lineare Homologie mittels einer Computer Software untersucht. Mehrere dieser Peptide entsprachen Domänen des viralen Hüllproteins, wie z.B. konformelle V3 loop Epitope and Epitope des linearen C-Terminus von gp120.

Im Rahmen dieser Arbeit wurden diese Mimotope auf Kreuzreaktivität mit anderen Seren von Rhesus Affen mit neutralisierenden Antikörpern untersucht. Dabei wurden insbesondere die Mimotope des V3 loops von anderen Seren erkannt. Des Weiteren wurden diese Phagen-Mimotope im Rahmen einer neuen DNA prime/phage boost Strategie zur Immunisierung verwendet. Mäuse wurden einmalig mit HIV-1 clade C gp160 DNA immunisiert und anschließend mehrfach mit rekombinanten Phagen geboostet. Mittels dieser Strategie sollte das Immunsystem auf einige, spezielle Epitope des viralen Hüllproteins fokussiert werden (Immunofocusing). Hierbei wurden HIV-1 clade gp160-bindende Antikörper und breit-neutralisierende Antikörper induziert.

Des Weiteren konnten zum ersten Mal neutralisierende Antikörper gegen den C-terminus von gp120, einer konservierten Region des viralen Hüllproteins, induziert werden. Die Identifikation solcher konservierter Mimotope kann zur Entwicklung von einem HIV-1 Impfstoff beitragen, der breit neutralisierende Antikörper induziert, die vor einer Infektion schützen können.

6 REFERENCES

1. UNAIDS. 2010. UNAIDS Report on the Global AIDS Epidemic 2010.
2. Walker BD, Burton DR. 2008. Toward an AIDS vaccine. *Science* 320: 760-4
3. Rowland-Jones S. 2008. A winding road towards an HIV vaccine. *Eur J Immunol* 38: 13-4
4. Barouch DH, Korber B. 2010. HIV-1 vaccine development after STEP. *Annu Rev Med* 61: 153-67
5. Steinbrook R. 2007. One step forward, two steps back--will there ever be an AIDS vaccine? *N Engl J Med* 357: 2653-5
6. Barre-Sinoussi F, Chermann JC, Rey F, Nugeyre MT, Chamaret S, Gruest J, Dauguet C, Axler-Blin C, Vezinet-Brun F, Rouzioux C, Rozenbaum W, Montagnier L. 1983. Isolation of a T-lymphotropic retrovirus from a patient at risk for acquired immune deficiency syndrome (AIDS). *Science* 220: 868-71
7. Gallo RC, Salahuddin SZ, Popovic M, Shearer GM, Kaplan M, Haynes BF, Palker TJ, Redfield R, Oleske J, Safai B, et al. 1984. Frequent detection and isolation of cytopathic retroviruses (HTLV-III) from patients with AIDS and at risk for AIDS. *Science* 224: 500-3
8. Levy JA, Hoffman AD, Kramer SM, Landis JA, Shimabukuro JM, Oshiro LS. 1984. Isolation of lymphocytopathic retroviruses from San Francisco patients with AIDS. *Science* 225: 840-2

9. Rabson AB, Martin MA. 1985. Molecular organization of the AIDS retrovirus. *Cell* 40: 477-80
10. Coffin J, Haase A, Levy JA, Montagnier L, Oroszlan S, Teich N, Temin H, Toyoshima K, Varmus H, Vogt P, et al. 1986. Human immunodeficiency viruses. *Science* 232: 697
11. Clavel F, Guetard D, Brun-Vezinet F, Chamaret S, Rey MA, Santos-Ferreira MO, Laurent AG, Dauguet C, Katlama C, Rouzioux C, et al. 1986. Isolation of a new human retrovirus from West African patients with AIDS. *Science* 233: 343-6
12. Viruses ICoTo. 2009. Taxonomy of Viruses.
13. Flint SJ, American Society for Microbiology. 2009. *Principles of virology*. Washington, DC: ASM Press
14. Perrin L, Kaiser L, Yerly S. 2003. Travel and the spread of HIV-1 genetic variants. *Lancet Infect Dis* 3: 22-7
15. Thomson MM, Perez-Alvarez L, Najera R. 2002. Molecular epidemiology of HIV-1 genetic forms and its significance for vaccine development and therapy. *Lancet Infect Dis* 2: 461-71
16. Julg B, Goebel FD. 2005. HIV genetic diversity: any implications for drug resistance? *Infection* 33: 299-301
17. Wyatt R, Sodroski J. 1998. The HIV-1 envelope glycoproteins: fusogens, antigens, and immunogens. *Science* 280: 1884-8

18. Kindt TJ, Goldsby RA, Osborne BA, Kuby J. 2007. *Kuby immunology*. New York: W.H. Freeman. xxii, 574, A-31, G-12, AN-27, I-27 p. pp.
19. Peterlin BM, Trono D. 2003. Hide, shield and strike back: how HIV-infected cells avoid immune eradication. *Nat Rev Immunol* 3: 97-107
20. Frankel AD, Young JA. 1998. HIV-1: fifteen proteins and an RNA. *Annu Rev Biochem* 67: 1-25
21. Doms RW, Trono D. 2000. The plasma membrane as a combat zone in the HIV battlefield. *Genes Dev* 14: 2677-88
22. Berger EA, Doms RW, Fenyo EM, Korber BT, Littman DR, Moore JP, Sattentau QJ, Schuitemaker H, Sodroski J, Weiss RA. 1998. A new classification for HIV-1. *Nature* 391: 240
23. Karlsson Hedestam GB, Fouchier RA, Phogat S, Burton DR, Sodroski J, Wyatt RT. 2008. The challenges of eliciting neutralizing antibodies to HIV-1 and to influenza virus. *Nat Rev Microbiol* 6: 143-55
24. Pantaleo G, Graziosi C, Demarest JF, Cohen OJ, Vaccarezza M, Gantt K, Muro-Cacho C, Fauci AS. 1994. Role of lymphoid organs in the pathogenesis of human immunodeficiency virus (HIV) infection. *Immunol Rev* 140: 105-30
25. Pope M, Haase AT. 2003. Transmission, acute HIV-1 infection and the quest for strategies to prevent infection. *Nat Med* 9: 847-52
26. Das AT, Berkhout B. 1995. Efficient extension of a misaligned tRNA-primer during replication of the HIV-1 retrovirus. *Nucleic Acids Res* 23: 1319-26

-
27. McMichael AJ, Borrow P, Tomaras GD, Goonetilleke N, Haynes BF. 2010. The immune response during acute HIV-1 infection: clues for vaccine development. *Nat Rev Immunol* 10: 11-23
 28. Lackner AA, Veazey RS. 2007. Current concepts in AIDS pathogenesis: insights from the SIV/macaque model. *Annu Rev Med* 58: 461-76
 29. Levy JA. 2009. HIV pathogenesis: 25 years of progress and persistent challenges. *AIDS* 23: 147-60
 30. Simon V, Ho DD. 2003. HIV-1 dynamics in vivo: implications for therapy. *Nat Rev Microbiol* 1: 181-90
 31. Pantaleo G, Menzo S, Vaccarezza M, Graziosi C, Cohen OJ, Demarest JF, Montefiori D, Orenstein JM, Fox C, Schragger LK, et al. 1995. Studies in subjects with long-term nonprogressive human immunodeficiency virus infection. *N Engl J Med* 332: 209-16
 32. Mikhail M, Wang B, Saksena NK. 2003. Mechanisms involved in non-progressive HIV disease. *AIDS Rev* 5: 230-44
 33. Kaslow RA, Carrington M, Apple R, Park L, Munoz A, Saah AJ, Goedert JJ, Winkler C, O'Brien SJ, Rinaldo C, Detels R, Blattner W, Phair J, Erlich H, Mann DL. 1996. Influence of combinations of human major histocompatibility complex genes on the course of HIV-1 infection. *Nat Med* 2: 405-11
 34. Agrawal L, Lu X, Qingwen J, VanHorn-Ali Z, Nicolescu IV, McDermott DH, Murphy PM, Alkhatib G. 2004. Role for CCR5Delta32 protein in resistance to R5, R5X4, and X4 human immunodeficiency virus type 1 in primary CD4+ cells. *J Virol* 78: 2277-87

35. Humbert M, Antoni S, Brill B, Landersz M, Rodes B, Soriano V, Wintergerst U, Knechten H, Staszewski S, von Laer D, Dittmar MT, Dietrich U. 2007. Mimotopes selected with antibodies from HIV-1-neutralizing long-term non-progressor plasma. *Eur J Immunol* 37: 501-15
36. Parren PW, Gauduin MC, Koup RA, Poignard P, Fiscicaro P, Burton DR, Sattentau QJ. 1997. Relevance of the antibody response against human immunodeficiency virus type 1 envelope to vaccine design. *Immunol Lett* 57: 105-12
37. Fenouillet E, Gluckman JC, Jones IM. 1994. Functions of HIV envelope glycans. *Trends Biochem Sci* 19: 65-70
38. Liu J, Bartesaghi A, Borgnia MJ, Sapiro G, Subramaniam S. 2008. Molecular architecture of native HIV-1 gp120 trimers. *Nature* 455: 109-13
39. Pantophlet R, Burton DR. 2006. GP120: target for neutralizing HIV-1 antibodies. *Annu Rev Immunol* 24: 739-69
40. Zwick MB, Saphire EO, Burton DR. 2004. gp41: HIV's shy protein. *Nat Med* 10: 133-4
41. Modrow S, Hahn BH, Shaw GM, Gallo RC, Wong-Staal F, Wolf H. 1987. Computer-assisted analysis of envelope protein sequences of seven human immunodeficiency virus isolates: prediction of antigenic epitopes in conserved and variable regions. *J Virol* 61: 570-8
42. Willey RL, Rutledge RA, Dias S, Folks T, Theodore T, Buckler CE, Martin MA. 1986. Identification of conserved and divergent domains within the envelope gene of the acquired immunodeficiency syndrome retrovirus. *Proc Natl Acad Sci U S A* 83: 5038-42

43. Kwong PD, Wyatt R, Robinson J, Sweet RW, Sodroski J, Hendrickson WA. 1998. Structure of an HIV gp120 envelope glycoprotein in complex with the CD4 receptor and a neutralizing human antibody. *Nature* 393: 648-59
44. Zolla-Pazner S. 2004. Identifying epitopes of HIV-1 that induce protective antibodies. *Nat Rev Immunol* 4: 199-210
45. Diskin R, Marcovecchio PM, Bjorkman PJ. 2010. Structure of a clade C HIV-1 gp120 bound to CD4 and CD4-induced antibody reveals anti-CD4 polyreactivity. *Nat Struct Mol Biol* 17: 608-13
46. Montero M, van Houten NE, Wang X, Scott JK. 2008. The membrane-proximal external region of the human immunodeficiency virus type 1 envelope: dominant site of antibody neutralization and target for vaccine design. *Microbiol Mol Biol Rev* 72: 54-84, table of contents
47. Wyatt R, Kwong PD, Desjardins E, Sweet RW, Robinson J, Hendrickson WA, Sodroski JG. 1998. The antigenic structure of the HIV gp120 envelope glycoprotein. *Nature* 393: 705-11
48. Kwong PD, Wyatt R, Sattentau QJ, Sodroski J, Hendrickson WA. 2000. Oligomeric modeling and electrostatic analysis of the gp120 envelope glycoprotein of human immunodeficiency virus. *J Virol* 74: 1961-72
49. Burton DR, Desrosiers RC, Doms RW, Koff WC, Kwong PD, Moore JP, Nabel GJ, Sodroski J, Wilson IA, Wyatt RT. 2004. HIV vaccine design and the neutralizing antibody problem. *Nat Immunol* 5: 233-6
50. McMichael AJ. 2006. HIV vaccines. *Annu Rev Immunol* 24: 227-55

51. Keating GM, Noble S. 2003. Recombinant hepatitis B vaccine (Engerix-B): a review of its immunogenicity and protective efficacy against hepatitis B. *Drugs* 63: 1021-51
52. Belshe RB, Graham BS, Keefer MC, Gorse GJ, Wright P, Dolin R, Matthews T, Weinhold K, Bolognesi DP, Sposto R, et al. 1994. Neutralizing antibodies to HIV-1 in seronegative volunteers immunized with recombinant gp120 from the MN strain of HIV-1. NIAID AIDS Vaccine Clinical Trials Network. *JAMA* 272: 475-80
53. Francis DP, Gregory T, McElrath MJ, Belshe RB, Gorse GJ, Migasena S, Kitayaporn D, Pitisuttitham P, Matthews T, Schwartz DH, Berman PW. 1998. Advancing AIDSVAX to phase 3. Safety, immunogenicity, and plans for phase 3. *AIDS Res Hum Retroviruses* 14 Suppl 3: S325-31
54. Pitisuttithum P, Gilbert P, Gurwith M, Heyward W, Martin M, van Griensven F, Hu D, Tappero JW, Choopanya K. 2006. Randomized, double-blind, placebo-controlled efficacy trial of a bivalent recombinant glycoprotein 120 HIV-1 vaccine among injection drug users in Bangkok, Thailand. *J Infect Dis* 194: 1661-71
55. Flynn NM, Forthal DN, Harro CD, Judson FN, Mayer KH, Para MF. 2005. Placebo-controlled phase 3 trial of a recombinant glycoprotein 120 vaccine to prevent HIV-1 infection. *J Infect Dis* 191: 654-65
56. Ferrantelli F, Ruprecht RM. 2002. Neutralizing antibodies against HIV -- back in the major leagues? *Curr Opin Immunol* 14: 495-502
57. Mc Cann CM, Song RJ, Ruprecht RM. 2005. Antibodies: can they protect against HIV infection? *Curr Drug Targets Infect Disord* 5: 95-111

58. Robbins JB, Schneerson R, Szu SC. 1995. Perspective: hypothesis: serum IgG antibody is sufficient to confer protection against infectious diseases by inactivating the inoculum. *J Infect Dis* 171: 1387-98
59. Hilleman MR. 2001. Overview of the pathogenesis, prophylaxis and therapeutics of viral hepatitis B, with focus on reduction to practical applications. *Vaccine* 19: 1837-48
60. Baba TW, Liska V, Hofmann-Lehmann R, Vlasak J, Xu W, Aychunie S, Cavacini LA, Posner MR, Katinger H, Stiegler G, Bernacky BJ, Rizvi TA, Schmidt R, Hill LR, Keeling ME, Lu Y, Wright JE, Chou TC, Ruprecht RM. 2000. Human neutralizing monoclonal antibodies of the IgG1 subtype protect against mucosal simian-human immunodeficiency virus infection. *Nat Med* 6: 200-6
61. Conley AJ, Kessler JA, 2nd, Boots LJ, McKenna PM, Schleif WA, Emini EA, Mark GE, 3rd, Katinger H, Cobb EK, Lunceford SM, Rouse SR, Murthy KK. 1996. The consequence of passive administration of an anti-human immunodeficiency virus type 1 neutralizing monoclonal antibody before challenge of chimpanzees with a primary virus isolate. *J Virol* 70: 6751-8
62. Ferrantelli F, Rasmussen RA, Buckley KA, Li PL, Wang T, Montefiori DC, Katinger H, Stiegler G, Anderson DC, McClure HM, Ruprecht RM. 2004. Complete protection of neonatal rhesus macaques against oral exposure to pathogenic simian-human immunodeficiency virus by human anti-HIV monoclonal antibodies. *J Infect Dis* 189: 2167-73
63. Ferrantelli F, Hofmann-Lehmann R, Rasmussen RA, Wang T, Xu W, Li PL, Montefiori DC, Cavacini LA, Katinger H, Stiegler G, Anderson DC, McClure HM, Ruprecht RM. 2003. Post-exposure prophylaxis with human monoclonal

- antibodies prevented SHIV89.6P infection or disease in neonatal macaques. *AIDS* 17: 301-9
64. Hofmann-Lehmann R, Vlasak J, Rasmussen RA, Smith BA, Baba TW, Liska V, Ferrantelli F, Montefiori DC, McClure HM, Anderson DC, Bernacky BJ, Rizvi TA, Schmidt R, Hill LR, Keeling ME, Katinger H, Stiegler G, Cavacini LA, Posner MR, Chou TC, Andersen J, Ruprecht RM. 2001. Postnatal passive immunization of neonatal macaques with a triple combination of human monoclonal antibodies against oral simian-human immunodeficiency virus challenge. *J Virol* 75: 7470-80
65. Mascola JR, Lewis MG, Stiegler G, Harris D, VanCott TC, Hayes D, Louder MK, Brown CR, Sapan CV, Frankel SS, Lu Y, Robb ML, Katinger H, Birx DL. 1999. Protection of Macaques against pathogenic simian/human immunodeficiency virus 89.6PD by passive transfer of neutralizing antibodies. *J Virol* 73: 4009-18
66. Mascola JR, Stiegler G, VanCott TC, Katinger H, Carpenter CB, Hanson CE, Beary H, Hayes D, Frankel SS, Birx DL, Lewis MG. 2000. Protection of macaques against vaginal transmission of a pathogenic HIV-1/SIV chimeric virus by passive infusion of neutralizing antibodies. *Nat Med* 6: 207-10
67. Parren PW, Marx PA, Hessel AJ, Luckay A, Harouse J, Cheng-Mayer C, Moore JP, Burton DR. 2001. Antibody protects macaques against vaginal challenge with a pathogenic R5 simian/human immunodeficiency virus at serum levels giving complete neutralization in vitro. *J Virol* 75: 8340-7
68. Veazey RS, Shattock RJ, Pope M, Kirijan JC, Jones J, Hu Q, Ketas T, Marx PA, Klasse PJ, Burton DR, Moore JP. 2003. Prevention of virus transmission to macaque monkeys by a vaginally applied monoclonal antibody to HIV-1 gp120. *Nat Med* 9: 343-6

-
69. Kramer VG, Siddappa NB, Ruprecht RM. 2007. Passive immunization as tool to identify protective HIV-1 Env epitopes. *Curr HIV Res* 5: 642-55
70. Binley JM, Wrin T, Korber B, Zwick MB, Wang M, Chappey C, Stiegler G, Kunert R, Zolla-Pazner S, Katinger H, Petropoulos CJ, Burton DR. 2004. Comprehensive cross-clade neutralization analysis of a panel of anti-human immunodeficiency virus type 1 monoclonal antibodies. *J Virol* 78: 13232-52
71. Ferrantelli F, Kitabwalla M, Rasmussen RA, Cao C, Chou TC, Katinger H, Stiegler G, Cavacini LA, Bai Y, Cotropia J, Ugen KE, Ruprecht RM. 2004. Potent cross-group neutralization of primary human immunodeficiency virus isolates with monoclonal antibodies--implications for acquired immunodeficiency syndrome vaccine. *J Infect Dis* 189: 71-4
72. Kitabwalla M, Ferrantelli F, Wang T, Chalmers A, Katinger H, Stiegler G, Cavacini LA, Chou TC, Ruprecht RM. 2003. Primary African HIV clade A and D isolates: effective cross-clade neutralization with a quadruple combination of human monoclonal antibodies raised against clade B. *AIDS Res Hum Retroviruses* 19: 125-31
73. Xu W, Smith-Franklin BA, Li PL, Wood C, He J, Du Q, Bhat GJ, Kankasa C, Katinger H, Cavacini LA, Posner MR, Burton DR, Chou TC, Ruprecht RM. 2001. Potent neutralization of primary human immunodeficiency virus clade C isolates with a synergistic combination of human monoclonal antibodies raised against clade B. *J Hum Virol* 4: 55-61
74. Calarese DA, Lee HK, Huang CY, Best MD, Astronomo RD, Stanfield RL, Katinger H, Burton DR, Wong CH, Wilson IA. 2005. Dissection of the carbohydrate specificity of the broadly neutralizing anti-HIV-1 antibody 2G12. *Proc Natl Acad Sci U S A* 102: 13372-7
-

75. Posner MR, Hideshima T, Cannon T, Mukherjee M, Mayer KH, Byrn RA. 1991. An IgG human monoclonal antibody that reacts with HIV-1/GP120, inhibits virus binding to cells, and neutralizes infection. *J Immunol* 146: 4325-32
76. Saphire EO, Parren PW, Pantophlet R, Zwick MB, Morris GM, Rudd PM, Dwek RA, Stanfield RL, Burton DR, Wilson IA. 2001. Crystal structure of a neutralizing human IGG against HIV-1: a template for vaccine design. *Science* 293: 1155-9
77. Zwick MB, Jensen R, Church S, Wang M, Stiegler G, Kunert R, Katinger H, Burton DR. 2005. Anti-human immunodeficiency virus type 1 (HIV-1) antibodies 2F5 and 4E10 require surprisingly few crucial residues in the membrane-proximal external region of glycoprotein gp41 to neutralize HIV-1. *J Virol* 79: 1252-61
78. Haynes BF, Fleming J, St Clair EW, Katinger H, Stiegler G, Kunert R, Robinson J, Scearce RM, Plonk K, Staats HF, Ortel TL, Liao HX, Alam SM. 2005. Cardiolipin polyspecific autoreactivity in two broadly neutralizing HIV-1 antibodies. *Science* 308: 1906-8
79. Coeffier E, Clement JM, Cussac V, Khodaei-Boorane N, Jehanno M, Rojas M, Dridi A, Latour M, El Habib R, Barre-Sinoussi F, Hofnung M, Leclerc C. 2000. Antigenicity and immunogenicity of the HIV-1 gp41 epitope ELDKWA inserted into permissive sites of the MalE protein. *Vaccine* 19: 684-93
80. McGaughey GB, Citron M, Danzeisen RC, Freidinger RM, Garsky VM, Hurni WM, Joyce JG, Liang X, Miller M, Shiver J, Bogusky MJ. 2003. HIV-1 vaccine development: constrained peptide immunogens show improved binding to the anti-HIV-1 gp41 MAb. *Biochemistry* 42: 3214-23

81. Zhou T, Xu L, Dey B, Hessel AJ, Van Ryk D, Xiang SH, Yang X, Zhang MY, Zwick MB, Arthos J, Burton DR, Dimitrov DS, Sodroski J, Wyatt R, Nabel GJ, Kwong PD. 2007. Structural definition of a conserved neutralization epitope on HIV-1 gp120. *Nature* 445: 732-7
82. Javaherian K, Langlois AJ, McDanal C, Ross KL, Eckler LI, Jellis CL, Profy AT, Rusche JR, Bolognesi DP, Putney SD, et al. 1989. Principal neutralizing domain of the human immunodeficiency virus type 1 envelope protein. *Proc Natl Acad Sci U S A* 86: 6768-72
83. Putney SD, Matthews TJ, Robey WG, Lynn DL, Robert-Guroff M, Mueller WT, Langlois AJ, Ghrayeb J, Petteway SR, Jr., Weinhold KJ, et al. 1986. HTLV-III/LAV-neutralizing antibodies to an E. coli-produced fragment of the virus envelope. *Science* 234: 1392-5
84. Goudsmit J, Debouck C, Melen RH, Smit L, Bakker M, Asher DM, Wolff AV, Gibbs CJ, Jr., Gajdusek DC. 1988. Human immunodeficiency virus type 1 neutralization epitope with conserved architecture elicits early type-specific antibodies in experimentally infected chimpanzees. *Proc Natl Acad Sci U S A* 85: 4478-82
85. Mascola JR, Snyder SW, Weislow OS, Belay SM, Belshe RB, Schwartz DH, Clements ML, Dolin R, Graham BS, Gorse GJ, Keefer MC, McElrath MJ, Walker MC, Wagner KF, McNeil JG, McCutchan FE, Burke DS. 1996. Immunization with envelope subunit vaccine products elicits neutralizing antibodies against laboratory-adapted but not primary isolates of human immunodeficiency virus type 1. The National Institute of Allergy and Infectious Diseases AIDS Vaccine Evaluation Group. *J Infect Dis* 173: 340-8

-
86. Hioe CE, Xu S, Chigurupati P, Burda S, Williams C, Gorny MK, Zolla-Pazner S. 1997. Neutralization of HIV-1 primary isolates by polyclonal and monoclonal human antibodies. *Int Immunol* 9: 1281-90
87. Gorny MK, VanCott TC, Hioe C, Israel ZR, Michael NL, Conley AJ, Williams C, Kessler JA, 2nd, Chigurupati P, Burda S, Zolla-Pazner S. 1997. Human monoclonal antibodies to the V3 loop of HIV-1 with intra- and interclade cross-reactivity. *J Immunol* 159: 5114-22
88. Gorny MK, Xu JY, Karwowska S, Buchbinder A, Zolla-Pazner S. 1993. Repertoire of neutralizing human monoclonal antibodies specific for the V3 domain of HIV-1 gp120. *J Immunol* 150: 635-43
89. Gorny MK, Williams C, Volsky B, Revesz K, Cohen S, Polonis VR, Honnen WJ, Kayman SC, Krachmarov C, Pinter A, Zolla-Pazner S. 2002. Human monoclonal antibodies specific for conformation-sensitive epitopes of V3 neutralize human immunodeficiency virus type 1 primary isolates from various clades. *J Virol* 76: 9035-45
90. Conley AJ, Gorny MK, Kessler JA, 2nd, Boots LJ, Ossorio-Castro M, Koenig S, Lineberger DW, Emini EA, Williams C, Zolla-Pazner S. 1994. Neutralization of primary human immunodeficiency virus type 1 isolates by the broadly reactive anti-V3 monoclonal antibody, 447-52D. *J Virol* 68: 6994-7000
91. Krachmarov CP, Kayman SC, Honnen WJ, Trochev O, Pinter A. 2001. V3-specific polyclonal antibodies affinity purified from sera of infected humans effectively neutralize primary isolates of human immunodeficiency virus type 1. *AIDS Res Hum Retroviruses* 17: 1737-48
92. Gorny MK, Revesz K, Williams C, Volsky B, Louder MK, Anyangwe CA, Krachmarov C, Kayman SC, Pinter A, Nadas A, Nyambi PN, Mascola JR,
-

- Zolla-Pazner S. 2004. The v3 loop is accessible on the surface of most human immunodeficiency virus type 1 primary isolates and serves as a neutralization epitope. *J Virol* 78: 2394-404
93. Poignard P, Moulard M, Golez E, Vivona V, Franti M, Venturini S, Wang M, Parren PW, Burton DR. 2003. Heterogeneity of envelope molecules expressed on primary human immunodeficiency virus type 1 particles as probed by the binding of neutralizing and nonneutralizing antibodies. *J Virol* 77: 353-65
94. Andris JS, Johnson S, Zolla-Pazner S, Capra JD. 1991. Molecular characterization of five human anti-human immunodeficiency virus type 1 antibody heavy chains reveals extensive somatic mutation typical of an antigen-driven immune response. *Proc Natl Acad Sci U S A* 88: 7783-7
95. Cormier EG, Dragic T. 2002. The crown and stem of the V3 loop play distinct roles in human immunodeficiency virus type 1 envelope glycoprotein interactions with the CCR5 coreceptor. *J Virol* 76: 8953-7
96. Suphaphiphat P, Thitithanyanont A, Paca-Uccaralertkun S, Essex M, Lee TH. 2003. Effect of amino acid substitution of the V3 and bridging sheet residues in human immunodeficiency virus type 1 subtype C gp120 on CCR5 utilization. *J Virol* 77: 3832-7
97. Vancott TC, Polonis VR, Loomis LD, Michael NL, Nara PL, Birx DL. 1995. Differential role of V3-specific antibodies in neutralization assays involving primary and laboratory-adapted isolates of HIV type 1. *AIDS Res Hum Retroviruses* 11: 1379-91
98. Spenlehauer C, Saragosti S, Fleury HJ, Kirn A, Aubertin AM, Moog C. 1998. Study of the V3 loop as a target epitope for antibodies involved in the

- neutralization of primary isolates versus T-cell-line-adapted strains of human immunodeficiency virus type 1. *J Virol* 72: 9855-64
99. Zolla-Pazner S, O'Leary J, Burda S, Gorny MK, Kim M, Mascola J, McCutchan F. 1995. Serotyping of primary human immunodeficiency virus type 1 isolates from diverse geographic locations by flow cytometry. *J Virol* 69: 3807-15
100. Zwick MB, Bonnycastle LL, Menendez A, Irving MB, Barbas CF, 3rd, Parren PW, Burton DR, Scott JK. 2001. Identification and characterization of a peptide that specifically binds the human, broadly neutralizing anti-human immunodeficiency virus type 1 antibody b12. *J Virol* 75: 6692-9
101. Bou-Habib DC, Roderiquez G, Oravec T, Berman PW, Lusso P, Norcross MA. 1994. Cryptic nature of envelope V3 region epitopes protects primary monocyctotropic human immunodeficiency virus type 1 from antibody neutralization. *J Virol* 68: 6006-13
102. Cavacini L, Posner M. 2004. Native HIV type 1 virion surface structures: relationships between antibody binding and neutralization or lessons from the viral capture assay. *AIDS Res Hum Retroviruses* 20: 435-41
103. Stamatatos L, Zolla-Pazner S, Gorny MK, Cheng-Mayer C. 1997. Binding of antibodies to virion-associated gp120 molecules of primary-like human immunodeficiency virus type 1 (HIV-1) isolates: effect on HIV-1 infection of macrophages and peripheral blood mononuclear cells. *Virology* 229: 360-9
104. Holmes EC. 2001. On the origin and evolution of the human immunodeficiency virus (HIV). *Biol Rev Camb Philos Soc* 76: 239-54
105. Huet T, Cheynier R, Meyerhans A, Roelants G, Wain-Hobson S. 1990. Genetic organization of a chimpanzee lentivirus related to HIV-1. *Nature* 345: 356-9

-
106. Hirsch VM, Olmsted RA, Murphey-Corb M, Purcell RH, Johnson PR. 1989. An African primate lentivirus (SIVsm) closely related to HIV-2. *Nature* 339: 389-92
107. Hu SL. 2005. Non-human primate models for AIDS vaccine research. *Curr Drug Targets Infect Disord* 5: 193-201
108. Connor RI, Sheridan KE, Ceradini D, Choe S, Landau NR. 1997. Change in coreceptor use correlates with disease progression in HIV-1--infected individuals. *J Exp Med* 185: 621-8
109. Zhu T, Mo H, Wang N, Nam DS, Cao Y, Koup RA, Ho DD. 1993. Genotypic and phenotypic characterization of HIV-1 patients with primary infection. *Science* 261: 1179-81
110. Song RJ, Chenine AL, Rasmussen RA, Ruprecht CR, Mirshahidi S, Grisson RD, Xu W, Whitney JB, Goins LM, Ong H, Li PL, Shai-Kobiler E, Wang T, McCann CM, Zhang H, Wood C, Kankasa C, Secor WE, McClure HM, Strobert E, Else JG, Ruprecht RM. 2006. Molecularly cloned SHIV-1157ipd3N4: a highly replication-competent, mucosally transmissible R5 simian-human immunodeficiency virus encoding HIV clade C Env. *J Virol* 80: 8729-38
111. Kwong PD, Wyatt R, Majeed S, Robinson J, Sweet RW, Sodroski J, Hendrickson WA. 2000. Structures of HIV-1 gp120 envelope glycoproteins from laboratory-adapted and primary isolates. *Structure* 8: 1329-39
112. Smith GP, Petrenko VA. 1997. Phage Display. *Chem Rev* 97: 391-410
113. Enshell-Seijffers D, Smelyanski L, Vardinon N, Yust I, Gershoni JM. 2001. Dissection of the humoral immune response toward an immunodominant epitope of HIV: a model for the analysis of antibody diversity in HIV+ individuals. *FASEB J* 15: 2112-20
-

-
114. Felici F, Galfre G, Luzzago A, Monaci P, Nicosia A, Cortese R. 1996. Phage-displayed peptides as tools for characterization of human sera. *Methods Enzymol* 267: 116-29
 115. Meola A, Delmastro P, Monaci P, Luzzago A, Nicosia A, Felici F, Cortese R, Galfre G. 1995. Derivation of vaccines from mimotopes. Immunologic properties of human hepatitis B virus surface antigen mimotopes displayed on filamentous phage. *J Immunol* 154: 3162-72
 116. Prezzi C, Nuzzo M, Meola A, Delmastro P, Galfre G, Cortese R, Nicosia A, Monaci P. 1996. Selection of antigenic and immunogenic mimics of hepatitis C virus using sera from patients. *J Immunol* 156: 4504-13
 117. Roccasecca R, Folgari A, Ercole BB, Puntoriero G, Lahm A, Zucchelli S, Tafi R, Pezzanera M, Galfre G, Tramontano A, Mondelli MU, Pessi A, Nicosia A, Cortese R, Meola A. 2001. Mimotopes of the hyper variable region 1 of the hepatitis C virus induce cross-reactive antibodies directed against discontinuous epitopes. *Mol Immunol* 38: 485-92
 118. Scala G, Chen X, Liu W, Telles JN, Cohen OJ, Vaccarezza M, Igarashi T, Fauci AS. 1999. Selection of HIV-specific immunogenic epitopes by screening random peptide libraries with HIV-1-positive sera. *J Immunol* 162: 6155-61
 119. Konigs C, Rowley MJ, Thompson P, Myers MA, Scealy M, Davies JM, Wu L, Dietrich U, Mackay CR, Mackay IR. 2000. Monoclonal antibody screening of a phage-displayed random peptide library reveals mimotopes of chemokine receptor CCR5: implications for the tertiary structure of the receptor and for an N-terminal binding site for HIV-1 gp120. *Eur J Immunol* 30: 1162-71
 120. Riemer AB, Forster-Waldl E, Bramswig KH, Pollak A, Zielinski CC, Pehamberger H, Lode HN, Scheiner O, Jensen-Jarolim E. 2006. Induction of

- IgG antibodies against the GD2 carbohydrate tumor antigen by vaccination with peptide mimotopes. *Eur J Immunol* 36: 1267-74
121. Saphire EO, Montero M, Menendez A, van Houten NE, Irving MB, Pantophlet R, Zwick MB, Parren PW, Burton DR, Scott JK, Wilson IA. 2007. Structure of a high-affinity "mimotope" peptide bound to HIV-1-neutralizing antibody b12 explains its inability to elicit gp120 cross-reactive antibodies. *J Mol Biol* 369: 696-709
122. Sticht J, Humbert M, Findlow S, Bodem J, Muller B, Dietrich U, Werner J, Krausslich HG. 2005. A peptide inhibitor of HIV-1 assembly in vitro. *Nat Struct Mol Biol* 12: 671-7
123. Bublil EM, Yeger-Azuz S, Gershoni JM. 2006. Computational prediction of the cross-reactive neutralizing epitope corresponding to the [corrected] monoclonal [corrected] antibody b12 specific for HIV-1 gp120. *FASEB J* 20: 1762-74
124. Bublil EM, Freund NT, Mayrose I, Penn O, Roitburd-Berman A, Rubinstein ND, Pupko T, Gershoni JM. 2007. Stepwise prediction of conformational discontinuous B-cell epitopes using the Mapitope algorithm. *Proteins* 68: 294-304
125. Huang J, Gutteridge A, Honda W, Kanehisa M. 2006. MIMOX: a web tool for phage display based epitope mapping. *BMC Bioinformatics* 7: 451
126. Mayrose I, Penn O, Erez E, Rubinstein ND, Shlomi T, Freund NT, Bublil EM, Ruppin E, Sharan R, Gershoni JM, Martz E, Pupko T. 2007. Pepitope: epitope mapping from affinity-selected peptides. *Bioinformatics* 23: 3244-6
127. Moreau V, Granier C, Villard S, Laune D, Molina F. 2006. Discontinuous epitope prediction based on mimotope analysis. *Bioinformatics* 22: 1088-95

-
128. Schreiber A, Humbert M, Benz A, Dietrich U. 2005. 3D-Epitope-Explorer (3DEX): localization of conformational epitopes within three-dimensional structures of proteins. *J Comput Chem* 26: 879-87
129. Humbert M, Rasmussen RA, Song R, Ong H, Sharma P, Chenine AL, Kramer VG, Siddappa NB, Xu W, Else JG, Novembre FJ, Strobert E, O'Neil SP, Ruprecht RM. 2008. SHIV-1157i and passaged progeny viruses encoding R5 HIV-1 clade C env cause AIDS in rhesus monkeys. *Retrovirology* 5: 94
130. Siddappa NB, Song R, Kramer VG, Chenine AL, Velu V, Ong H, Rasmussen RA, Grisson RD, Wood C, Zhang H, Kankasa C, Amara RR, Else JG, Novembre FJ, Montefiori DC, Ruprecht RM. 2009. Neutralization-sensitive R5-tropic simian-human immunodeficiency virus SHIV-2873Nip, which carries env isolated from an infant with a recent HIV clade C infection. *J Virol* 83: 1422-32
131. Huang CC, Tang M, Zhang MY, Majeed S, Montabana E, Stanfield RL, Dimitrov DS, Korber B, Sodroski J, Wilson IA, Wyatt R, Kwong PD. 2005. Structure of a V3-containing HIV-1 gp120 core. *Science* 310: 1025-8
132. Humbert M, Rasmussen RA, Ong H, Kaiser FM, Hu SL, Ruprecht RM. 2008. Inducing cross-clade neutralizing antibodies against HIV-1 by immunofocusing. *PLoS One* 3: e3937
133. Rasmussen RA, Ong H, Kittel C, Ruprecht CR, Ferrantelli F, Hu SL, Polacino P, McKenna J, Moon J, Travis B, Ruprecht RM. 2006. DNA prime/protein boost immunization against HIV clade C: safety and immunogenicity in mice. *Vaccine* 24: 2324-32
134. Sharon M, Kessler N, Levy R, Zolla-Pazner S, Gorlach M, Anglister J. 2003. Alternative conformations of HIV-1 V3 loops mimic beta hairpins in

- chemokines, suggesting a mechanism for coreceptor selectivity. *Structure* 11: 225-36
135. Rosen O, Chill J, Sharon M, Kessler N, Mester B, Zolla-Pazner S, Anglister J. 2005. Induced fit in HIV-neutralizing antibody complexes: evidence for alternative conformations of the gp120 V3 loop and the molecular basis for broad neutralization. *Biochemistry* 44: 7250-8
136. Gorny MK, Williams C, Volsky B, Revesz K, Wang XH, Burda S, Kimura T, Konings FA, Nadas A, Anyangwe CA, Nyambi P, Krachmarov C, Pinter A, Zolla-Pazner S. 2006. Cross-clade neutralizing activity of human anti-V3 monoclonal antibodies derived from the cells of individuals infected with non-B clades of human immunodeficiency virus type 1. *J Virol* 80: 6865-72
137. Derdeyn CA, Decker JM, Bibollet-Ruche F, Mokili JL, Muldoon M, Denham SA, Heil ML, Kasolo F, Musonda R, Hahn BH, Shaw GM, Korber BT, Allen S, Hunter E. 2004. Envelope-constrained neutralization-sensitive HIV-1 after heterosexual transmission. *Science* 303: 2019-22
138. Li B, Decker JM, Johnson RW, Bibollet-Ruche F, Wei X, Mulenga J, Allen S, Hunter E, Hahn BH, Shaw GM, Blackwell JL, Derdeyn CA. 2006. Evidence for potent autologous neutralizing antibody titers and compact envelopes in early infection with subtype C human immunodeficiency virus type 1. *J Virol* 80: 5211-8
139. Galfre G, Monaci P, Nicosia A, Luzzago A, Felici F, Cortese R. 1996. Immunization with phage-displayed mimotopes. *Methods Enzymol* 267: 109-15
140. Zuercher AW, Miescher SM, Vogel M, Rudolf MP, Stadler MB, Stadler BM. 2000. Oral anti-IgE immunization with epitope-displaying phage. *Eur J Immunol* 30: 128-35

141. Davis D, Morein B, Akerblom L, Lovgren-Bengtsson K, van Gils ME, Bogers WM, Teeuwesen VJ, Heeney JL. 1997. A recombinant prime, peptide boost vaccination strategy can focus the immune response on to more than one epitope even though these may not be immunodominant in the complex immunogen. *Vaccine* 15: 1661-9
142. Keller PM, Arnold BA, Shaw AR, Tolman RL, Van Middlesworth F, Bondy S, Rusiecki VK, Koenig S, Zolla-Pazner S, Conard P, et al. 1993. Identification of HIV vaccine candidate peptides by screening random phage epitope libraries. *Virology* 193: 709-16
143. Zolla-Pazner S, Cohen SS, Krachmarov C, Wang S, Pinter A, Lu S. 2008. Focusing the immune response on the V3 loop, a neutralizing epitope of the HIV-1 gp120 envelope. *Virology* 372: 233-46

FIGURES

Figure:	Title:	Page:
Figure 1.1	Global prevalence of HIV-1 in 2009	1
Figure 1.2	HIV-1 Virion Structure	4
Figure 1.3	Interaction of HIV-1 Env with its primary receptor CD4 and its secondary receptor CCR5	6
Figure 1.4	The HIV-1 Life Cycle	7
Figure 1.5	The natural course of HIV-1 infection	9
Figure 1.6	Ribbon diagram of a clade C core gp120 structure (CAP210)	12
Figure 1.7	Schematic illustration of gp41 domains and the epitopes of the human mAbs 2F5 and 4E10	13
Figure 1.8	Modeling of the HIV-1 envelope spike showing epitopes of broadly nmAbs	16
Figure 2.1	Map of the pPEPTIDE Cloning Vector 1	26
Figure 3.1	Serial passage of SHIV-1157i in rhesus monkeys for viral adaptation	38
Table 3.1	IC ₅₀ for selected rhesus monkeys with high-titer nAb activity	38
Figure 3.2	Selection of HIV-1 clade C Env-specific mimotopes	40
Figure 3.3	Location of mimotope A12.2 on gp120	41
Table 3.2	Alignment of mimotopes selected with serum from monkey RKI-8 with the sequence of homologous gp160 _{SHIV-1157ip}	42
Figure 3.4	The conformational dependence of mimotope A12.2 by dot spot analysis with phage affinity-purified serum antibodies	43
Figure 3.5	Amplification of phage mimotope DNA via PCR	44
Figure 3.6	Digestion of phage mimotope DNA samples	45
Figure 3.7	Digestion of pPEPTIDE Cloning Vector DNA	45
Figure 3.8	Site-directed mutagenesis	46
Figure 3.9	Restriction analysis of AIV3p12.7 plasmid DNA samples	47
Figure 3.10	Expression screen	47
Figure 3.11	Protein purification	48
Figure 3.12	Purified proteins of V3 loop group and both controls	48
Figure 3.13	Detection of AIV3p12.5 with RKI-8 sera and sera of the Top-Ten Cohort by Western blot	49
Figure 3.14	Detection of AIV12.4 with RKI-8 sera and sera of the Top-Ten Cohort by Western blot	50

FIGURES

Figure:	Title:	Page:
Figure 3.15	Detection of AIV3p12.6 with RKI-8 sera and sera of the Top-Ten Cohort by Western blot	50
Figure 3.16	Reactivity profile of mimotope fusion proteins by ELISA	51
Figure 3.17	Reactivity profile of V3 loop mimotope fusion proteins under native and reduced conditions by ELISA	52
Figure 3.18	Cross-reactivity of mimotope fusion protein AIII12.11 with RKI-8 sera of different time points	53
Figure 3.19	Cross-reactivity of mimotope fusion protein AIV12.1 with RKI-8 sera of different time points	53
Figure 3.20	Cross-reactivity of mimotope fusion protein AIV12.4 with RKI-8 sera of different time points	54
Figure 3.21	Cross-reactivity of mimotope fusion protein AIV3p12.6 with RKI-8 sera of different time points	54
Figure 3.22	Cross-reactivity of RAO-8 serum with mimotope fusion proteins	55
Figure 3.23	Cross-reactivity of RTs-7 serum with mimotope fusion proteins	56
Figure 3.24	Cross-reactivity of RJA-9 serum with mimotope fusion proteins	56
Figure 3.25	Schedule for immunizations and blood collections in mouse study	57
Figure 3.26	Analysis of post-phage boost (4 th bleed) mouse immune sera	58
Figure 3.27	Analysis of immune mouse sera after DNA prime/phage boosting or DNA prime/phage + gp160 boosting	59
Figure 3.28	Reducing Env ELISA	61
Figure 3.29	Binding to individual mimotopes of the V3 loop group after 4 th boost	63
Figure 3.30	Binding to individual mimotopes of the V3 loop group after 5 th boost	63
Figure 3.31	Binding to individual mimotopes of the C-terminus group after 4 th boost	64
Figure 3.32	Binding to individual mimotopes of the C-terminus group after 5 th boost	64
Figure 3.33	Binding to individual mimotopes of the IDR group after 4 th boost	65
Figure 3.34	Binding to individual mimotopes of the IDR group after 5 th boost	65
Figure 3.35	Binding to individual mimotopes of the KLIC group after 4 th boost	66
Figure 3.36	Binding to individual mimotopes of the KLIC group after 5 th boost	66

ACKNOWLEDGMENTS

First of all, I would like to thank my wonderful principal investigator Ruth Ruprecht for giving me the opportunity to conduct my M.D. thesis in her laboratory. I will always remember her infinite enthusiasm and her contagious passion for research, which have re-confirmed my plans to pursue an academic career as a physician-scientist.

I would also like to thank my friend and advisor Michael Humbert who supervised me during my stay in Boston for his commitment and patience. Michael has always re-sparked my enthusiasm during times of frustration and despair. I could not have asked for a better mentor.

In addition, I would like to thank Prof. Dr. Axel Rethwilm for being my supervisor in Germany.

I want to thank all members of the Ruprecht laboratory for making my stay such a memorable experience, in particular Victor Kramer and his wife Jessica, Helena Ong, Susan Sharp, Klemens Wassermann, Gaia Scarangella and Robert Rasmussen.

Furthermore, I would like to thank my roommates Andreas Volk and Tarek Abdel-Aziz for saving me from insanity given the hygienic and social conditions in our accommodation.

I would also like to thank Alex Koglin for maintaining my blood glucose levels in the normal range through regular administration of Au-Bon-Pain pastries.

Last but not least, I want to thank my parents for always supporting my plans and ideas. This thesis is dedicated to them.
